The Messenger

No. 178 – Quarter 4 | 2019

ELT M4 — The Largest Adaptive Mirror Ever Built
A Celebration of GRAVITY Science
The ESO Summer Research Programme 2019

ESO, the European Southern Observatory, is the foremost intergovernmental astronomy organisation in Europe. It is supported by 16 Member States: Austria, Belgium, the Czech Republic, Denmark, France, Finland, Germany, Ireland, Italy, the Netherlands, Poland, Portugal, Spain, Sweden, Switzerland and the United Kingdom, along with the host country of Chile and with Australia as a Strategic Partner. ESO's programme is focussed on the design, construction and operation of powerful ground-based observing facilities. ESO operates three observatories in Chile: at La Silla, at Paranal, site of the Very Large Telescope, and at Llano de Chajnantor. ESO is the European partner in the Atacama Large Millimeter/submillimeter Array (ALMA). Currently ESO is engaged in the construction of the Extremely Large Telescope.

The Messenger is published, in hardcopy and electronic form, four times a year. ESO produces and distributes a wide variety of media connected to its activities. For further information, including postal subscription to The Messenger, contact the ESO Department of Communication at:

ESO Headquarters
Karl-Schwarzschild-Straße 2
85748 Garching bei München, Germany
Phone +498932006-0
information@eso.org

The Messenger
Editor: Gaitee A. J. Hussain
Layout, Typesetting, Graphics:
Jutta Boxheimer, Mafalda Martins
Design, Production: Jutta Boxheimer
Proofreading: Peter Grimley
www.eso.org/messenger/

Printed by FIBO Druck- und Verlags GmbH
Fichtenstraße 8, 82061 Neuried, Germany

ISSN 0722-6691

Contents

Front cover: Simulation of the orbits of stars very close to the supermassive black hole at the heart of the Milky Way, Sgr A*. One of these stars, S2, is the perfect laboratory to test Einstein's general theory of relativity as it passes very close to the black hole, with an orbital period of 16 years. S2's orbit has been monitored with ESO's telescopes since the 1990's and continues at even greater precision with GRAVITY. Credit: ESO/L. Calçada/spaceengine.org

DOI: 10.18727/0722-6691/5162

ELT M4 — The Largest Adaptive Mirror Ever Built

Elise Vernet[1]
Michele Cirasuolo[1]
Marc Cayrel[1]
Roberto Tamai[1]
Aglae Kellerer[1]
Lorenzo Pettazzi[1]
Paul Lilley[1]
Pablo Zuluaga[1]
Carlos Diaz Cano[1]
Bertrand Koehler[1]
Fabio Biancat Marchet[1]
Juan Carlos Gonzalez[1]
Mauro Tuti[1]
+ the ELT Team

[1] ESO

The Extremely Large Telescope (ELT) is at the core of ESO's vision to deliver the largest optical and infrared telescope in the world. Continuing our series of Messenger articles describing the optical elements of the ELT, we focus here on the quaternary mirror (M4), a true technological wonder; it is the largest deformable mirror ever made. In combination with M5, M4 is vital to delivering the sharp (diffraction-limited) images needed for science by correcting for atmospheric turbulence and the vibrations of the telescope itself. Here we describe the main characteristics of M4, the challenges and complexity involved in the production of this unique adaptive mirror, and its manufacturing status.

Background: how the ELT works

Let's briefly recall how the ELT works. The optical design of the ELT is based on a novel five-mirror scheme capable of collecting and focusing the light from astronomical sources and feeding state-of-the-art instruments for the purposes of imaging and spectroscopy. The light is collected by the giant primary mirror 39 metres in diameter, relayed via the M2 and M3 mirrors (each of which has a diameter of ~ 4 metres) to the M4 and M5 mirrors that form the core of the adaptive optics of the telescope; the light then reaches the instruments on one or other of the two Nasmyth platforms. This design provides an unvignetted field of view (FoV) of 10 arcminutes in diameter on the sky, ~ 80 square arcminutes (approximately a ninth of the full moon). Thanks to the combined use of M4 and M5, the optical system is capable of correcting for atmospheric turbulence and the vibration of the telescope structure itself induced by motion and wind.

This adaptive capability is crucial to allowing the ELT to reach its diffraction limit, which is ~ 8 milliarcseconds (mas) in the *J*-band (at λ ~ 1.2 µm) and ~ 14 mas in the *K*-band. In so doing the ELT will be able to yield images 15 times sharper than the Hubble Space Telescope and with much greater sensitivity. Translated into astrophysical terms this means opening up new discovery spaces, from exoplanets closer to their stars, to black holes, to the building blocks of galaxies both in the local Universe and billions of light years away. For example, the ELT will be able to detect and characterise extrasolar planets in the habitable zone around our closest star Proxima Centauri, or to resolve giant molecular clouds (the building blocks of star formation) down to ~ 50 parsecs in distant galaxies at z ~ 2 (and even smaller structures for sources that are gravitationally lensed by foreground clusters) with an unprecedented sensitivity.

The quaternary mirror (M4)

M4 is the main adaptive mirror of the telescope. The term "adaptive mirror" means that its surface can be deformed to correct for atmospheric turbulence, as well as for the fast vibration of the telescope structure induced by its motion and the wind. In the case of M4, more than 5000 actuators are used to change the shape of the mirror up to 1000 times per second.

In combination with the M5 mirror, M4 forms the core of the adaptive optics of the ELT. With a diameter of 2.4 metres, M4 will be the largest adaptive mirror ever built. By comparison, current adaptive mirrors are just over 1 metre in diameter, for example the 1.1-m M2 adaptive secondary on the VLT UT4 telescope (Yepun).

Adaptive mirror technology was translated into an industrial product for astronomy more than two decades ago by the Italian companies Microgate s.r.l and ADS, internationally known under the consortium name of AdOptica. Many 8-metre telescopes now have a metre-scale adaptive mirror. The same technology is now being adapted to serve the ELT, in order to produce a mirror with an area five times larger. The M4 mirror uses the same principle as a loudspeaker; the mirror is made of a very thin shell levitating 100 microns away from its reference surface (this corresponds to the thickness of a standard A4 sheet of paper) and it acts like a membrane which deforms under the effect of about 5000 voice coil actuators. A voice coil actuator is a type of direct drive linear motor and the name "voice coil" comes from one of its first historical applications, vibrating the paper cone of a loudspeaker. It consists of a permanent magnetic field assembly and a coil assembly. The current flowing through the coil assembly interacts with the permanent magnetic field and generates a force that can be reversed by changing the polarity of the current.

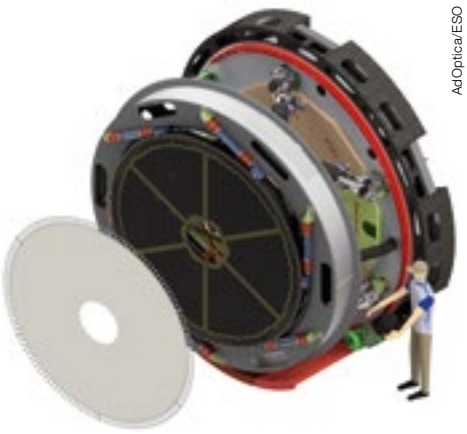
AdOptica/ESO

Figure 1. Rendering of the M4 adaptive mirror unit for the ELT.

Depending on the current injected into the coil the mirror can be pushed or pulled up to a distance of 90 microns from its mean position. With the help of a very fast and precise set of capacitive sensors and amplifiers that are co-located with the voice coil actuators, the mirror's position is measured 70 000 times per second to an accuracy of a few tens of nanometres (the size of the smallest virus) with the actuators being driven up to 1000 times per second.

M4 is made of several state-of-the-art components, the mirror and its reference

Figure 2. (Left) One of the shell mirrors of the M4 in Zerodur©.

Figure 3. (Right) The reference body in silicon-carbide being inspected after brazing the six parts.

structure being two of the most critical ones. The mirror is an assembly of six optically polished thin shells, or petals, made of the low-expansion glass-ceramic Zerodur© (manufactured by Schott GmbH). The six petals are obtained from a 35 mm-thick blank, which is polished and thinned down to a thickness of less than 2 mm — necessary to achieve the desired flexibility for shaping the mirror — and then finally cut into a precise shape by Safran Reosc (France; see Figure 2).

In order to adjust the shapes of the thin shells, a rigid and sufficiently accurate flat reference structure is also needed to hold the petals. This structure must be stiff enough to provide a good reference surface, whatever the orientation of the telescope. It also needs to hold all the actuators, which will deform and change the shape of the six petals.

The 2.7-metre diameter lightweight structure is made of Boostec® silicon carbide, one of the stiffest materials available (stiffer than steel, carbon fibre or beryllium). Its surface has more than 5000 holes which will hold the actuators (see Figure 4), while the back surface is composed of several ribs to reinforce the structure. Owing to its large dimensions, the silicon carbide structure is made of six parts brazed together, similar to the Herschel primary mirror which was manufactured more than a decade ago. The manufacture of the structure is significantly challenging, not only because of the depth, length, and thickness of the ribs, but also given the requirements on its straightness, as well as the number and accuracy of the actuator holes.

The back of the reference structure is supported by a 12-point whiffletree and laterally at six points on the mirror edge. The overall M4 sub-system is mounted on six position actuators (a hexapod system), which provide the fine alignment of the mirror. It is further mounted on a rotating mechanism (called a switcher) which is used to select the Nasmyth focus to which the light will be directed.

Manufacturing the M4

Safran Reosc (France) started to manufacture the thin segment mirrors in 2017 and four thin shells are now ready for integration in Italy. The remaining eight shells still need to be delivered in order to have two sets of six shells each (during ELT operation one set is integrated on M4, while the other is being recoated). The reference body manufacturing also began in 2017 and six segments have been brazed in the last few months. The reference surface will need to be lapped to 5 microns flatness before being delivered to Italy.

To have a mirror fully tested in Chile by early 2024, AdOptica has to ensure the procurement and manufacture of all the other components, including all the voice coil actuators and more than 60% of the permanent magnets, which are already in house and are waiting to be integrated. In addition, more than half of the electronics boards are either ready or under calibration, and most of the mechanical parts are ready, including the reference structure cell support and its whiffletree.

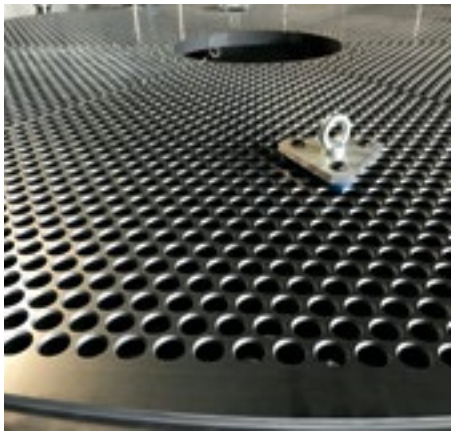

Mersen Boostec

Figure 4. Detail of the M4 reference body.

The final integration will start at AdOptica once the reference structure has been delivered. Given the number of components that need to be assembled to a high degree of precision, the integration will be a lengthy task requiring procedures to ensure that the assembly and calibration meet requirements. It should take 1.5 years to fully integrate the M4 mirror and start the final calibration of each mirror segment and their associated capacitive sensors. A test tower is being specially developed to verify and test the M4. It will be used in Europe to calibrate the M4 unit before being transferred to Chile where it will be used before the mirror is installed on the telescope and kept on-site for any future major maintenance activities that may be required.

DOI: 10.18727/0722-6691/5163

NEAR: First Results from the Search for Low-Mass Planets in α Cen

Markus Kasper[1]
Robin Arsenault[1]
Ulli Käufl[1]
Gerd Jakob[1]
Serban Leveratto[1]
Gerard Zins[1]
Eric Pantin[2]
Philippe Duhoux[1]
Miguel Riquelme[1]
Jean-Paul Kirchbauer[1]
Johann Kolb[1]
Prashant Pathak[1]
Ralf Siebenmorgen[1]
Christian Soenke[1]
Eloy Fuenteseca[1]
Michael Sterzik[1]
Nancy Ageorges[3]
Sven Gutruf[3]
Dirk Kampf[3]
Arnd Reutlinger[3]
Olivier Absil[4]
Christian Delacroix[4]
Anne-Lise Maire[4]
Elsa Huby[5]
Olivier Guyon[6,7]
Pete Klupar[7]
Dimitri Mawet[8]
Garreth Ruane[8]
Mikael Karlsson[9]
Kjetil Dohlen[10]
Arthur Vigan[10]
Mamadou N'Diaye[11]
Sascha Quanz[12]
Alexis Carlotti[13]

[1] ESO
[2] AIM, CEA, CNRS, Université Paris-Saclay, Université Paris Diderot, Sorbonne Paris Cité, Gif-sur-Yvette, France
[3] Kampf Telescope Optics (KT Optics), Munich, Germany
[4] University of Liège, Liège, Belgium
[5] Observatoire de Paris-Meudon, France
[6] Subaru Telescope, Tokyo, Japan
[7] Breakthrough Initiatives, Mountainview, USA
[8] Caltech, Pasadena, USA
[9] Uppsala University, Sweden
[10] Laboratoire d'Astrophysique Marseille, France
[11] Observatoire de la Côte d'Azur, Nice, France
[12] Eidgenössische Technische Hochschule Zürich, Switzerland
[13] Institude de Planétologie et d'Astrophysique de Grenoble, France

ESO, in collaboration with the Breakthrough Initiatives, has modified the VLT mid-infrared imager VISIR to greatly enhance its ability as a planet finder. It has conducted a 100-hour observing campaign to search for low-mass planets around both components of the binary α Centauri, part of the closest stellar system to the Earth. Using adaptive optics and high-performance coronagraphy, the instrument reached unprecedented contrast and sensitivity allowing it to see Neptune-sized planets in the habitable zone, if present. The experiment allowed us to characterise the current limitations of the instrument. We conclude that the detection of rocky planets similar to Earth in the habitable zone of the α Centauri System is already possible with 8-metre-class telescopes in the thermal infrared.

From an idea to the telescope

The α Centauri system is uniquely suited to the search for signatures of low-mass planets in the thermal infrared. The *N*-band at around 10 µm is best suited for such observations, because this is where a planet with a temperature like Earth's is brightest. The α Centauri binary consists of the solar-type stars α Centauri A and B, and the planet-hosting (Anglada-Escudé et al., 2016) M-dwarf star Proxima Centauri. In a previous Messenger article (Kasper et al., 2017), we provided details of how we planned to modify the existing VISIR instrument to conduct the necessary observations with the Very Large Telescope (VLT). This article describes how VISIR was moved to UT4, the innovations and new technologies that were implemented and how they work, concluding with the execution of the NEAR (New Earths in the α Centauri Region) experiment — a unique 100-hour observation of the α Centauri system, which took place in early June 2019.

Three years were needed to develop the NEAR experiment from the initial idea, from the Phase A review held in July 2016 to the observing campaign in June 2019. Between January and July 2018, ESO's mid-infrared detector test facility Thermal Infrared MultiMode Instrument (TIMMI2), a decommissioned instrument from the ESO 3.6-metre telescope at La Silla, was modified and used to carry out the acceptance tests of the internal chopper. This was followed by a performance evaluation of the Annular Groove Phase Mask (AGPM) coronagraph with a dedicated optical setup incorporating a line-tunable CO_2 laser, elliptical mirrors and germanium lenses. Four AGPM coronagraphs were tested, three specifically optimised for the NEAR filter (10–12.5 µm) and an older sample manufactured in 2012 and optimised for wavelengths between 11 and 13.1 µm. Surprisingly, the older coronagraph performed best, with a rejection ratio of up to 400 at 10.5 µm, and a contrast level of $< 10^{-4}$ at 3 λ/D.

After passing Provisional Acceptance Europe (PAE) in November 2018, the NEAR hardware was shipped to Paranal. At the same time, VISIR was dismounted from UT3 (Melipal) and brought to Paranal's New Integration Hall (NIH) in preparation for the on-site installation starting in early January 2019. As expected, three cool-downs of VISIR were required to successfully implement all the new modifications. First, the aperture wheel was rearranged with the help of the Paranal mechanical workshop to include two new AGPMs and a special optical mask (ZELDA, N'Diaye et al., 2014) to measure and pre-compensate optical aberrations in the instrument. New Lyot filters were mounted and mechanically centred with the cold stop of VISIR to an accuracy of better than 175 µm (i.e., 1% of the pupil diameter). The internal chopper, the wavefront sensor arm and the calibration unit were installed with the help of the contractor KT Optics, and all units were successfully tested. In particular, the alignment of the calibration unit, which uses an elliptical mirror with an aberration-free field of view of around 0.1 mm in diameter was laborious and required some modifications of the mechanical mounts on-site.

Following the completion of the assembly integration and verification (AIV) activities, VISIR was transported and mounted to UT4 (Yepun) in mid-March 2019 (see Figure 1). After measuring the expected residual misalignment between the instrument and telescope pupil on-sky on 24 March, VISIR was taken off the telescope again for adjustment by tilting

the instrument, and some fine adjustment of the wavefront sensor arm. On-sky commissioning started on 3 April 2019 and lasted for 10 half-nights, during which the various new functions were tested, and operational procedures were tuned.

Technical innovations, observing modes and performance

NEAR implements several technologies which are either completely new for *N*-band astronomy or have not previously been tested on-sky at this wavelength. For example, the experiment confirmed that atmospheric water vapour content does not significantly impact the adaptive optics (AO) corrected *N*-band image quality, and that mid-infrared spectral filters can be overcoated with chromium masks implementing Lyot stops or apodisers for the coronagraph. We also, for the first time, implemented an alternative altitude cable wrap (see Figure 1), which could also greatly facilitate the operation of other Cassegrain instruments.

Chopping, internal and external

Among the new technologies is an internal chopping device, the so-called Dicke Switch, which is described in more detail in Kasper et al. (2017). We tested the Dicke Switch at chopping frequencies up to 10 Hz during commissioning, and it substantially reduces the detector's Excess Low Frequency Noise (ELFN) as foreseen. There is an expected mismatch in the spatial distribution of the sky and internal background, but this mismatch turns out to be stable in time and can be well modelled or subtracted by nodding techniques. This device can be used when external chopping is not possible — when, for example, the source size exceeds the throw range of an external chopper.

The second option, external chopping using the Deformable Secondary Mirror (DSM), worked flawlessly. This option was initially deemed a risky approach, because the chopping action is seen by the AO and could have disturbed its operation. However, the clever design of the DSM and the Standard Platform for Adaptive optics Real Time Applications (SPARTA)[2] made sure that DSM chopping observations are highly efficient and almost transparent to the instrument. In addition, the α Centauri binary offers the possibility of chopping with an amplitude corresponding to the separation between the two stars of about 5 arcseconds in 2019, placing all the time a scientifically interesting target on the coronagraphic mask and doubling the efficiency. Because of these advantages, we used external chopping with the DSM for the α Centauri observations, and Figure 2 illustrates the data as seen by the detector during the two chopping cycles on the left and middle panels, and the chopping subtracted image of the two on the right.

ESO/NEAR Collaboration

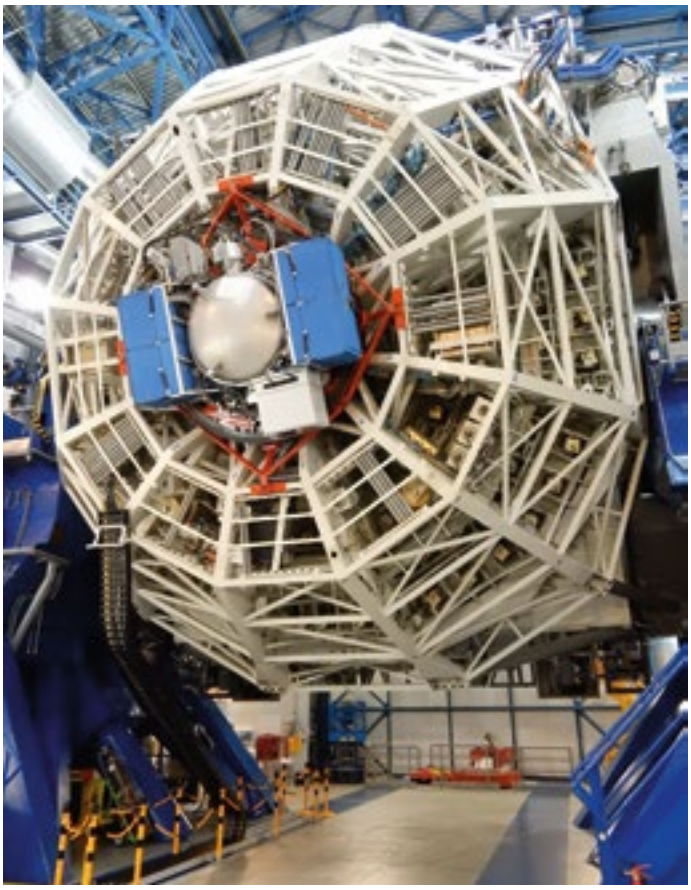

Figure 1. (Left) VISIR mounted on UT4 and ready for NEAR. The alternative altitude cable wrap connecting the instrument to the electronics racks and helium compressors on the azimuth platform can be seen on the left hanging down from the mirror cell.

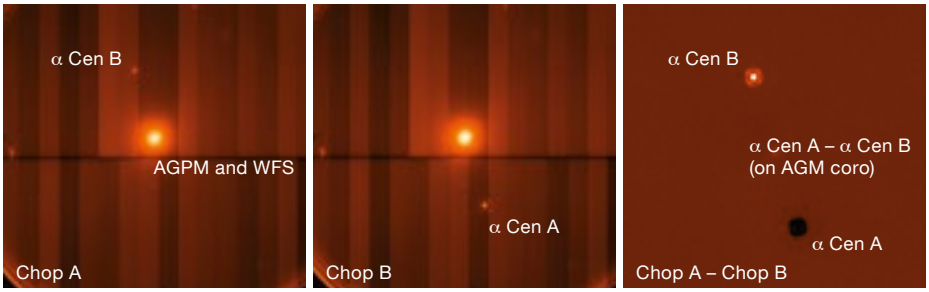

Figure 2. (Below) Illustration of the VISIR data acquisition of α Centauri with chopping.

Coronagraph modes and centring

The light from the star at the location where we search for planets can be suppressed using two different concepts in NEAR. The first is the AGPM, a technical realisation of a Vortex coronagraph using a sub-wavelength grating etched into a diamond substrate (Mawet et al., 2005). The second is a shaped pupil mask

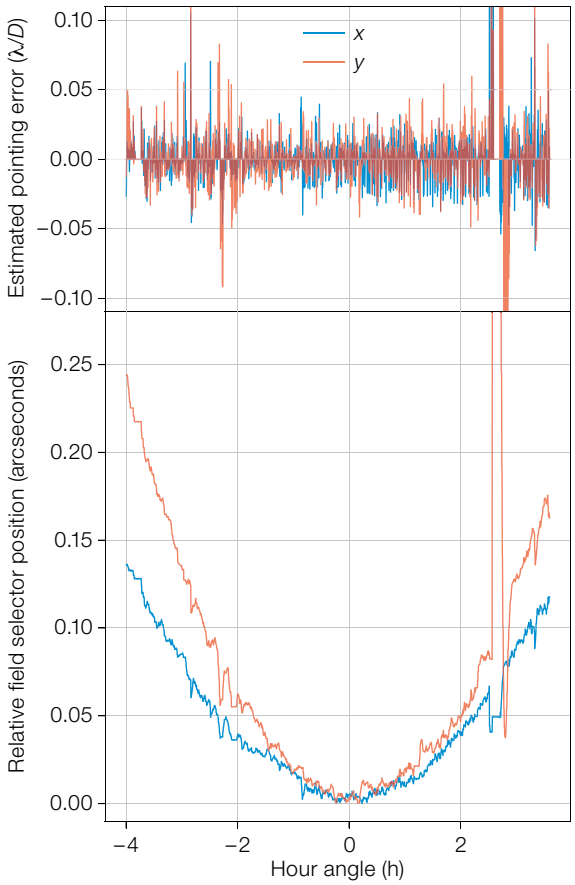

Figure 3. (Left) Top: The shifting movement of the star behind the AGPM is measured by the QACITS algorithm in a closed loop during a NEAR observing night. The horizontal axis shows the hour angle and the colours refer to the *x* and *y* directions. Over 4 hours, centered on meridian passage, the rms estimation is 0.015 λ/*D* for both the *x* and *y* directions. Bottom: The relative positions of the field selector recorded in the same night. The variation in the position of the field selector is due to differential atmospheric refraction between the AO wavefront-sensing channel and the science channel of VISIR. There was an AO interruption at hour angle ~ 2.5–3.

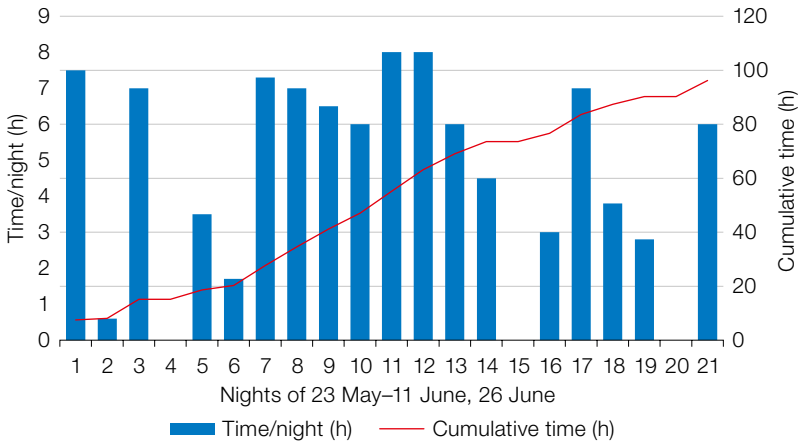

Figure 4. (Above) Hours of open shutter time over the duration of the NEAR campaign. Only small amounts of data could be collected between 24 and 28 May and between 5 and 11 June, owing to mediocre (mostly cloudy) observing conditions.

(Carlotti et al., 2012), which does not suppress the overall light intensity, but modifies the light distribution in the focal plane so as to carve out a dark high-contrast region at the relevant angular separation. Both concepts work well and improve the contrast by a factor of between 50 and 100. What tipped the balance towards the AGPM as the choice for the NEAR campaign was the higher throughput, resulting in a moderately improved sensitivity overall and, more importantly, the suppression of the high-intensity stellar image, thus avoiding detector electronics "ghosts".

As with all small inner working angle coronagraphs, the AGPM performance is sensitive to small offsets of the star behind the coronagraph (for example, slow drifts). In order to actively control the centring of α Centauri behind the AGPM during the observation, we implemented an algorithm called "Quadrant Analysis of Coronagraphic Images for Tip-tilt Sensing" (QACITS; Huby et al., 2015). This method estimates the offsets directly from the images recorded on the detector. The tests during the commissioning phase allowed us to optimise the QACITS algorithm parameters and the observing strategy. It was shown that background residuals after chopping have to be subtracted from the images analysed by QACITS. After tuning, QACITS was able to automatically centre the star on the AGPM and keep it there with an accuracy of 0.015 λ/*D* rms, almost one-hundredth of a resolution element (Figure 3).

One hundred hours of observations

ESO allocated 20 observing nights for the NEAR campaign between 23 May and 11 June 2019 to observe the α Centauri system. Even though the observing efficiency of NEAR is very high, with very small overheads for telescope sky offsets and data transfer (well below 10%), the campaign struggled to collect the 100 hours of data desired.

Figure 4 shows the campaign progress in data hours collected per night. The maximum possible time for which α Centauri could be observed at an airmass smaller than two is about seven hours in a good observing night. Figure 4 shows, however, that there were several consecutive nights during the first and last weeks of the campaign when either no or only small amounts of data were recorded. These nights suffered from extended periods of cloud coverage. Even thin high clouds, which can be acceptable for observations in the near-infrared, are very detrimental for thermal infrared observations, because they lead to very high fluctuations in throughput and sky background.

Solid N_2 on the coronagraph

There were, of course, a number of smaller and larger problems during the long campaign and lots of stories to tell. Here is a particularly interesting one, which concerns one of the unknown unknowns that we encountered.

During the first few nights of the campaign, we noticed that the contrast provided by the coronagraph was less effective than during commissioning, with a continuing slow degradation every other night. While we were expecting a suppression of the central point spread function (PSF) by a factor of about 120, we started

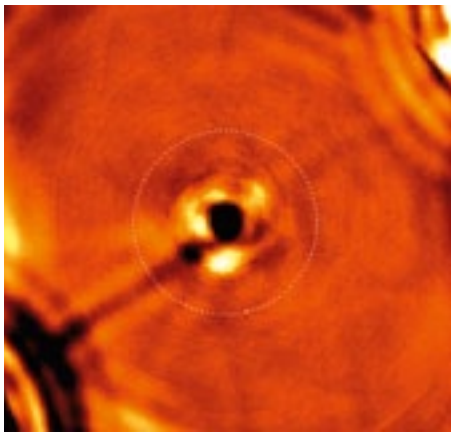

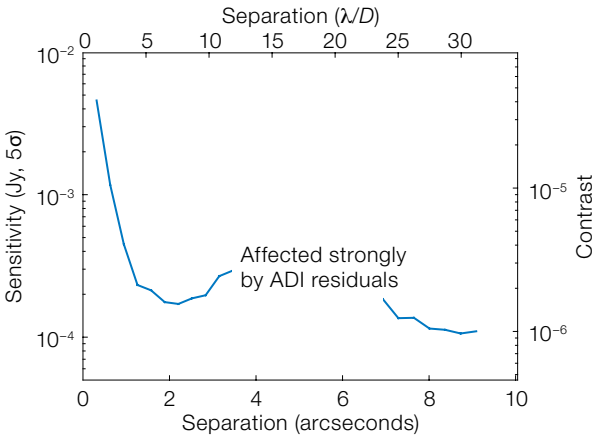

Figure 5. Left: The deepest ever view of the habitable zone (indicated by the dashed circle) around α Centauri A; the 76-hour image obtained during the NEAR campaign — ~ 6 × 6 arcseconds. Right: Sensitivity and contrast estimated from the deep image as a function of radial distance to the centre.

with a factor of 80, which degraded to only a factor of 40 about a week into the campaign. Somewhat frustratingly, none of the typical external effects that degrade coronagraph efficiency (for example, Lyot stop misalignments or optical aberrations) could explain the shape of the residual image that we observed. It really looked like an intrinsic degradation of the coronagraphic mask itself.

Could air, entering the cryostat through a known tiny leak, freeze out on the 20-Kelvin cold coronagraphic mask and produce the loss of contrast? A back-of-the-envelope estimate showed that such a leak could indeed build up an ice layer of a few microns thickness every day. With the refractive index of solid nitrogen, the main constituent of air, ice partly entering the grooves of the AGPM coronagraphic mask could change the optical depth of the grooves sufficiently to degrade the performance.

So, how were we to test this theory, and even more importantly, fix it during the campaign as it was running? Solid nitrogen starts to sublimate at a sufficiently high rate to de-ice the coronagraph mask at temperatures that are only moderately higher than the nominal 20 Kelvin. It turned out that the temperature after the first stage of the instrument warmup, lasting just a few hours, is 35–40 Kelvin. Tricking the PLC-controlled system into stopping the warmup sequence after the first stage and going into cooling again was risky (a glitch could have resulted in a full warmup which would have taken out VISIR for several days), but it paid off. A procedure was developed to carry out the mini-warmup and cool-down in the morning and be back in business in less than 10 hours, sufficiently quick to be ready for the following observing night. And it was a success! The coronagraphic rejection recovered with each mini-warmup, and starting from 1 June we repeated this procedure approximately every three days.

The data and preliminary results

The campaign data were taken at a VISIR/NEAR detector frame rate of 166 Hz, i.e., the detector integration time (DIT) was 6 ms. Chopping ran at 8.33 Hz for most of the campaign, and each chopping half-cycle thus lasted 60 ms. During this time span, 48 ms or 8 DITs were averaged into a single frame, and 12 ms or 2 DITs were skipped for the transition of the DSM between the two chopping positions. Each 30-second data file consists of 500 half-cycle frames, and the 100 hours of data add up to 6 million frames or 6 Tb.

Before entering advanced high-contrast imaging data reduction, some pre-processing was necessary to remove bad frames and reduce the data volume to a more manageable size. We removed frames with extremely high or variable background produced, for example, by thin clouds or low encircled energy for the off-axis stars during ineffective AO correction, and frames with low coronagraphic suppression through bad centring of the PSF on the coronagraph mask. Finally, we cropped the images to 400 × 400 pixels, carefully centred them to the position between the two off-axis PSFs and binned the surviving 76 hours of data to 1-minute time resolution, which is short enough to avoid any noticeable smearing of the images because of field rotation. This procedure compressed the full campaign into ~ 4600 frames or 3 Gb.

A relatively simple high-contrast imaging analysis can help evaluate the detection limits reached during the campaign. By sorting all the frames according to their parallactic angle, we run a PSF calibration procedure based on principal component analysis using all the frames, i.e., processing the campaign as a whole rather than night-by-night. The calibrated images are then combined using noise-weighted averages in order to properly take into account the rather large variations in the sky background.

Figure 5 shows the result of this simple data reduction and the contrast sensitivity achieved. The 5σ background-limited sensitivity far away from the star is of the order of 100 μJy, which is consistent with our initial goals. At ~ 1.1-arcsecond separation, i.e., at the angular size of the habitable zone around α Centauri A, the sensitivity is reduced to about 250 μJy mostly by the central glow of the AGPM. This does not yet mean that a point source can readily be detected at this level, but first estimates using a fake injected source show that a planet of ~ 350 μJy brightness corresponding to a temperate Neptune could indeed be seen.

No planet candidate of the size of Neptune or larger was found in the data so far. While we were obviously hoping for a

detection, the result can also be seen as good news for the existence of rocky planets, which may therefore still exist in the habitable zone of α Centauri in a stable orbit. There is also a roughly 35% chance that an existing planet would have been hidden by the star as the result of an unfavourable projected orbital position during our single-epoch observation. In addition, the image in Figure 5 shows some straight lines connecting the coronagraphic centre field with the off-axis stellar image to the lower left. These streaks appear because of a small persistence in the detector, i.e., the pixels remember the stars being dragged over the detector during the chopping transition. This feature is difficult to model and may hide another 5–10% of the possible planet orbits.

Beyond NEAR

Preliminary results of the NEAR commissioning and experiment have triggered substantial interest within the community in this facility, and also for other astronomical observations. ESO therefore issued a call for Science Demonstration proposals, which received a lot of attention and resulted in 26 proposals being submitted for NEAR observing time. Two periods of Science Demonstration were allocated in September and December 2019 to conduct roughly half of the proposed programmes.

While no planet candidates have been found so far, NEAR is already a very successful collaboration between ESO, the Breakthrough Initiatives[1] and many partners in the exoplanet and mid-infrared astronomy communities. Several key technologies for mid-infrared high-contrast imaging were successfully tested on-sky, and many important assumptions were validated — for example, the scaling of the achieved signal-to-noise ratio with the square-root of the observing time.

All raw data obtained during the 100-hour α Centauri campaign are publicly available, and a condensed easy-to-use 3 Gb package of all the good frames is available on request[3]. The on-sky contrast at 3 λ/D and the *N*-band sensitivity are unprecedented in ground-based astronomy by a large margin — more than one order of magnitude. The sensitivity limits are well understood and could be improved further by a factor 2–2.5, mainly by removing the AGPM glow by introducing a small optical relay incorporating a cold pupil stop in front of the AGPM. But this is still not the limit for mid-infrared observations from the ground. A novel lower-noise detector technology is emerging, which promises to double the sensitivity once more. These next-generation detectors would allow the VLT to probe the rocky planet regime in the habitable zone around α Centauri. When combined with similar instruments at the other southern hemisphere 8-metre-class telescopes, Gemini South and Magellan, true Earth analogues could soon be discovered.

Acknowledgements

The NEAR experiment greatly benefited, and still benefits, from the exchange with the exoplanet and mid-infrared scientific community on both sides of the Atlantic. We would like to thank Derek Ives for access to the Infrared Lab at ESO, Paranal's mechanical workshop for the excellent support during the integration on-site, and Rus Belikov, Eduardo Bendek, Anna Boehle, Bernhard Brandl, Christian Marois, Mike Meyer and Kevin Wagner for very helpful discussions and their interest in the data analysis. Many thanks go also to our industrial partners KT Optics, Optoline and the Infrared Multilayer Laboratory of the University of Reading (now Oxford), for their R&D spirit and their willingness to stay with us during the rapid development of the experiment.

References

Anglada-Escudé, G. et al. 2016, Nature, 536, 437
Carlotti, A. et al. 2012, Proc. SPIE, 8442, 844254
Huby, E. et al. 2015, A&A, 584, A74
Ives, D. et al. 2014, Proc. SPIE, 9154, 91541J
Kasper, M. et al. 2017, The Messenger, 169, 16
Lagage, P. O. et al. 2004, The Messenger, 117, 12
Mawet, D. et al. 2005, ApJ, 633, 1191
N'Diaye, M. et al. 2014, Proc. SPIE, 9148, 91485H

Links

[1] Breakthrough Initiatives webpage: http://breakthroughinitiatives.org
[2] SPARTA: https://www.eso.org/sci/facilities/develop/ao/tecno/sparta.html
[3] Data can be requested via e-mail from Prashant Pathak (ppathak@eso.org) or Markus Kasper (mkasper@eso.org

ESO/NEAR Collaboration

The NEAR experiment being mounted on the Cassegrain focus of the VLT's UT4 (Yepun).

DOI: 10.18727/0722-6691/5164

Report on Status of ESO Public Surveys and Current Activities

Magda Arnaboldi[1]
Nausicaa Delmotte[1]
Dimitri Gadotti[1]
Michael Hilker[1]
Gaitee Hussain[1]
Laura Mascetti[2]
Alberto Micol[1]
Monika Petr-Gotzens[1]
Marina Rejkuba[1]
Jörg Retzlaff[1]
Chiara Spiniello[1,3]
Bruno Leibundgut[1]
Martino Romaniello[1]

[1] ESO
[2] Terma GmbH, Darmstadt, Germany
[3] Astronomical Observatory of Capodimonte, Naples, Italy[a]

This report on the status of the ESO Public Surveys includes a brief overview of their legacy value and scientific impact. Their legacy is ensured by their homogeneity, sensitivity, large sky coverage in multiple filters, large number of targets, wavelength coverage and spectral resolution, which make them useful for the community at large, extending beyond the scientific goals identified by the survey teams. In May 2019, as almost all first-generation imaging and spectroscopic surveys completed their observations and second-generation imaging surveys got well underway, the Public Survey Panel reviewed the scientific impact of these projects. The review was based on a quantitative assessment of the number of refereed publications from the survey teams and archive users. It included the number of citations, the number of data releases and statistics on access to archive data by the user community. The ESO Users Committee also discussed the availability and usage of ESO Public Survey data by the community during their yearly meeting in April 2019. We describe the status of these projects with respect to their observing plans, highlight the most recent data releases and provide links to the resulting science data products.

ESO Public Surveys: overview of engagement rules and status

By design, the ESO Public Surveys cover a variety of research areas, from the detection of planets via micro-lensing, through stellar variability and evolution, the Milky Way and Local Group galaxies, to extragalactic astronomy, galaxy evolution, the high-redshift Universe and cosmology. Differently from Large Programmes, these projects are planned to span more than four semesters and last for many years. For example, the latest call for the Cycle 2 survey projects for the Visible and Infrared Survey Telescope for Astronomy (VISTA) required them to span a time interval of more than three years. These survey projects all have a legacy value for the community at large in addition to the science goals identified by the proposing teams.

ESO science policies for Public Surveys

The selection of ESO Public Surveys is a two-step process which starts with the submission of letters of intent. On the basis of these letters, the Public Survey Panel (PSP) formulates a coherent, well-balanced scientific programme that takes into account any synergies among teams in the community and the international survey projects. The PSP then provides recommendations to ESO including a list of the teams that should be invited to submit full proposals on the basis of the ranking of the descriptions of their science projects as provided in the letters of intent. In so doing, the PSP fosters active collaborations within the community by asking independent teams to join, encouraging them to optimise science goals and observing strategies, and sharing resources.

Once the proposals have been recommended for approval by the PSP and the Observing Programmes Committee, data acquisition for each ESO Public Survey starts. This involves the review and assessment of each survey management plan by the ESO Survey Team. The survey management plan is an essential tool for the survey team, as well as for operations at ESO; it details the data acquisition plan, and the allocated resources for data processing and analysis, including the timeline for the delivery of science data products over the entire duration of the survey project. The approval of the survey management plan is further confirmed by the agreement signed between ESO's Director General (DG) and the Principal Investigator (PI) of each survey.

The agreement between the DG and the PI specifies the milestones for the data releases and their content and responsibility for the scientific quality and accuracy of the data products, which is to be warranted by the Public Survey team under the leadership of the PI. The agreement states that a final release which includes the reprocessing of the entire data set is expected upon completion of data acquisition for each survey. This final data release should take place within one year of completion of the data acquisition for any survey. The PSP was set up to periodically review the progress of the surveys and to assess compliance with the specification of the survey products. In May 2019, a PSP review took place to evaluate the scientific impact of the active Public Surveys.

Operations for ESO Public Surveys

The ESO Public Survey observations — whether in service mode or visitor mode — are carried out according to the process defined by the ESO Data Flow System. The raw data acquired for ESO Public Surveys are immediately public. Once the Public Survey teams have carried out data reduction to remove instrumental signatures, calibrate the data and complete the measurements defined by their scientific goals, ESO assists the survey teams to define and package their data products in a manner consistent with the ESO Science Archive and Virtual Observatory standards and in agreement with the specifications in the survey management plans. The goal is to integrate science data products from the Public Surveys into the ESO Archive, together with the entire archive content from the La Silla Paranal Observatory. This is done via the Phase 3 process, which is an audit process that certifies the integrity, consistency and data quality of the products available from the ESO Archive and ensures a homogeneous

user experience once the data are published through the Archive.

ESO Public Survey status

A total of twenty Public Surveys[1] have been carried out by consortia in the community and are actively supported by ESO. The majority have completed data acquisition using ESO facilities and are in the process of publishing science data products via the ESO archive.

ESO Public Surveys were launched in 2005 with an initial call for the optical imaging surveys at the VLT Survey Telescope (VST; Capaccioli & Schipani, 2011), followed by a call for the near-infrared surveys (Cycle 1) in 2007 (Arnaboldi et al., 2007) at VISTA (Sutherland et al., 2015). Once the imaging surveys were under way, ESO opened a first call for Public Spectroscopic Surveys in 2011, followed by a second call for the VIMOS Public Spectroscopic Surveys in 2015. The call for Cycle 2 VISTA imaging Public Surveys was opened in 2015 and the selected surveys began in April 2017 (Arnaboldi et al., 2017). Four of the seven Cycle 2 VISTA surveys exploit the time domain: for example, following up exotic transients like the optical-near-infrared echo of gravitational wave (GW) events (VinRouge); studying the 3D shape of the Milky Way bulge (VVVX) via astrometry — to test stellar evolution models and microlensing, and to obtain proper motion membership (VVVX, VISIONS); or detecting high-*z* supernovae (SN) in cosmological deep fields (VEILS). Two of the seven Cycle 2 surveys, VVVX and the Continuing UltraVISTA, follow up the successful Cycle 1 surveys, very much in the spirit of other surveys such as the Sloan Digital Sky Survey (SDSS).

In the optical, the VST Public Surveys completed their data acquisition in Period 104. The V-ATLAS survey was granted an extension by the PSP to acquire the *u'g'r'*-band imaging of chosen sub-areas. The data acquisition for this extension is ongoing and completion is expected in Period 105. In Figure 1 we show the cumulative curves of data acquisition for the VST surveys. The data acquisition for the Cycle 1 VISTA imaging surveys was completed between 2015 and 2018, except for the VHS South Pole fields. The data acquisition for the Cycle 2 VISTA imaging surveys is two-thirds complete. In Figure 2 we show the cumulative curves of data acquisition for all VISTA surveys. The data acquisition for the four spectroscopic surveys, including the two that were carried out with the VIMOS spectrograph, has also been completed.

In Tables 1 and 2 we provide a summary of the observational parameters for the twenty ESO Public Surveys and the total observing time — in hours for the imaging surveys and in nights for the spectroscopic surveys.

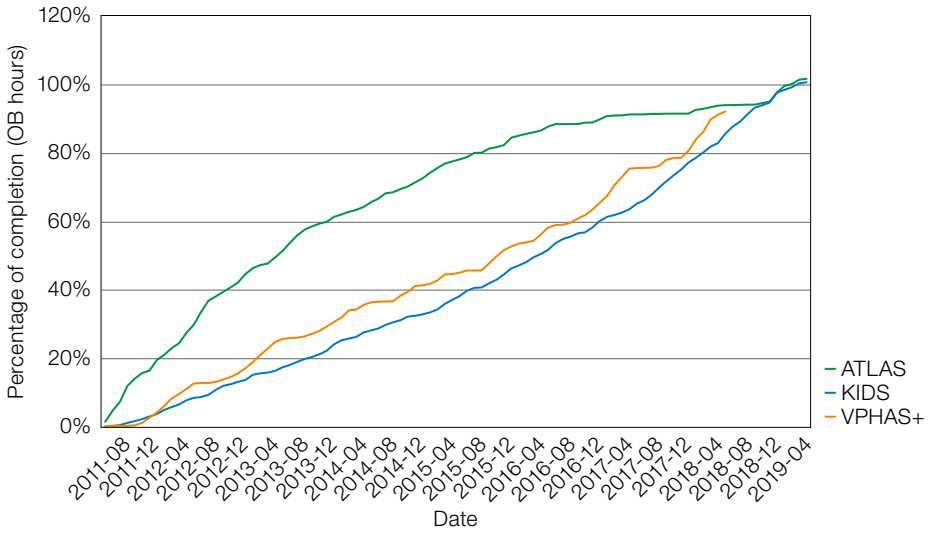

Figure 1. (Upper) Cumulative curves for the completion of the VST surveys. The VST ATLAS survey was extended after the completion of the observing plan to allow further coverage in the *u'g'r'*-bands (as outlined in its Survey Management Plan). The VPHAS+ curve is below 100% because the PI requested that it be terminated early.

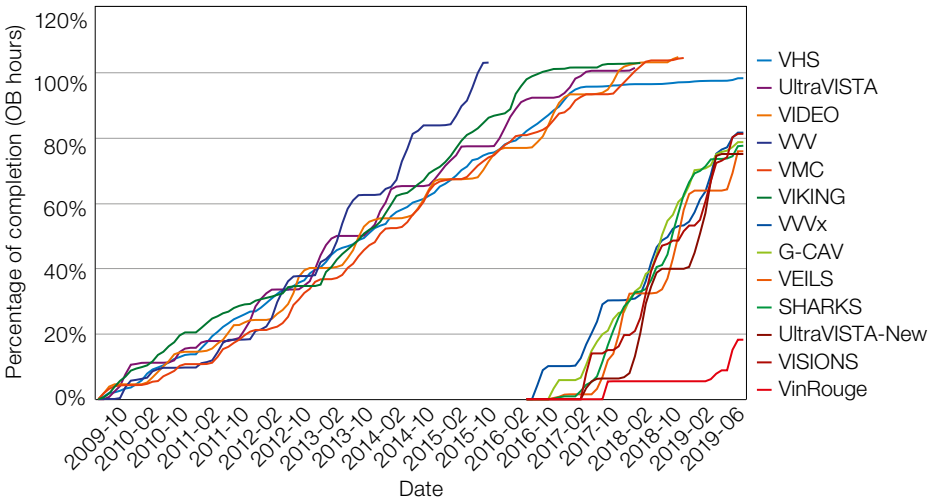

Figure 2. (Lower) Cumulative curves of completion for Cycle 1 and 2 VISTA Surveys. The cumulative curves of completion can reach values over 100% for Public Surveys that were compensated for time corresponding to low-quality observations (OBs with a D grade). Public Survey teams can ask for compensation via reports submitted to the OPC.

Scientific impact of ESO Public Surveys

A standard reference metric for the assessment of scientific impact is given by the number of refereed publications from the Public Survey teams. Given the legacy value of these projects and the science data products readily available for download via the ESO Archive, other

VST Survey ID	Science	Area (square degrees)	Filters	Magnitude limits	Total time (hours)
KiDS — Kilo-Degree Survey http://kids.strw.leidenuniv.nl/ (de Jong et al., 2013)	Extragalactic	1350[b]	*u' g' r' i'*	24.1 24.6 24.4 23.4	3421
ATLAS http://astro.dur.ac.uk/Cosmology/vstatlas/ (Shanks et al., 2013)	Wide area/baryon acoustic oscillations	4700[c]	*u' g' r' i' z*	22.0 22.2 22.2 21.3 20.5	1585
VPHAS+ — VST Photometric Hα Survey of the Southern Galactic Plane http://www.vphas.eu (Drew et al., 2013)	Stellar astrophysics	1800[d]	*u' g'* Hα *r' i'*	21.8 22.5 21.6 22.5 21.8	1200

VISTA Cycle 1	Science	Area (square degrees)	Filters	Magnitude limits	Total time (hours)
UltraVISTA http://home.strw.leidenuniv.nl/~ultravista/ (McCracken et al., 2013)	Deep high-*z*	1.7 Deep 0.73 Ultra deep	*Y J H Ks* NB118	25.7 25.5 25.1 24.5 26.7 26.6 26.1 25.6 26.0	1832
VHS — VISTA Hemisphere Survey http://www.ast.cam.ac.uk/~rgm/vhs/ (McMahon et al., 2013)	Southern sky	17 800	*Y J H Ks*	21.2 21.1 20.6 20.0	4623
VIDEO — VISTA Deep Extragalactic Observations Survey https://www.eso.org/sci/observing/PublicSurveys/sciencePublicSurveys.html (Jarvis et al., 2013)	Deep high-*z*	12	*Z Y J H Ks*	25.7 24.6 24.5 24.0 23.5	2073
VVV — VISTA Variables in the Via Lactea http://vvvsurvey.org/ (Hempel et al., 2014)	Milky Way	560	*Z Y J H Ks*	21.9 21.1 20.2 18.2 18.1	2205
VIKING — VISTA Kilo-Degree Infrared Galaxy Survey http://www.astro-wise.org/ (Edge et al., 2013)	Extragalactic	1500	*Z Y J H Ks*	23.1 22.3 22.1 21.5 21.2	2424
VMC — VISTA Magellanic Clouds Survey http://star.herts.ac.uk/~mcioni/vmc/ (Cioni et al., 2013)	Resolved star formation history	180	*Y J Ks*	21.9 21.4 20.3	2047

VISTA Cycle 2	Science	Area (square degrees)	Filters	Magnitude limits	Total time (hours)
VINROUGE* — Kilonova counterparts to gravitational wave sources http://www.star.le.ac.uk/nrt3/VINROUGE/ (Tanvir et al., 2017)	Kilonova counterparts to GW sources	300	*Y J Ks*	21.0 21.0 20.1	77
Cont. UltraVISTA — Completing the legacy of UltraVISTA http://home.strw.leidenuniv.nl/~ultravista/	High-*z*	0.75	*J H Ks*	26.0 25.7 25.3	567
VVVX* — Extending VVV to higher Galactic latitudes http://vvvsurvey.org/	Milky Way	1700	*J H Ks*	Ks = 17.5	1631
VEILS* — VISTA Extragalactic Infrared Legacy Survey http://www.ast.cam.ac.uk/~mbanerji/VEILS/veils_index.html	Galaxy evolution, AGN, SN	9	*J Ks*	*J* < 23.5 *Ks* < 22.5	847
G-CAV — Galaxy Clusters At VIRCAM http://www.oats.inaf.it/index.php/en/2014-09-12-12-59-22/tematiche-di-ricerca/macroarea-1-en/670-galaxy_cluster.html	Galaxy clusters	30	*Y J Ks*	24.5 24 23	440
VISIONS* — VISTA star formation atlas https://visions.univie.ac.at	Star formation atlas	550	*J H Ks*	21.5 20.5 19.5	449
SHARKS — Southern Herschel-Atlas Regions *Ks*-band survey https://www.iac.es/sharks/	Near-infrared counterparts for radio sources	300	*Ks*	22.7	929

Table 1. (Upper) VLT Survey Telescope Public Surveys. These projects began operations in October 2011 and data acquisition is now completed according to their survey management plans. The total number of completed hours is reported to the 30 September 2019 date.

Table 2. (Centre) Cycle 1 VISTA Public Surveys; these projects began operations in April 2010 and are now all completed but for the VHS subareas close to the South Galactic Pole. The total number of completed hours is reported to the 30 September 2019 date.

Table 3. (Lower) Cycle 2 VISTA Public Surveys began operations in April 2017. The four Cycle 2 VISTA surveys that explore the time domain are indicated by an asterisk in the table. The total number of completed hours by 30 September 2019 is shown in the last column.

Public Spectroscopic Survey ID and homepage	Science topic	Number of targets/spectra	Spectral resolution	Total time (nights)
Gaia–ESO http://www.gaia-eso.eu/ (Randich et al., 2013)	Milky Way, stellar populations	200 000	20 000	282.5
PESSTO — Public ESO Spectroscopic Survey of Transient Objects http://www.pessto.org/ (Smartt et al., 2013)	Transient, SN progenitors	150	~ 2500	384.0
VANDELS http://vandels.inaf.it (McLure et al., 2017)	Physics of galaxies in the early universe CANDELS, UDS & CDFS fields	2700	~ 1500	142.7
LEGA-C — Large Early Galaxy Astrophysics Census http://www.mpia.de/home/legac/index.html (van der Wel et al., 2016)	Dynamics of galaxies at z = 0.6–1.0	3100	~ 1500	99.8

Table 4. Public Spectroscopic Surveys. PESSTO and Gaia–ESO began operations in 2012 and were completed in 2017. The surveys using the VIsible Multi Object Spectrograph (VIMOS), called VANDELS and LEGA-C, began operations in 2015 and were completed in March 2018, before the decommissioning of the VIMOS spectrograph.

independent archives (for example, the VISTA science archive, Vizier) or the Public Survey webpages have also been made available to those in the community interested in accessing data products for their independent scientific explorations.

The ESO library routinely monitors refereed publications, based on data acquired from ESO approved observing programmes. This includes papers published by PIs/co-investigators (CoIs) as well as archive papers. Archive papers come in two flavours: *archive only* and *archive plus PI* publications. In *archive only* papers, none of the authors of these refereed publications are listed as PIs or CoIs of the approved Public Survey proposals. In the case of *archive plus PI* publications, science data products from the ESO Public Surveys are used together with data owned by a PI or CoI of an ESO programme to achieve their scientific published results. In the case of ESO Public Surveys, the total number of refereed publications by teams and archive users was 848 by 30 September 2019. Of these refereed publications, 172 (20.3%) are *archive only* and 84 (10%) are *archive plus PI* since 2010 (from ESO telbib[2]). The total number of citations from ESO Public Survey refereed publications is 26 266. In Figure 3 we provide the histogram of the cumulative number of refereed publications and citations per survey project.

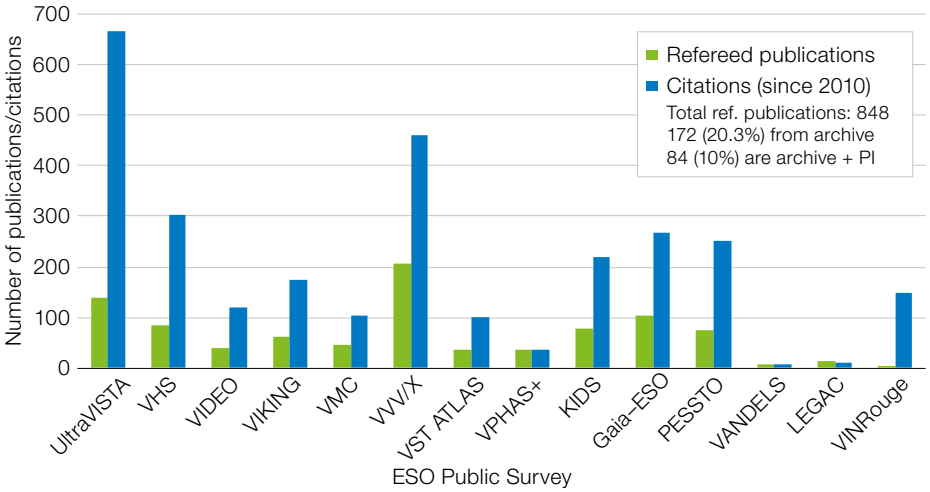

Figure 3. Histogram of the cumulative number of refereed publications and citations (divided by 10) for each ESO Public Survey.

Published data releases

Because of the extensive amount of time allocated using ESO facilities, the science policies for ESO Public Surveys entail the submission and publication of the science data products from these projects into the ESO Archive. The publication process for science data products extends well after the completion of the data acquisition. This additional time is used by the Public Survey teams to execute global calibrations of the entire data volume and to carry out the relevant measurements required to achieve their scientific goals. The ultimate publication of the results of these steps is contained in the final catalogue release. All twenty ESO Public Surveys are currently involved in the publication of their science data products via the ESO Archive.

The Public Survey teams adopted a range of strategies to deal with the data volumes from their respective surveys. Some rely on the support of data centres while others have developed their own specific infrastructures. Five out of six Cycle 1 VISTA surveys and two out of three VST surveys received extensive support from the dedicated data centres, CASU[3] and WFAU[4]. The deep UltraVISTA and Continuing UltraVISTA surveys relied on dedicated support from CASU, TERAPIX[5] and CALET[6] centre at the IAP in Paris, while the KIDS survey is supported by Astro-WISE[7]. The Cycle 2 VISTA surveys have adopted different strategies compared to the first generation, with a larger number receiving tailored support to their data processing from their respective science institutes.

For the Public Spectroscopic Surveys, Gaia-ESO, PESSTO, LEGA-C and VANDELS, the teams built their data reduction infrastructure based on previous experience they had acquired through managing large programmes at ESO and

scientific networks (for example, PESSTO–WISeREP).

All survey teams have successfully published several data releases for some of their science data through the Phase 3 process (Arnaboldi et al., 2014); an overview of these releases is available via this webpage[8]. Since January 2019, the total volume of science data products released from the ESO Public Surveys amounts to 27.4 Tb, including ancillary files. The data releases published this year include: the fourth data release of KIDS (> 1000 square degrees) and UltraVISTA (deep stacked images of the COSMOS field from observations acquired between December 2009 and June 2016); the proper motion of selected stars in the Milky Way disc and bulge from the VVV near-infrared Astrometric Catalogue (VIRAC); accurate PSF-fitting photometry of the 300 square degrees around the Galactic centre; and the fifth data release of VMC with full coverage of the Small Magellanic Cloud. All data releases were promptly advertised via the Archive/Phase 3 web pages, followed up with specific announcements on the ESO science page, the Science Newsletter[9] and the ESO archive community forum[10].

The most recent data releases join a large number of data collections from the ESO Public Surveys that can be browsed using the Archive Science Portal[11]. The science data products from the ESO Public Surveys amount to a total volume of 68.6 Tb (nearly 8.5×10^5 files) which are currently accessible via the ESO Archive. The science data products that can be actively queried and downloaded amount to nearly 320 000 catalogue files, half a million astrometrically and photometrically calibrated images, and 56 000 1D extracted spectra. In Figure 4 we show a collection of on-sky footprints of the data releases published during the last year by the ESO Public Survey teams.

Data download statistics

In Figure 5 we show the cumulative curves of the data volume (Gb) and the number of files downloaded by the community for each ESO Public Survey. The lower chart shows the numbers of catalogues, the numbers of distinct users and the numbers of queries carried out using the ESO catalogue query interface[12] to access ESO Public Survey catalogues. On average, users of the ESO catalogue query interface carry out at least 21 independent queries to access catalogue records.

An enhanced archive capability allowing programmatic access[13] results in anonymous exploration and retrieval of catalogue records (and other products) via Virtual Observatory tools, for example, Aladin and Topcat. This new service allows users to repeat queries in an automated fashion, in order to perform more complex queries by combining data from different surveys or other content of the ESO Science Archive, thereby enhancing the scientific use of the catalogue content of the ESO Archive. One interesting statistic is the number of distinct users — 1583 users from 77 different countries — who have downloaded ESO Public Survey science products published via the ESO Archive. To place this in context, the fraction of distinct users who access

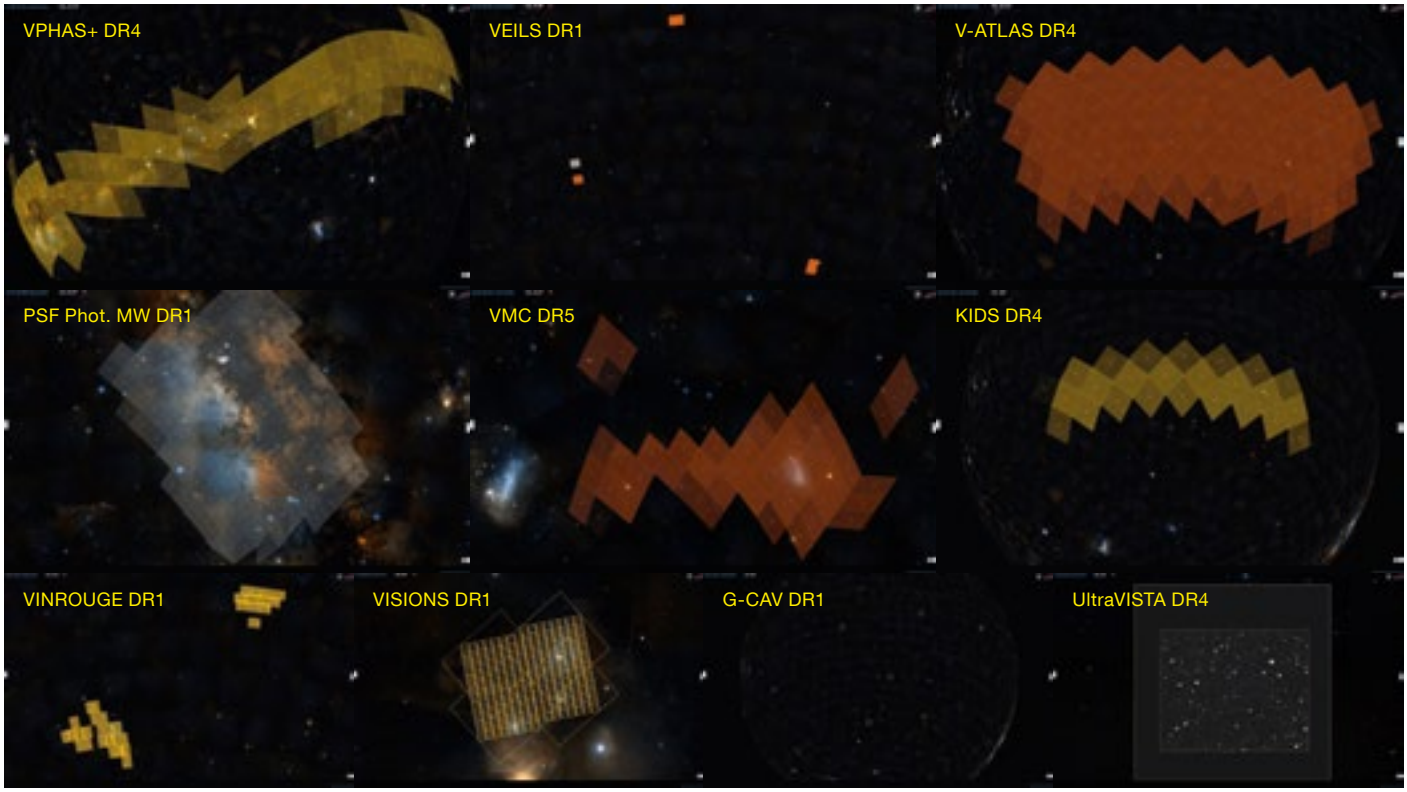

Figure 4. Montage of the footprints of the data releases from the ESO Public Surveys published by 2019, as shown on the ESO Archive Science Portal interactive interface.

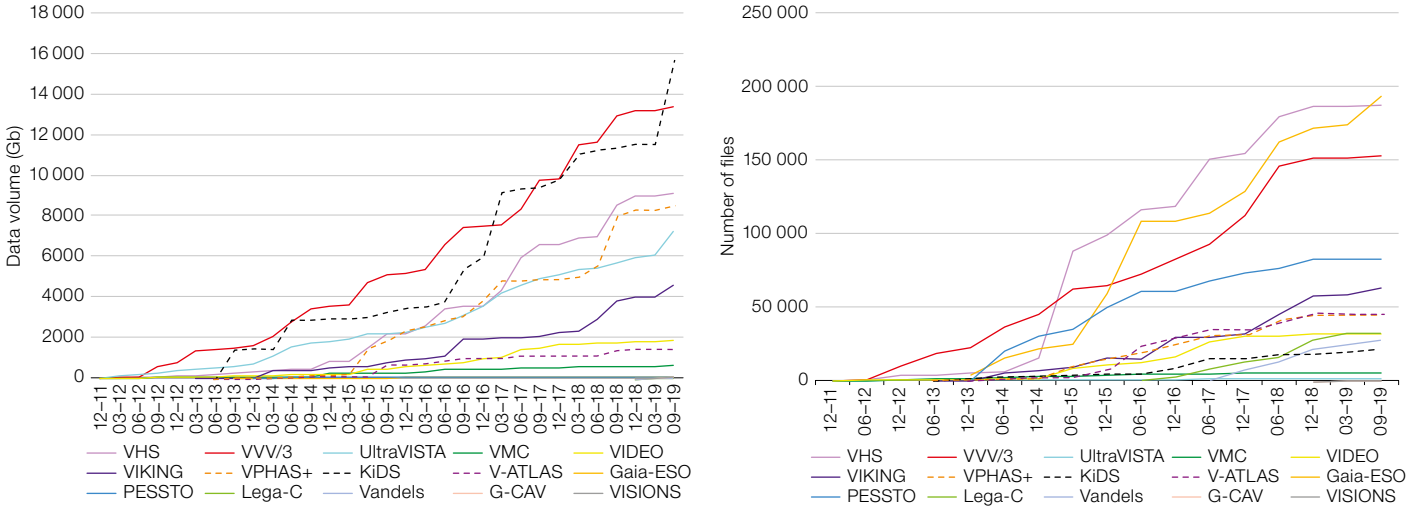

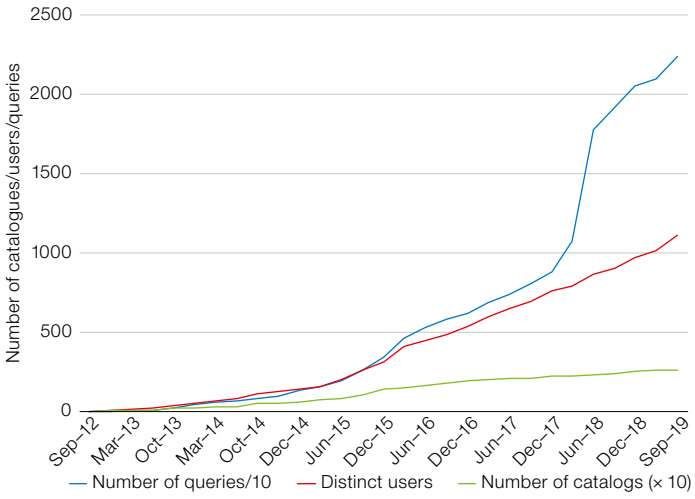

Figure 5. Charts showing the cumulative data volume (upper left) and numbers of files downloaded (upper right) for each ESO Public Survey. The lower chart shows the cumulative curves for the number of catalogues (× 10), the number of distinct users, and number of queries (× 0.1) related to the ESO Public Surveys downloaded using the ESO catalogue query interface.

data products from ESO Public Surveys is 46% of the total number of users (3457) who have downloaded science data products from the ESO Archive.

How ESO promotes Public Survey science

ESO promotes science results from Public Surveys via science/photo press releases and community workshops. The most recent photo release of the new image of the Large Magellanic Cloud[14] celebrated the 500th anniversary of its first being seen by Europeans (during the voyage of the explorer Ferdinand Magellan). Among the science press releases, we particularly note those on the 3D structure of the bulge of the Milky Way[15], the constraints on the clumpiness of the dark matter distribution in the Universe[16], and the first light from a gravitational wave source[17].

Three community workshops were organised by ESO in 2012, 2015 and 2019 to support survey science and operations at ESO. The most recent was the 4MOST community workshop (see also The Messenger 175[18], and Liske & Mainieri, 2019). A workshop focused on the next-generation galaxy evolution surveys is currently being organised in Perth, Australia in February 2020. This second Australia-ESO conference will discuss the future coordination of these surveys with multi-wavelength facilities in the southern hemisphere.

Community awareness of ESO Public Surveys: feedback from the User Community poll

In April 2019 the ESO Public Surveys were identified as the special topic for the User Community (UC) poll. The results of this UC poll showed that more than 60% of the ESO users who responded were aware of the ESO Public Surveys. About 25% of UC poll participants (excluding all Survey PIs/CoIs) had used archive data from Public Surveys to complement other datasets. This was the most frequent usage of these data products according to the results of the poll.

The science data products from ESO Public Surveys were retrieved from the ESO Archive in the vast majority of cases. The UC poll participants who had used science data products from Public Surveys for their own science reported that they had published between one and three peer-reviewed papers based on these data. Finally, most users who had participated in the surveys or used Public Survey data provided a positive assessment of their utility, scheduling, rate of progress/publication, and the effectiveness of communication with ESO. Regarding the services provided by ESO, i.e., archive interfaces and Phase 3, the vast majority of the users were “satisfied” or “very satisfied”, with the ESO Archive being the preferred site for data retrieval. The release description published together with an active release was considered

the most reliable/useful documentation to support the scientific use of the available data products.

The Public Survey Panel review

Membership and evolution of the Public Survey Panel

In 2005, the Public Survey Panel (PSP) was set up as a subpanel to the Observing Programmes Committee, its role being later extended to include monitoring of the progress of the Public Survey projects. Four chairs organised the work of the panel: Duccio Macchetto, Simon White, Danny Lennon, and Miguel Mas Hesse (the current chair). From 2005 to 2012, ESO set up three separate panels: the VISTA, VST imaging, and Spectroscopic Public Survey Panels; the VISTA and VST Panels were later merged. Since 2018 there has been only one panel for all ESO Public Surveys, whether imaging or spectroscopy. In the near future, the PSP will advise ESO on the selection of 4MOST surveys (see de Jong et al., 2019).

The PSP review in May 2019

As most of the Public Surveys completed their data acquisition in 2019, the goal and objectives of the PSP review held in May at the ESO headquarters were to assess the scientific success of the Public Surveys using criteria that included published results in refereed journals, the progress of the analysis, potential scientific extensions, complementarity with other telescopes, activities to promote the surveys, and the use of survey data products for independent projects in the community. The PIs of the twenty active Public Surveys were invited to the review and asked to address the above criteria during their presentations. All PIs but one attended the review and contributed to a lively and constructive discussion. The PSP report was presented to the Scientific Technical Committee at its meeting in October 2019.

Outlook and Conclusions

While work on the scientific analysis continues for the twenty Public Surveys, ESO announced 2019 a call for letters of intent for 4MOST Community Surveys on 26 November 2019. The community surveys will access up to 30% of the available time on the 4MOST spectrograph on VISTA over a period of five years. These projects will complement the GTO surveys that were presented during the 4MOST workshop at ESO in May and are described in the special issue of the Messenger in March 2019[7].

Large surveys are considered a key tool in observational astronomy because they allow explorations that go beyond individual targeted observations. They are characterised by large investments that comprise dedicated telescopes and instruments, a wide community of astronomers involved in the science projects and extended networks for the data distribution and analysis. The scientific success of such survey projects includes the legacy value of science products that are made available through the archives for further scientific exploration by the community. ESO Public Surveys are an example of an effective implementation of this strategy, with the goal of supporting the scientific advancement of its community.

Acknowledgements

The authors would like to thank colleagues at the La Silla Paranal Observatory for their work, and support by the science operations of the ESO Public Surveys. They wish to acknowledge the colleagues from the ESO Directorate of Engineering who supported the development of the tools required for carrying out Phase 1, Phase 2 and Phase 3 operations for ESO Public Surveys and the Archive science interfaces. The authors thank the ESO library team for their careful monitoring of the refereed publications. The authors wish to thank the PIs of the Public Surveys and their collaborators, including the data centres at CASU[3], WFAU[4], Astro-WISE[14] (Astronomical Wide-field Imaging System for Europe) and TERAPIX[5], for their hard work and support of the ESO mission. Finally, ESO wish to thank the PSP chairs and the colleagues in the community who served as members in the different PSPs for their efforts and their support with the definition of how to execute the survey programmes.

References

Arnaboldi, M. et al. 2007, The Messenger, 127, 28
Arnaboldi, M. et al. 2014, The Messenger, 156, 24
Arnaboldi, M. et al. 2017, The Messenger, 168, 15
Capaccioli, M. & Schipani, P. 2011, The Messenger, 146, 2
Cioni, M.-R. et al. 2013, The Messenger, 154, 23
de Jong, R. 2019, The Messenger, 175, 3
de Jong, R. et al. 2013, The Messenger, 154, 44
Drew, J. E. et al. 2013, The Messenger, 154, 41
Edge, A. et al. 2013, The Messenger, 154, 32
Hempel, M. et al. 2014, The Messenger, 155, 29
Jarvis, M. J. et al. 2013, The Messenger, 154, 26
Liske, J. & Mainieri, V. 2019, The Messenger, 177, 61
McCracken, H. J. et al. 2013, The Messenger, 154, 29
McLure, R. et al. 2017, The Messenger, 167, 31
McMahon, R. et al. 2013, The Messenger, 154, 35
Randich, S. et al. 2013, The Messenger, 154, 47
Shanks, T. et al. 2013, The Messenger, 154, 38
Smartt, S. et al. 2013, The Messenger, 154, 50
Sutherland, W. et al. 2015, A&A, 575, 27
Tanvir, N. et al. 2017, ApJ, 848, 27
van der Wel, A. et al. 2016, The Messenger, 164, 36

Links

1 ESO Public Surveys Project webpage: http://www.eso.org/sci/observing/PublicSurveys/sciencePublicSurveys.html
2 ESO Telescope Bibliography telbib: http://telbib.eso.org
3 The Cambridge Astronomy Survey Unit: http://casu.ast.cam.ac.uk/
4 The Wide Field Astronomy Unit: http://www.roe.ac.uk/ifa/wfau/
5 TERAPIX: http://terapix.iap.fr/
6 CALET: https://calet.org/
7 Astro-WISE: http://www.astro-wise.org/
8 ESO Phase 3 Data Releases: http://eso.org/rm/publicAccess#/dataReleases
9 ESO Science Newsletter: http://www.eso.org/sci/publications/newsletter/
10 ESO Archive Community Forum: https://esocommunity.userecho.com/
11 ESO Archive Science Portal: https://archive.eso.org/scienceportal/
12 ESO catalogue query interface: https://www.eso.org/qi/
13 ESO Archive Programmatic Access webpage: http://archive.eso.org/programmatic/
14 VISTA image of LMC: https://www.eso.org/public/news/eso1914/
15 VISTA image of Milky Way bulge: https://www.eso.org/public/news/eso1339/
16 VISTA image from KIDS survey: https://www.eso.org/public/news/eso1642/
17 First Light from Gravitational Wave Source: https://www.eso.org/public/news/eso1733/
18 Messenger issue dedicated to 4MOST GTO surveys: https://www.eso.org/sci/publications/messenger/archive/no.175-mar19/messenger-no175.pdf

Notes

[a] Astrofit2 Marie Skłodowska-Curie Fellow
[b] The survey area was reduced from the original approved coverage to coincide with the VIKING footprint.
[c] The survey area was increased to 4700 square degrees after approval by the PSP; data-taking is currently active.
[d] The survey area was reduced from that approved by the PSP following a request by the PI to end the survey early.

DOI: 10.18727/0722-6691/5165

MUSE Spectral Library

Valentin D. Ivanov [1]
Lodovico Coccato [1]
Mark J. Neeser [1]
Fernando Selman [1]
Alessandro Pizzella [2,3]
Elena Dalla Bontà [2,3]
Enrico M. Corsini [2,3]
Lorenzo Morelli [4]

[1] ESO
[2] Dipartimento di Fisica e Astronomia "G. Galilei", Università di Padova, Italy
[3] INAF–Osservatorio Astronomico di Padova, Italy
[4] Instituto de Astronomía y Ciencias Planetarias, Universidad de Atacama, Copiapó, Chile

Empirical stellar spectral libraries have applications in both extragalactic and stellar studies. We have assembled the MUSE Spectral Library (MSL), consisting of 35 high-quality spectra of stars covering the Hertzsprung–Russell diagram, and verified the continuum shape of our spectra with synthetic broadband colours. We also report indices from the Lick system, derived from the new observations. Our data demonstrate that integral field units (IFUs) are excellent tools for building spectral libraries with reliable continuum shapes that can be used as templates for extragalactic studies.

Introduction and sample

Empirical stellar spectral libraries are a universal tool in modern astronomy, with applications in both extragalactic and galactic stellar studies. They can have multiple uses: to match and remove continua to reveal weak emission lines; as templates to measure stellar kinematics in galaxies; and to measure stellar parameters such as effective temperatures and surface gravities. Theoretical stellar models can have significant weaknesses; for example, Sansom et al. (2013) found discrepancies in Balmer lines and the incomplete treatment of molecules (also shown by Castelli, Gratton & Kurucz, 1997). This occasionally leads to poorly predicted broad-band colours. At the same time, the typical empirical libraries suffer from low resolution and/or sparse coverage of the parameter space (Pickles, 1998; Le Borgne et al., 2003; Yan et al., 2018).

Spectral datasets that are available include the Elodie library (Soubiran et al., 1998; Prugniel & Soubiran, 2001; Le Borgne et al., 2004) and the X-shooter Spectral Library (XSL; Chen et al., 2014). The latter showcases the problems that increasing resolution and multi-order cross-dispersed spectrographs bring; synthetic broadband optical (UBV) colours show poor agreement with observed colours from the Bright Star Catalogue (on average at ~ 7%; see Table 5 and Figure 26 in Chen et al., 2014). The differences are likely related to pulsating variable stars observed at different phases. Slit losses are another issue; for many stars these are caused by the attenuation of flux, or other losses inherent to slit-based spectrographs.

We embarked on a project to build an empirical spectral library without slit losses using the MUSE (Multi-Unit Spectroscopic Explorer; Bacon et al., 2010) IFU, with the goal of spanning all of the major sequences on the Hertzsprung–Russell diagram and serving as a benchmark for the shapes of other theoretical and empirical spectra. Our final products are spectra suitable for galactic modelling, stellar classification and other applications. Here we report on our first sample of 35 MSL spectra.

Our initial sample numbered 33 XSL stars[1]. In addition, HD 193256 and HD 193281B serendipitously fell inside the MUSE field of view. The full sample is described in Table 1 of Ivanov et al. (2019).

Observations and data reduction

The spectra were obtained with MUSE at the European Southern Observatory (ESO) Very Large Telescope, Unit Telescope 4 (Yepun), on Cerro Paranal, Chile. Table A.1 in Ivanov et al. (2019) gives the observing log. We obtained six exposures for each target, except for HD 204155 which was observed 12 times. We placed the science targets at the same spaxels as the spectrophotometric standards to minimise any residual systematics from the instrument.

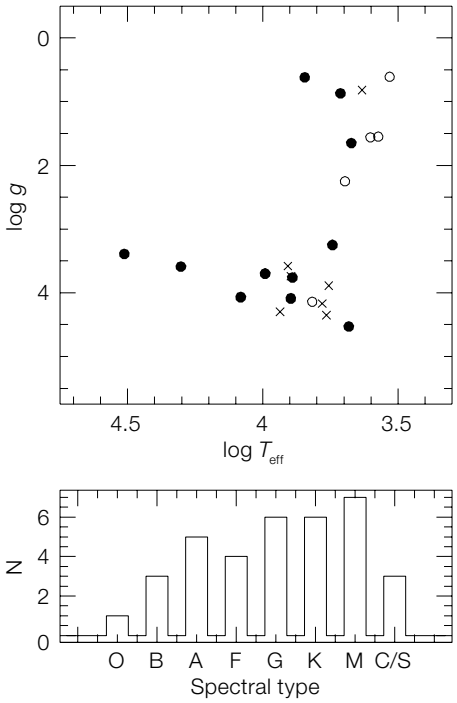

Figure 1. Properties of the MSL stars. Top: surface gravity log g vs. effective temperature T_{eff} for stars with [Fe/H] ≤ –0.5 dex (crosses), –0.5 < [Fe/H] < 0.0 dex (open circles), and [Fe/H] ≥ 0.0 dex (filled circles). Bottom: distribution of the stars by spectral type.

Data reduction was performed with the ESO MUSE pipeline (v. 2.6) within the ESOReflex 3 environment (Freudling et al., 2013). The 1D spectra were extracted using a circular aperture with a radius of 6 arcseconds. This number was selected after experiments with different aperture sizes, to guarantee that "aperture" losses led to less than a 1% change in the overall slope of the spectra from the blue to the red.

Three stars were treated differently, without major loss of continuum fidelity. For the asymptotic giant branch star [B86] 133 we reduced the extraction aperture radius to 4 arcseconds to avoid contamination from nearby sources. For HD 193256 the aperture had a radius of 4.6 arcseconds, and the sky annulus had an inner radius of 4.6 arcseconds and a width of 2 arcseconds because the star was close to the edge of the MUSE field of view. HD 193281 is a binary with a separation of ~ 3.8 arcseconds. We disentangled the two spectra as described in Ivanov et al. (2019).

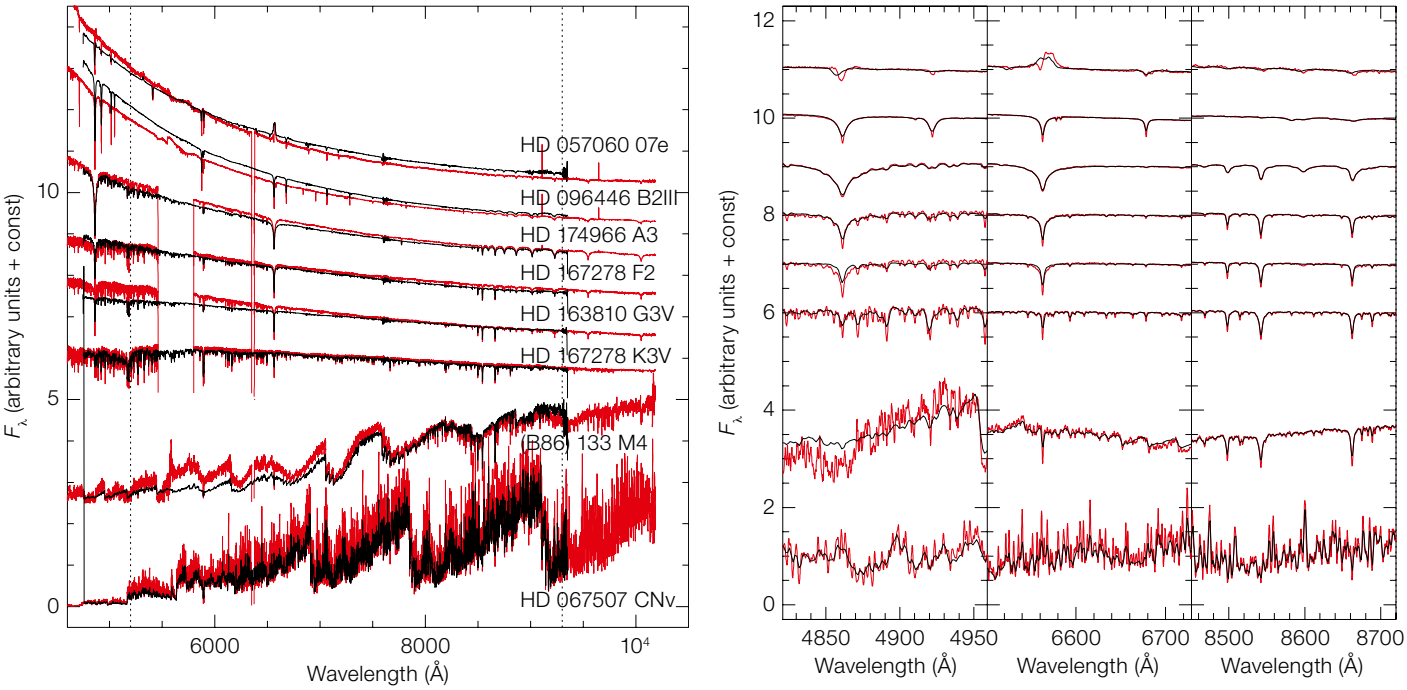

Figure 2. Comparison of a subset of our MSL spectra (black) with the XSL spectra (red; boxcar smoothed over 8 pixels). The spectra are normalised to unity between the two vertical dotted lines shown on the left, and shifted vertically for display purposes. Left: entire MUSE spectral range; right: zoom around the Hβ, Hα, and Ca triplet features (left to right). No radial velocity correction is applied.

The final MSL spectra have signal-to-noise ratios S/N > 70–200 and are available via the ESO MUSE webpage[2] or via CDS/VizieR[3]. The Lick indices (Worthey et al., 1994) that fall within the wavelength range covered by MUSE were measured in the new MSL spectra (Table C.1 in Ivanov et al., 2019).

Analysis and discussion

We demonstrate excellent agreement between the 6 (or 12 in the case of HD 204155) individual observations (Figures 2 and A.1 in Ivanov et al., 2019). A direct comparison of the MSL and XSL spectra for eight randomly selected stars across the spectral type sequence is shown in select wavelength ranges in Figure 2. In most cases, the agreement on a scale of a few hundred pixels — in other words, within the same X-shooter spectral order — is excellent. However, on a larger scale we find deviations between the XSL and MSL spectra. We fitted second-order polynomials to the ratios and extrapolated them over the full wavelength range covered by the XSL library to demonstrate that, if these trends hold, the overall peak-to-peak flux differences can easily reach ~ 20%, meaning that the overall continua of the cross-dispersed spectra is somewhat ill-defined.

Finally, we calculated synthetic Sloan Digital Sky Survey (SDSS) colours from both MSL and XSL spectra (Figure 5 in Ivanov et al., 2019). The MUSE sequences are slightly tighter than the XSL ones, confirming that the IFU MUSE spectra have more reliable shapes. This is expected in light of the slit losses and the imperfect order stitching of the XSL spectra. Furthermore, X-shooter has three arms and is in effect three different instruments; some of the colours can mix fluxes from the different arms, which may contribute to the larger scatter.

Acknowledgements

This paper is based on observations made with the ESO VLT at the La Silla Paranal Observatory (Programme ID 099.D-0623). We have made extensive use of SIMBAD at the Centre de Données astronomiques Strasbourg (CDS) and of the VizieR tool and CDS, Strasbourg, France. Enrico M. Corsini, Elena Dalla Bontà, Lorenzo Morelli, and Alessandro Pizzella acknowledge financial support from Padua University through grants DOR1715817/17, DOR1885254/18, DOR1935272/19, and BIRD164402/16.

References

Bacon, R. et al. 2010, Proc. SPIE, 7735, 773508
Castelli, F., Gratton, R. G. & Kurucz, R. L. 1997, A&A, 318, 841
Chen, Y.-P. et al. 2014, A&A, 565, A117
Freudling, W. et al. 2013, A&A, 559, A96
Ivanov, V. D. et al. 2019, A&A, 629, 100
Le Borgne, J.-F. et al. 2003, A&A, 402, 433
Le Borgne, D. et al. 2004, A&A, 425, 881
Pickles, A. J. 1998, PASP, 110, 863
Prugniel, P. & Soubiran, C. 2001, A&A, 369, 1048
Sansom, A. E. et al. 2013, MNRAS, 435, 952
Soubiran, C. et al. 1998, A&AS, 133, 221
Yan, R. et al. 2019, ApJ, 883, 175
Worthey, G. et al. 1994, ApJS, 94, 687

Links

[1] The XSL library: http://xsl.u-strasbg.fr/
[2] The MUSE spectral library at the ESO MUSE webpage: https://www.eso.org/sci/facilities/paranal/sciops/tools/MUSE_Spectral_Library.html
[3] The MUSE spectral library at VizieR/CDS: http://cdsarc.u-strasbg.fr/viz-bin/cat/J/A+A/629/A100

Enrico Sacchetti/ESO

The VLTI delay lines at Paranal lie inside a 168-metre tunnel, forming an essential part of a complicated optical system that feeds interferometric instruments such as GRAVITY.

DOI: 10.18727/0722-6691/5166

Spatially Resolving the Quasar Broad Emission Line Region

GRAVITY Collaboration

Roberto Abuter[8]
Matteo Accardo[8]
Tobias Adler[3]
António Amorim[6]
Narsireddy Anugu[7,29,30]
Gerardo Ávila[8]
Michi Bauböck[1]
Myriam Benisty[5,12]
Jean-Philippe Berger[5]
Joachim M. Bestenlehner[22,3]
Hervé Beust[5]
Nicolas Blind[9]
Mickaël Bonnefoy[5]
Henri Bonnet[8]
Pierre Bourget[8]
Jérôme Bouvier[5]
Wolfgang Brandner[3]
Roland Brast[8]
Alexander Buron[1]
Leonard Burtscher[14]
Faustine Cantalloube[3]
Alessio Caratti o Garatti[16,3]
Paola Caselli[1]
Frédéric Cassaing[10]
Frédéric Chapron[2]
Benjamin Charnay[2]
Élodie Choquet[37]
Yann Clénet[2]
Claude Collin[2]
Vincent Coudé du Foresto[2]
Ric Davies[1]
Casey Deen[1]
Françoise Delplancke-Ströbele[8]
Roderick Dembet[8]
Frédéric Derie[8]
Willem-Jan de Wit[8]
Jason Dexter[1]
Tim de Zeeuw[1,14]
Catherine Dougados[5]
Guillaume Dubus[5]
Gilles Duvert[5]
Monica Ebert[3]
Andreas Eckart[4,13]
Frank Eisenhauer[1]
Michael Esselborn[8]
Fabio Eupen[4]
Pierre Fédou[2]
Miguel C. Ferreira[6]
Gert Finger[8]
Natascha M. Förster Schreiber[1]
Feng Gao[1]
César Enrique García Dabó[8]
Rebeca Garcia Lopez[16,3]
Paulo J. V. Garcia[7]
Éric Gendron[2]
Reinhard Genzel[1,15]
Ortwin Gerhard[1]
Juan Pablo Gil[8]
Stefan Gillessen[1]
Frédéric Gonté[8]
Paulo Gordo[6]
Damien Gratadour[2]
Alexandra Greenbaum[40]
Rebekka Grellmann[4]
Ulrich Grözinger[3]
Patricia Guajardo[8]
Sylvain Guieu[5]
Maryam Habibi[1]
Pierre Haguenauer[8]
Oliver Hans[1]
Xavier Haubois[8]
Marcus Haug[8]
Frank Haußmann[1]
Thomas Henning[3]
Stefan Hippler[3]
Sebastian F. Hönig[27]
Matthew Horrobin[4]
Armin Huber[3]
Zoltan Hubert[5]
Norbert Hubin[8]
Christian A. Hummel[8]
Gerd Jakob[8]
Annemieke Janssen[36]
Alejandra Jimenez Rosales[1]
Lieselotte Jochum[8]
Laurent Jocou[5]
Jens Kammerer[8,41]
Martina Karl[20,21]
Andreas Kaufer[8]
Stefan Kellner[1]
Sarah Kendrew[11,3]
Lothar Kern[8]
Pierre Kervella[2]
Mario Kiekebusch[8]
Makoto Kishimoto[31]
Lucia Klarmann[3]
Ralf Klein[3]
Rainer Köhler[3]
Yitping Kok[1]
Johann Kolb[8]
Maria Koutoulaki[16,19,3,8]
Martin Kulas[3]
Lucas Labadie[4]
Sylvestre Lacour[2,8]
Anne-Marie Lagrange[5]
Vincent Lapeyrère[2]
Werner Laun[3]
Bernard Lazareff[5]
Jean-Baptiste Le Bouquin[5]
Pierre Léna[2]
Rainer Lenzen[3]
Samuel Lévêque[8]
Chien-Cheng Lin[3,18]
Magdalena Lippa[1]
Dieter Lutz[1]
Yves Magnard[5]
Anne-Lise Maire[23,3]
Leander Mehrgan[8]
Antoine Mérand[8]
Florentin Millour[37]
Paul Mollière[3]
Thibaut Moulin[5]
André Müller[3]
Eric Müller[8,3]
Friedrich Müller[3]
Hagai Netzer[32]
Udo Neumann[3]
Mathias Nowak[2]
Sylvain Oberti[8]
Thomas Ott[1]
Laurent Pallanca[8]
Johana Panduro[3]
Luca Pasquini[8]
Thibaut Paumard[2]
Isabelle Percheron[8]
Karine Perraut[5]
Guy Perrin[2]
Bradley M. Peterson[24,25,26]
Pierre-Olivier Petrucci[5]
Andreas Pflüger[1]
Oliver Pfuhl[8]
Than Phan Duc[8]
Jaime E. Pineda[1]
Philipp M. Plewa[1]
Dan Popovic[8]
Jörg-Uwe Pott[3]
Almudena Prieto[39]
Laurent Pueyo[11]
Sebastian Rabien[1]
Andrés Ramírez[8]
José Ricardo Ramos[3]
Christian Rau[1]
Tom Ray[16]
Miguel Riquelme[8]
Gustavo Rodríguez-Coira[2]
Ralf-Rainer Rohloff[3]
Daniel Rouan[2]
Gérard Rousset[2]
Joel Sanchez-Bermudez[3,17]
Marc Schartmann[1,33,34]
Silvia Scheithauer[3]
Markus Schöller[8]
Nicolas Schuhler[8]
Dominique Segura-Cox[1]
Jinyi Shangguan[1]
Thomas T. Shimizu[1]
Jason Spyromilio[8]
Amiel Sternberg[1,32]
Matthias Raphael Stock[21]
Odele Straub[1,2]
Christian Straubmeier[4]
Eckhard Sturm[1]
Marcos Suárez Valles[8]
Linda J. Tacconi[1]
Wing-Fai Thi[1]

Konrad R. W. Tristram[8]
Javier J. Valenzuela[8]
Roy van Boekel[3]
Ewine F. van Dishoeck[14]
Pierre Vermot[2]
Frédéric Vincent[2]
Sebastiano von Fellenberg[1]
Idel Waisberg[1]
Jason J. Wang[28]
Imke Wank[4]
Johannes Weber[1]
Gerd Weigelt[13]
Felix Widmann[1]
Ekkehard Wieprecht[1]
Michael Wiest[4]
Erich Wiezorrek[1]
Markus Wittkowski[8]
Julien Woillez[8]
Burkhard Wolff[8]
Pengqian Yang[3,35]
Senol Yazici[1,4]
Denis Ziegler[2]
Gérard Zins[8]

[1] Max Planck Institute for Extraterrestrial Physics, Garching, Germany
[2] LESIA, Observatoire de Paris, Université PSL, CNRS, Sorbonne Université, Université de Paris, Meudon, France
[3] Max-Planck-Institut für Astronomie, Heidelberg, Germany
[4] I Physikalisches Institut, Universität zu Köln, Germany
[5] Univ. Grenoble Alpes, CNRS, IPAG, Grenoble, France
[6] CENTRA and Universidade de Lisboa – Faculdade de Ciências, Lisboa, Portugal
[7] CENTRA and Universidade do Porto – Faculdade de Engenharia, Porto, Portugal
[8] ESO
[9] Observatoire de Genève, Université de Genève, Versoix, Switzerland
[10] DOTA, ONERA, Université Paris-Saclay, Châtillon, France
[11] European Space Agency, Space Telescope Science Institute, Baltimore, USA
[12] Unidad Mixta Internacional Franco-Chilena de Astronomía (CNRS UMI 3386), Departamento de Astronomía, Universidad de Chile, Las Condes, Santiago, Chile
[13] Max Planck Institute for Radio Astronomy, Bonn, Germany
[14] Sterrewacht Leiden, Leiden University, Leiden, the Netherlands
[15] Department of Physics, Le Conte Hall, University of California, Berkeley, USA
[16] Dublin Institute for Advanced Studies, Dublin, Ireland
[17] Instituto de Astronomía, Universidad Nacional Autónoma de México, Ciudad de México, Mexico
[18] Institute for Astronomy, University of Hawai'i, Honolulu, USA
[19] School of Physics, University College Dublin, Ireland
[20] Max Planck Institute for Physics, Munich, Germany
[21] TUM Department of Physics, Technical University of Munich, Garching, Germany
[22] Department of Physics and Astronomy, University of Sheffield, UK
[23] STAR Institute, Liège, Belgium
[24] Department of Astronomy, The Ohio State University, Columbus, USA
[25] Center for Cosmology and AstroParticle Physics, The Ohio State University, Columbus, USA
[26] Space Telescope Science Institute, Baltimore, USA
[27] School of Physics & Astronomy, University of Southampton, UK
[28] Department of Astronomy, California Institute of Technology, Pasadena, USA
[29] Steward Observatory, Department of Astronomy, University of Arizona, Tucson, USA
[30] University of Exeter, School of Physics and Astronomy, Exeter, UK
[31] Kyoto Sangyo University, Department of Astrophysics and Atmospheric Sciences, Japan
[32] School of Physics and Astronomy, Tel Aviv University, Israel
[33] Excellence Cluster Origins, Ludwig-Maximilians-Universität München, Garching, Germany
[34] Universitäts-Sternwarte München, Munich, Germany
[35] Shanghai Institute of Optics and Fine Mechanics, Chinese Academy of Sciences, China
[36] NOVA Optical Infrared Instrumentation Group at ASTRON, Dwingeloo, the Netherlands
[37] Aix Marseille Univ, CNRS, CNES, LAM, France
[38] Observatoire de la Côte d'Azur Lagrange, Boulevard de l'Observatoire, Nice, France
[39] Instituto de Astrofísica de Canarias, La Laguna, Spain
[40] University of Michigan Department of Astronomy, Ann Arbor, USA
[41] Research School of Astronomy & Astrophysics, Australian National University, Canberra, Australia

The angular resolution of the Very Large Telescope Interferometer (VLTI) and the excellent sensitivity of GRAVITY have led to the first detection of spatially resolved kinematics of high velocity atomic gas near an accreting supermassive black hole, revealing rotation on sub-parsec scales in the quasar 3C 273 at a distance of 550 Mpc. The observations can be explained as the result of circular orbits in a thick disc configuration around a 300 million solar mass black hole. Within an ongoing Large Programme, this capability will be used to study the kinematics of atomic gas and its relation to hot dust in a sample of quasars and Seyfert galaxies. We will measure a new radius-luminosity relation from spatially resolved data and test the current methods used to measure black hole mass in large surveys.

Introduction

Emission lines of atomic gas velocity-broadened to widths of 3000–10 000 km s^{-1} are a hallmark of quasars and are thought to trace the gravitational potential of the central supermassive black hole. Despite decades of study their physical origin remains unclear. The observed properties can be explained by emission from discrete, collapsed clouds or high-density regions of a continuous medium. The gas may be part of the inflow feeding the black hole or a continuous equatorial outflow. Assuming a gravitational origin, line widths combined with a measurement of the emission region size provide an estimate of the black hole mass.

Extensive monitoring campaigns use light echoes in a technique called reverberation mapping to measure the emission size, with ongoing work expanding the sample size from tens (Kaspi et al., 2000; Peterson et al., 2004) to hundreds (Du et al., 2016; Grier et al., 2017). The key result of these studies is that the size of the emitting region increases with

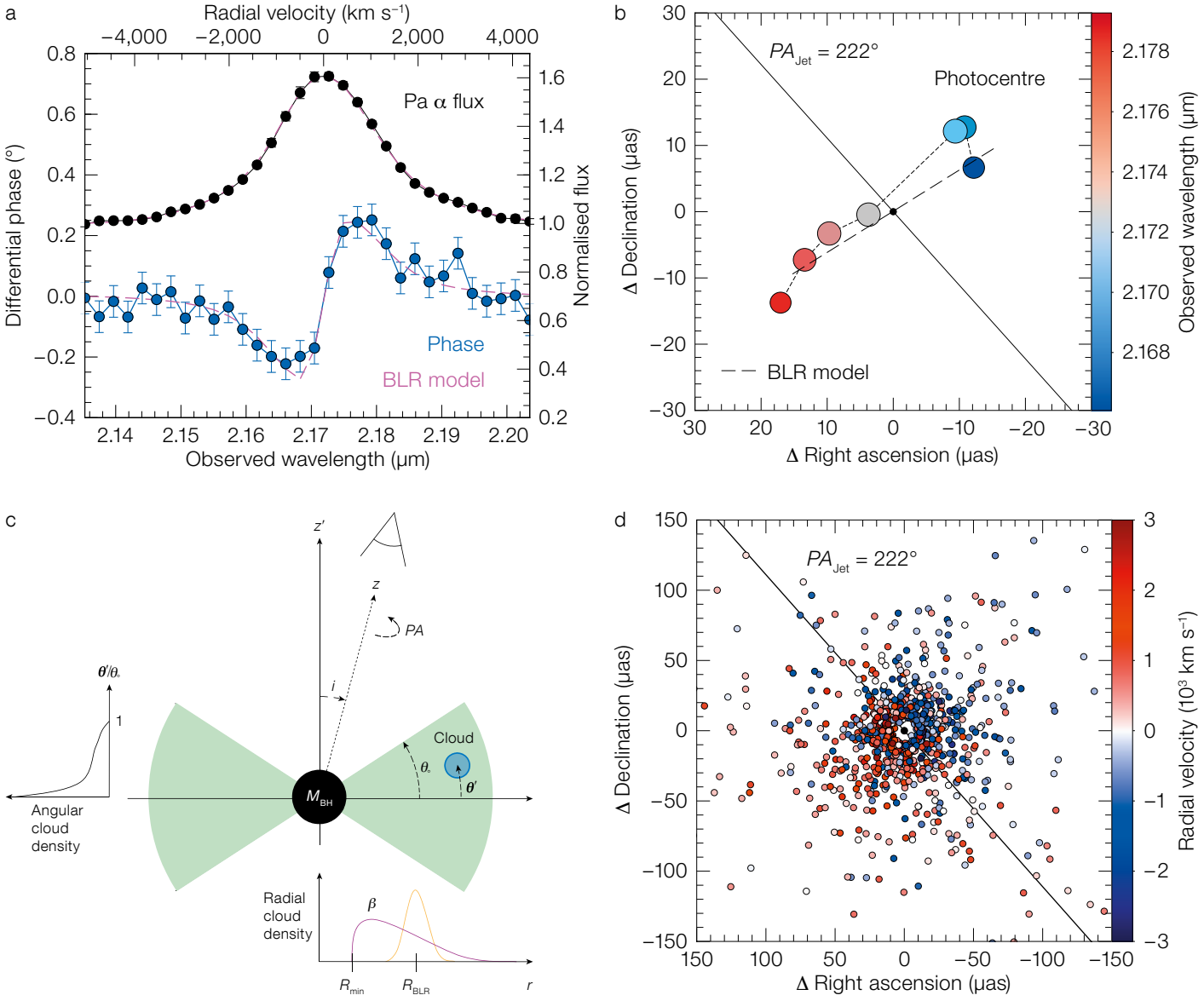

Figure 1. GRAVITY spatially resolves the broad emission line kinematics of 3C 273. (a) Paα line profile (black) and averaged differential phase (blue), showing non-zero phases and a change of sign across the broad emission line. (b) Photocentre positions measured at each line channel, showing a clear separation between red and blue which corresponds to a velocity gradient at a position angle perpendicular to the large-scale radio jet of 3C 273 (black line). This is the result of net ordered rotation of the line-emitting gas. By comparing a kinematic model of the emission region (c) to GRAVITY data, we find that a thick disc configuration viewed at low inclination best explains the data (d). The model also provides estimates of the mean emission radius and central black hole mass. Adapted from GRAVITY Collaboration (2018).

luminosity, roughly as $R \sim L^{1/2}$. That relationship can be understood as atomic gas emission being produced under optimal photoionisation conditions (constant received flux). This radius-luminosity relation allows "secondary" methods for estimating black hole masses using a single optical spectrum (replacing long campaigns to measure R via an estimate based on L). Secondary methods so far provide all available active galactic nucleus (AGN) black hole mass measurements in large samples and out to high redshift.

Interferometry provides an independent method for spatially resolving AGN central engines. The key components of AGN are small on the sky, at micro- to milliarcsecond scales, requiring long baselines at the VLTI and Keck Interferometer. AGN are also relatively faint sources, so far only detected in optical interferometry with 8–10-metre-class telescopes and instrumentation with excellent sensitivity. Continuum measurements with the Keck Interferometer (for example, Kishimoto et al., 2011) and the Astronomical Multi-BEam combineR (AMBER) on the VLTI (Weigelt et al., 2012) provide information about hot dust surrounding the nucleus. The broad line region (BLR) is even smaller (angular size < 0.1 milliarcseconds [mas]) and is impossible to resolve in standard

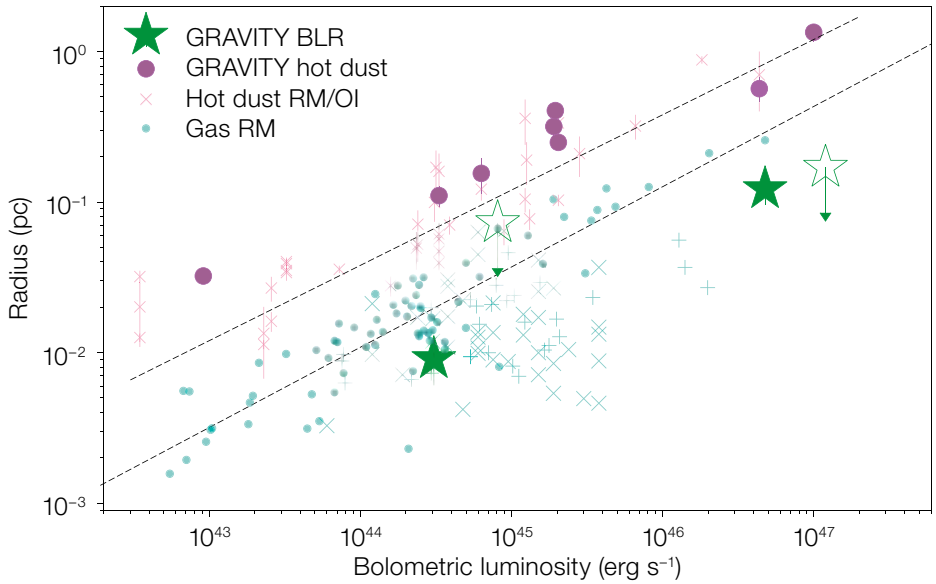

Figure 2. AGN radius-luminosity relationships measured for hot dust and atomic gas. The hot dust measurements include our new GRAVITY results (purple solid circles; see GRAVITY Collaboration, 2019a), as well as those from previous observations. For atomic gas, we have detected velocity gradients and measured the emission region size for the quasar 3C 273 (GRAVITY Collaboration, 2018) with another detection and upper limits in deep integrations for two other sources. With an ongoing large programme, we aim to expand the sample to roughly 10 AGN spanning four orders of magnitude in luminosity. The results can be compared to the large scatter found in reverberation mapping samples (different samples as smaller symbols) and to the $R \sim L^{0.5}$ relations found for both dust and atomic gas.

imaging, even with the VLTI. Instead, we can study its kinematics by measuring the photocentre shift of the atomic gas relative to the hot dust, as a function of wavelength (or velocity) across the emission line. The photocentre shift results in a small differential phase signal $\lesssim 1$ degree (Rakshit et al., 2015) whose detection requires high sensitivity and deep integrations. This is now possible with GRAVITY.

A case study in 3C 273

We observed 3C 273 with GRAVITY using the four Unit Telescopes (UTs) over eight nights between July 2017 and May 2018, with a total on-source integration time of 8 hours. By combining the data from all epochs, we measure the interferometric phase with a precision of ~ 0.1–0.2 degrees per baseline. An average of three of the six baselines shows the detection of an S-shaped phase signal, corresponding to a spatially resolved velocity gradient across the otherwise featureless broad Paα emission line (Figure 1a). From the phase data, we fit for a model-independent photocentre position at wavelength channels where the line emission is strong. We find a clear separation between blue and red channels (a velocity gradient, Figure 1b), with an orientation perpendicular to the large-scale radio jet. This demonstrates net rotation of the line emission region. The photocentre positions are measured with a typical precision of 5 μas per channel.

By adopting a kinematic model of the Paα emission region as a collection of orbiting gas clouds (following Pancoast et al., 2014 and Rakshit et al., 2015), we measure physical properties of the gas distribution and black hole. The data are consistent with a thick disc (opening angle of 45^{+9}_{-6} degrees) in Keplerian rotation around a supermassive black hole of $1.5–4.1 \times 10^{8}\ M_{\odot}$. The inclination and position angles agree with those inferred for the radio jet. The measured mean emission radius of $R_{\rm BLR} = 0.12 \pm 0.03$ pc (at an angular diameter distance of 548 Mpc) is a factor of about two smaller than reported in earlier RM studies (Kaspi et al., 2000; Peterson et al., 2004) although it is consistent with a recent one (Zhang et al., 2019). This first result supports the fundamental assumptions used in reverberation mapping and the secondary methods used to measure black hole mass. For more details, see GRAVITY Collaboration (2018).

Outlook

With an approved large programme we are carrying out observations of ~ 10 sources over the next two years, spanning four orders of magnitude in AGN luminosity. The data will provide information on the dominant kinematics and the degree of ordered motion in atomic gas in the broad emission line region, helping us to address the following questions: are the line widths primarily set by rotation in the black hole gravitational potential, or by polar outflow driven by radiation pressure? And is the velocity structure well ordered or randomised?

By modelling the line profile and differential phase data, we will measure the emission region size and construct a new radius-luminosity relationship. Our results can be compared with those obtained independently from reverberation techniques and used to constrain the physical origin of the atomic gas. We will also study the connection of the atomic gas to that of the hot dust continuum which we obtain using the same data (for example, GRAVITY Collaboration, 2019a & b). The angular size of both the hot dust and the atomic gas scales with optical flux, which makes interferometry well suited for studying luminous quasars like 3C 273 as well as nearby Seyfert galaxies. A future upgrade to the sensitivity of GRAVITY could further obtain kinematics, broad emission line region size, and black hole mass estimates for large samples out to a redshift $z \sim 2$.

Acknowledgements

This research was supported by Paris Observatory, Grenoble Observatory, by CNRS/INSU, by the *Programme National Cosmologie et Galaxies* (PNCG) of CNRS/INSU with INP and IN2P3, co-funded by CEA and CNES, by the *Programme National GRAM of CNRS/INSU* with INP and IN2P3, co-funded by CNES, by the *Programme National Hautes Energies* (PNHE) of CNRS/INSU with INP and IN2P3, co-funded by CEA and CNES, and by the *Programme National de Physique Stellaire* (PNPS) of CNRS/INSU, co-funded by CEA and CNES. It has also received funding from the following programmes: European Union's Horizon 2020 research and innovation programme (OPTICON Grant Agreement 730890), from the European Research Council (ERC) under the

European Union's Horizon 2020 research and innovation programme (Grant Agreement No. 743029), from the Irish Research Council (IRC Grant: GOIPG/2016/769) and SFI Grant 13/ERC/12907, from the Humboldt Foundation Fellowship and the ESO Fellowship programes, from the European Research Council under the European Union's Horizon 2020 research and innovation programme (Grant Agreement Nos. 2016–ADG–74302 [EASY], 2015-StG-677117 [SFH], 694513, and 742095 [SPIDI]), and was supported in part by the German Federal Ministry of Education and Research (BMBF) under the grants *Verbundforschung* #05A08PK1, #05A11PK2, #05A14PKA and #05A17PKA, by *Fundação para a Ciência e a Tecnologia*, Portugal (Grants UID/FIS/00099/2013, SFRH/BSAB/142940/2018 [P. G.] and PD/BD/113481/2015; M. F. in the framework of the Doctoral Programme IDPASC Portugal), by NSF grant AST 1909711, by the Heising-Simons Foundation 51 Pegasi b postdoctoral fellowship, from the *Direction Scientifique Générale of Onera* and by a Grant from Science Foundation Ireland under Grant number 18/SIRG/5597.

References

Peterson, B. M. et al. 2004, ApJ, 613, 682
Kaspi, S. et al. 2000, ApJ, 533, 631
Rakshit, S. et al. 2015, MNRAS, 447, 2420
GRAVITY Collaboration 2018, Nature, 563, 657
GRAVITY Collaboration 2019a, submitted to A&A, arXiv:1910.00593
GRAVITY Collaboration 2019b, submitted to A&A
Bentz, M. C. et al. 2013, ApJ, 767, 149
Du, P. et al. 2018, ApJ, 856, 6
Grier, C. J. et al. 2017, ApJ, 851, 21
Pancoast, A. et al. 2008, MNRAS, 445, 3073
Kishimoto, M. et al. 2011, A&A, 527, 121
Weigelt, G. et al. 2012, A&A Letters, 451, 9
Zhang, Z.-X. et al. 2019, ApJ, 876, 49

DOI: 10.18727/0722-6691/5167

An Image of the Dust Sublimation Region in the Nucleus of NGC 1068

GRAVITY Collaboration (see page 20)

The superb resolution of the Very Large Telescope Interferometer (VLTI) and the unrivalled sensitivity of GRAVITY have allowed us to reconstruct the first detailed image of the dust sublimation region in an active galaxy. In the nearby archetypal Seyfert 2 galaxy NGC 1068, the 2 µm continuum emission traces a highly inclined thin ring-like structure with a radius of 0.24 pc. The observed morphology challenges the picture of a geometrically and optically thick torus.

Introduction

NGC 1068 is one of the best studied nearby active galactic nuclei (AGN), in which accretion onto a central supermassive black hole contributes a significant fraction of the galaxy's total luminosity. The observation of broad polarised emission lines by Antonucci & Miller (1985) in the nucleus of this Seyfert galaxy was central to the development of the unified model that explains the differences between Seyfert 1 and Seyfert 2 objects as being due to the presence of a nuclear equatorial structure that both obscures and scatters the central emission depending on the line of sight.

Since the first seminal paper addressing its physical properties (Krolik & Begelman, 1988), and following numerous observations at many different wavelengths, the "torus" concept has evolved and been modified considerably. At the same time, increases in computational power have facilitated detailed modelling of clumpy torus structures. Such models are consistent with the near- to mid-infrared spectral energy distribution as well as dust reverberation measurements. Observations of almost two dozen galaxies using the MID-infrared Interferometric instrument (MIDI) on the VLTI have resolved the 1–3 pc scales where warm dust is responsible for the mid-infrared continuum (Burtscher et al., 2013 and references therein). However, measuring the size of the small (< 1 pc) region containing hot dust that emits at near-infrared wavelengths has been possible in very few galaxies. Also, until GRAVITY observed NGC 1068, there were no data showing spatial structure in this dust sublimation region.

Observations and Image Reconstruction

Data on NGC 1068 were obtained in November and December 2018 using GRAVITY and the four 8-metre UTs. Under superb conditions, with seeing ~ 0.5 arcseconds and a coherence time of up to 13 ms, it was possible to fringe-track on the nucleus of NGC 1068 despite its large size and moderate brightness. The data obtained were of excellent quality, with typically < 1% visibility and closure-phase accuracy. The wealth of information provided by the six VLTI baselines has enabled us to reconstruct a *K*-band image based on the obtained closure phases and visibilities with 3-milliarcsecond (mas) resolution.

We used the publicly available Multi-aperture image Reconstruction Algorithm (MiRA; Thiébaut, 2008) to generate the image shown in Figure 1, which contains a total flux of 155 mJy. The structures present are robust, having been reproduced consistently over a wide variety of parameter settings, and with a signal level much higher than that expected for spurious sources. Full details are in GRAVITY Collaboration (2019).

A new view of NGC 1068

The image in Figure 1 is dominated by knots of continuum arranged in a ring around a central hole, with the south-western side about a factor of two brighter than the north-eastern side. Fitting an

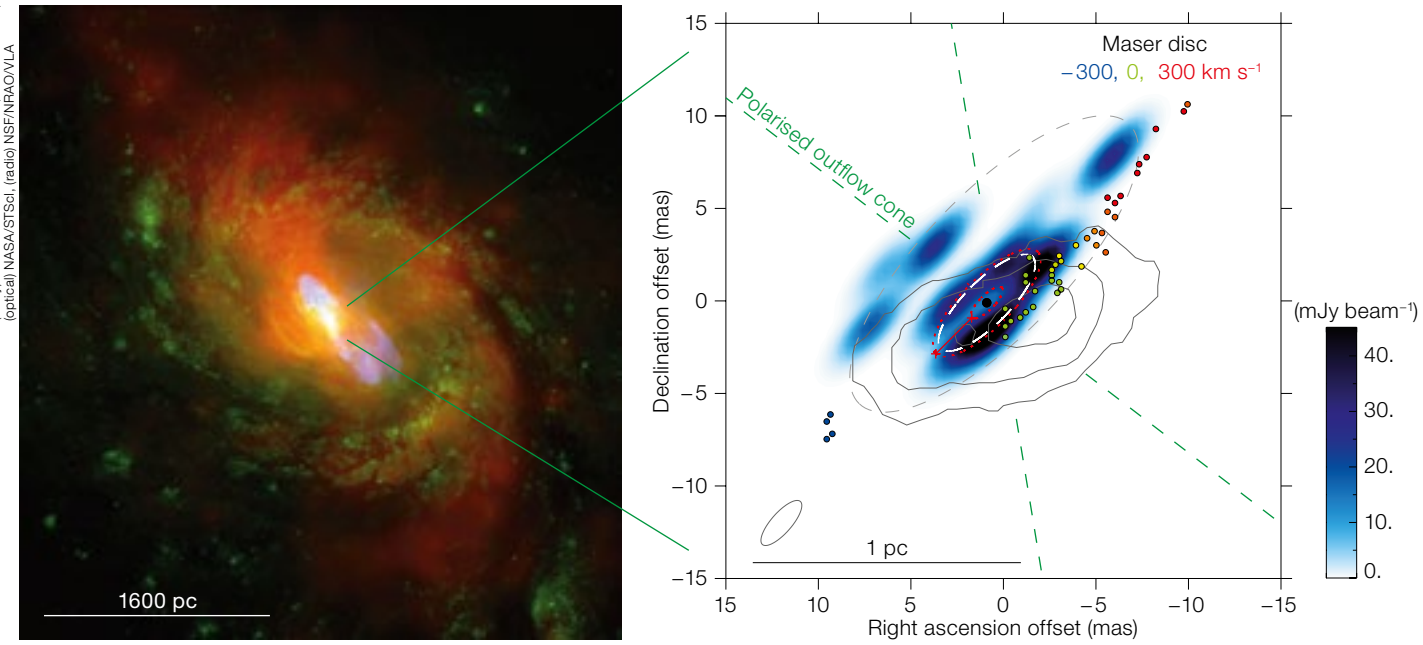

Figure 1. Left: Three-colour image of NGC 1068. The optical emission is shown in green, the X-ray in red and the radio jet in blue. Right: Reconstructed image of the 2 μm continuum (blue colour scale) in the central 2.1 pc of NGC 1068, showing the reconstructed beam size in the lower left. The white dashed ellipse, fitted to the brightest knots, traces a ring that matches the expected range of dust sublimation radii (orange dotted ellipses). The filled black circle in the centre of the ring, denoting the location of the AGN, has been matched to the kinematic centre derived from the maser kinematics, and hence fixes the relative position of the maser distribution. The radio continuum has been positioned using the masers as a coordinate reference. The green dashed lines outline the bipolar ionised outflow also seen in polarisation data. The grey dashed ellipse indicates the size of the 10-metre continuum in the MIDI data.

ellipse to these knots yields a position angle of 50 degrees west of north, an inclination of 70 degrees and a radius of about 0.24 pc. The size matches remarkably well the expected dust sublimation radius for large graphite grains in the radiation field of an AGN with an intrinsic bolometric luminosity of ~ 4×10^{45} erg s^{-1} as expected for NGC 1068. And if one aligns the central hole in the near-infrared continuum to the location of the central black hole inferred from the maser kinematics (Gallimore & Impellizzeri, 2019), then the positions of the lower-velocity maser spots match up remarkably well with the south-western side of the ring. This suggests that the masers and the hot dust trace a common disc, and hence that the brighter south-western side of the ring is the near side. This geometry is consistent with that implied by the jet and the ionisation cone, which are oriented toward us on the northern side.

The near-infrared continuum is very difficult to reconcile with geometrically thick clumpy torus models, which can only reproduce a ring-like structure in systems that are relatively face-on, and struggle to make the near side of the ring brighter. Similarly, the presence of a thin maser disc is inconsistent with a vertically extended structure, since this would impede the escape of far-infrared photons that would otherwise thermalise the population of masing molecules. In an additional test, we have compared the spectral energy distributions predicted by models with the photometry from MIDI and GRAVITY. For reasonable parameter ranges, the models tend to over-predict the mid-infrared continuum and have a near-infrared slope that is too shallow.

As an alternative, we considered whether the mid- and near-infrared continua have a common origin at all. Cool (~ 700 K) dust behind a screen of extinction provides an unexpectedly good fit to the spectral energy distribution, including the silicate dip. But the modest A_K ~ 0.9 magnitude extinction is far less than the lower limit of A_K ~ 6 magnitudes required by the non-detection of broad Brα at 4 μm (Lutz et al., 2000) and the high-column density implied by the HCN1–0 emission at 3 mm (García-Burillo et al., 2016; Imanishi et al., 2018).

Instead, our preferred interpretation is in terms of a hot dust disc close to the sublimation temperature. Dust at 1500 K behind a screen with A_K ~ 5.5 magnitude extinction is able to reproduce the slope of the near-infrared continuum. And a modest scale height of $h/r < 0.14$, as indicated by the data, is sufficient to couple the AGN luminosity to the dust disc because of the misalignment between it and the accretion disc. This scenario requires that most of the mid-infrared continuum originates in a different structure on larger scales. Disc-plus-wind models such as those described by Hönig (2019) would imply that the other structure is in fact the outflow driven by the AGN.

Conclusion

K-band observations with GRAVITY at a spatial resolution of 3 mas have resolved a ring-like structure on sub-parsec scales in the centre of NGC 1068. These observations do not support ideas of a geometrically and optically thick clumpy torus and instead trace a dusty disc around the AGN. The size matches that

expected for the dust sublimation region, and the apparent orientation is similar to that of the maser disc, arguing for a common origin. The structure and photometry are consistent with dust at ~ 1500 K behind A_K ~ 5.5 magnitudes of foreground extinction. This matches what is expected from the upper limit to the broad Brα line, and could originate in the dense and turbulent gas distribution observed on scales of 1–10 pc. In such a scenario, much of the mid-infrared continuum would originate in a separate structure, likely associated with the AGN-driven outflow.

Acknowledgements

See page 23.

References

Antonucci, R. R. J. & Miller, J. S. 1985, ApJ, 297, 621
Burtscher, L. et al. 2013, A&A, 558, 149
García-Burillo, S. et al. 2016, ApJ, 823, L12
Gallimore, J. & Impellizzeri, V. 2019, submitted to ApJ
GRAVITY Collaboration 2019, accepted by A&A
Hönig, S. F. 2019, accepted by ApJ
Imanishi, M. et al. 2018, ApJ, 853, L25
Krolik, J. H. & Begelman, M. C. 1988, ApJ, 329, 702
Lutz, D. et al. 2000, ApJ, 530, 733
Thiébaut, E. 2008, Proc. SPIE, 7013, 70131I

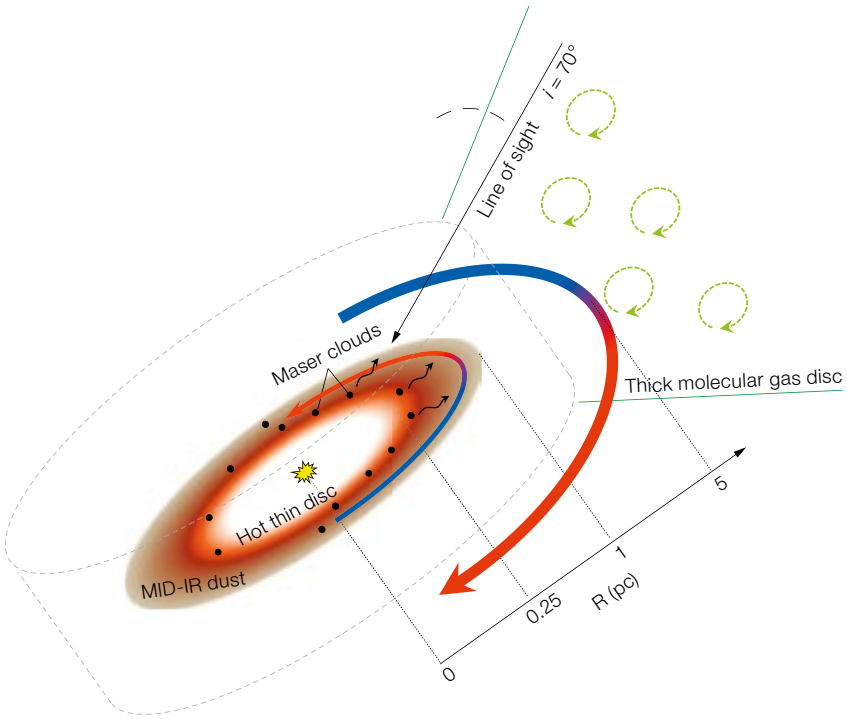

Figure 2. Sketch of the observed central structures. The *K*-band emission traces the inner rim of a thin disc of hot gas and dust, at or close to the dust sublimation radius of 0.24 pc. The inner water masers are cospatial with the hot *K*-band dust. The masers stretch out to 1 pc (Gallimore et al., 2001). Mid-infrared observations show warm dust on roughly the same scales as the outer masers, likely originating from the disc periphery. ALMA observations of HCN and HCO+ show a turbulent structure, which rotates in the opposite direction to the maser disc (Imanishi et al., 2018). The turbulence found in the molecular gas structure argues for a thick disc, which contains enough gas mass to reach column densities that screen the central region from the observer by A_K ~ 5.5 magnitudes.

DOI: 10.18727/0722-6691/5168

GRAVITY and the Galactic Centre

GRAVITY Collaboration (see page 20)

On a clear night, our home galaxy, the Milky Way, is visible as a starry ribbon across the sky. Its core is located in the constellation of Sagittarius, approximately where the bright glow is interrupted by the darkest dust filaments. There, hidden, lies a massive black hole. To peer through the obscuring clouds and see the stars and gas near the black hole we use GRAVITY. The main GRAVITY results are the detection of gravitational redshift, the most precise mass-distance measurement, the test of the equivalence principle, and the detection of orbital motion near the black hole.

The heart of the Milky Way

At the heart of the Milky Way, 26 000 light-years from Earth, is Sagittarius A* (Sgr A*, pronounced “Sag-A-star”), the closest massive black hole to us and, with a lensed angular diameter of 53 microarcseconds (μas), the largest one on the sky. It is embedded in hot gas and surrounded by a cluster of high velocity stars. They buzz around the black hole on trajectories which are, like the behaviour of the hot gas, governed by the gravitational field of the black hole.

With GRAVITY we are unravelling what is happening in the centre of our Galaxy with unprecedented angular resolution. The instrument operates at infrared wavelengths around 2 microns. GRAVITY combines the light beams of the four individual 8.2-metre Unit Telescopes at

Y. Beletsky/ESO

ESO/MPE/S. Gillessen et al.

Figure 1. Left: The sky above the VLT at Paranal. The laser of Unit Telescope 4 (Yepun) points at the Galactic centre. Right: Infrared image of the Galactic centre. For the interferometric GRAVITY observations the star IRS 16C was used as a reference star and the actual target was the star S2. The position of the centre, which harbours the (invisible) 4 million solar mass black hole known as Sgr A* is marked by the orange cross.

ESO's Very Large Telescope (VLT) in Chile to form the VLT Interferometer (VLTI). Together they achieve a spatial resolution equivalent to that of a telescope of approximately 130 metres in diameter (GRAVITY Collaboration, 2017). GRAVITY has also been equipped with a system to track interference fringes and it uses adaptive optics to correct for atmospheric turbulence in order to resolve small and faint structures in the sky.

Measurement of gravitational redshift in the Galactic centre

We have traced a partial astrometric and a full 16-year radial velocity orbit of the star S2 with GRAVITY on the VLTI and the Spectrograph for INtegral Field Observations in the Near Infrared (SINFONI) on the VLT. During its recent closest approach to the black hole, the pericentre passage in May 2018, we collected both astrometric and spectroscopic data. These data allowed the detection of the combined gravitational redshift and transverse Doppler effect on S2 for the first time. Gravitational redshift is one of the three classical tests of Einstein's general theory of relativity. Einstein was the first to accurately predict a gravitational time dilation, i.e., that a clock near a gravitational mass ticks slower than a distant reference clock. As a result of this effect an observer sees a photon emitted near a massive object at a longer, redder wavelength. This prediction has so far only been tested in weak gravity regimes like the gravitational fields of Earth, the Sun, and white dwarfs. With GRAVITY and SINFONI we were able to test the strong gravitational field of a massive black hole. During its recent closest approach to Sgr A* the spectral absorption lines in the light of S2 were significantly shifted towards redder wavelengths, in excellent agreement with Einstein's general theory of relativity (GRAVITY Collaboration 2018a).

Mass and Distance of the Galactic Black Hole

Our measurements of the position and radial velocity of S2 allow us to calculate both the mass of the black hole and the distance to the Galactic centre with unprecedented precision and accuracy. By combining the precise astrometry from GRAVITY with the spectral measurements of SINFONI, we can determine the distance to the Galactic centre to be 26 673 light-years and the black hole mass to be 4.1 million solar masses (GRAVITY Collaboration, 2019b).

Local position invariance

One of the cornerstones of general relativity is Einstein's equivalence principle. It consists of three parts: the weak equivalence principle, the local Lorentz invariance and the local position invariance (LPI). We use the orbit of S2 to test the LPI, which states that the results of a non-gravitational experiment are independent of the position in space-time.

The star S2 experiences very strong changes in gravitational potential in the course of its eccentric orbit around Sgr A*. This makes it a unique probe and allows us to test the LPI. The spectrum of S2 has absorption lines of helium and hydrogen, which are formed by atomic processes and are thus non-gravitational. We can observe how they change in wavelength as the star moves on its trajectory towards us, around the black hole, and away from us again. During the pericentre passage both the hydrogen and helium lines are redshifted. We did not detect a different shift of the two absorption lines. This puts a limit on the violation of the LPI to below 5%. While current tests on Earth have a much higher accuracy, our experiment in the Galactic centre laboratory tests gravitational field changes a million times larger (GRAVITY Collaboration, 2019a).

Flares

The Galactic centre black hole is, given its huge mass, surprisingly faint. That is, the hot gas that swirls around it has a comparatively low luminosity. Most of the radiation is emitted at radio and infrared wavelengths and is quasi-steady — it flickers only a little. In the near-infrared

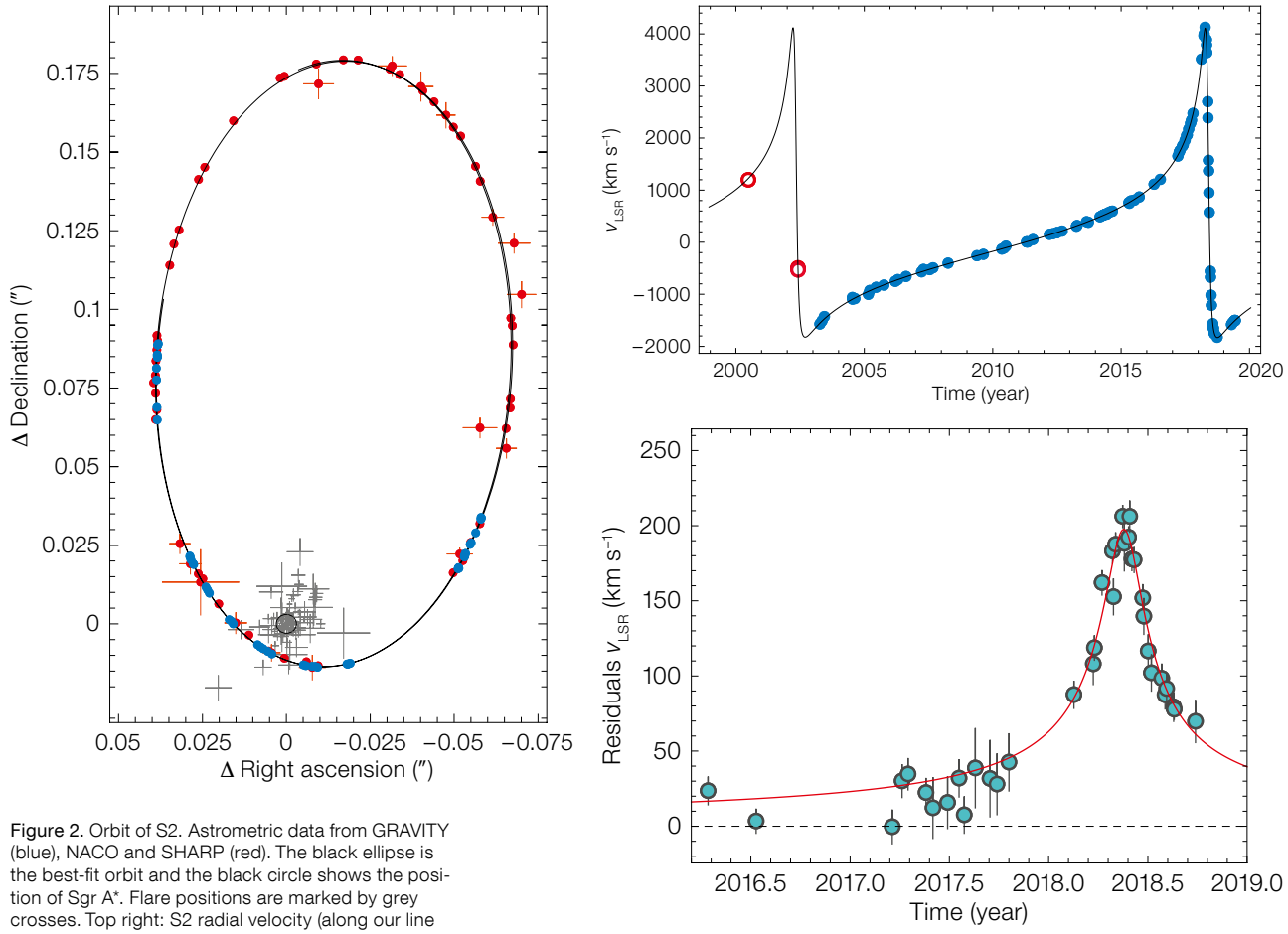

Figure 2. Orbit of S2. Astrometric data from GRAVITY (blue), NACO and SHARP (red). The black ellipse is the best-fit orbit and the black circle shows the position of Sgr A*. Flare positions are marked by grey crosses. Top right: S2 radial velocity (along our line of sight) measured over more than one orbit. Bottom right: The combined gravitational redshift and relativistic transverse Doppler effect manifest in an excess in the radial velocity of 200 km s^{-1}.

where GRAVITY and SINFONI operate, the long-term light curves are well described by a log-normal noise, indicating that there are statistical fluctuations in the way the hot gas is accreted by the black hole. On average, about once per day for 1–2 hours this slightly variable emission becomes a bright flare, and at times it contains so much energy that it even emits X-rays. The true nature of these flares seen at infrared and X-ray wavelengths is not yet known and may be explained as a hot spot in the gas or an ejected blob of gas (as in a jet).

Observations during the summer of 2018 with GRAVITY revealed that the emission near the black hole during an infrared flare moves in a loop around an unseen centre (GRAVITY Collaboration, 2018b). These loops are typically a few times larger than the event horizon of the black

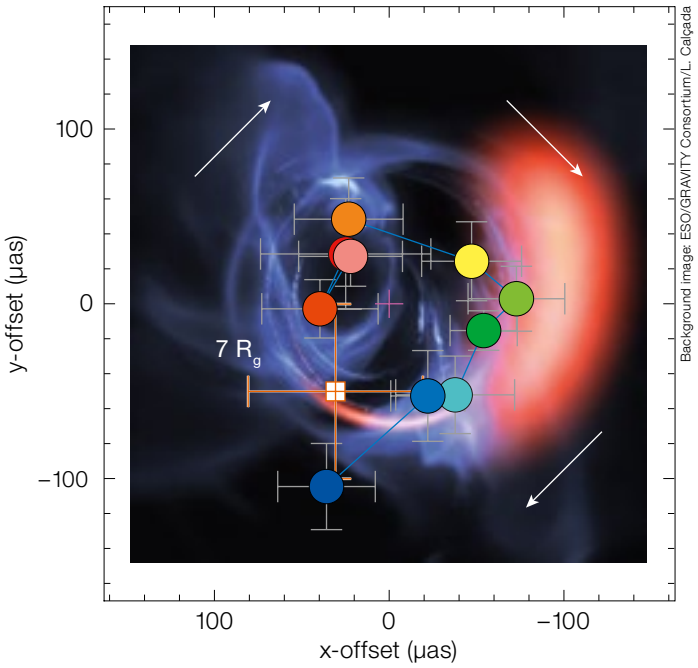

Figure 3. Projected orbit of the flare recorded on 22 July 2018 over its 30-minute duration (colour ranging from brown to dark blue indicates the time). The background shows a flare "hot spot" simulation.

hole and are consistent with a small region of heated electrons (a "hot spot"), moving in an orbit around the black hole. The GRAVITY observations also revealed changes in the polarisation angle over the course of the flare. In particular, as the centroid of the emission region completes one orbit around the black hole, the polarisation angle also makes a single loop. These polarisation measurements indicate the presence of a strong magnetic field in the immediate vicinity of the black hole and might indicate a magnetic origin of the flare.

What's next?

Continuing observations of S2 are expected to reveal a second relativistic effect on the star's orbit, namely the Schwarzschild precession. General relativity predicts that the orbit of S2 is not a closed Keplerian ellipse but an open rosette-like trajectory, where the periapse, i.e., the closest point to the black hole, shifts by a small angle per revolution which rotates the ellipse over time. Moreover, studying multiple flares as an ensemble will shed light on accretion properties, for example, the sense of rotation of the hot gas.

References

GRAVITY Collaboration 2017, A&A, 602, 23
GRAVITY Collaboration 2018a, A&A, 615, 15G
GRAVITY Collaboration 2018b, A&A, 618, 15
GRAVITY Collaboration 2019a, Phys. Rev. Lett., 122, 101102
GRAVITY Collaboration 2019b, A&A, 625, 10

DOI: 10.18727/0722-6691/5169

Spatially Resolved Accretion-Ejection in Compact Binaries with GRAVITY

GRAVITY Collaboration (see page 20)

The GRAVITY instrument at the Very Large Telescope Interferometer has led to the first spatially resolved observations of X-ray binaries at scales comparable to the binary orbit, providing unprecedented spatial information on their accretion-ejection mechanisms. In particular, observations of the hypercritical accretor SS433 have revealed a variety of spatial structures at the heart of this exotic microquasar, including bipolar outflows, super-Keplerian equatorial outflows and extended baryonic jets photoionised by collimated ultraviolet radiation.

X-ray binaries (XRBs) are composed of a compact object (neutron star or black hole) accreting matter from its donor star. The accretion process leads to a variety of inflow-outflow structures such as discs, streams, winds and jets. While large-scale jets are often resolved with very long baseline interferometry (VLBI) at radio wavelengths, capable of achieving approximately milliarcsecond (mas) spatial resolution, the inner parts of the accretion-ejection structures, at scales comparable to the binary orbit, had remained unresolved for a long time because the required sub-milliarcsecond spatial resolution is significantly beyond the diffraction limit of even extremely large telescopes. Resolving these structures is, in fact, challenging even for optical interferometry, since these sizes are below the canonical spatial resolution of an optical interferometer such as the Very Large Telescope Interferometer (VLTI), which is around 3 mas for a baseline of 100 metres. Therefore, in order to get to such scales, exquisite precision in the interferometric observables is required, which is best achieved with spectrally resolved measurements using strong emission lines. This technique is called spectral differential interferometry and it can be used to acquire robust velocity-resolved microarcsecond (μas) spatial information.

GRAVITY has led to a breakthrough in the ability to fringe-track on faint objects, allowing interferometric quantities to be measured in the near-infrared (NIR) at high spectral resolution (R ~ 4000) with unprecedented precision. When applied to X-ray binaries, this has led to the first spatially resolved observations of accretion-ejection structures at NIR wavelengths. Here, we review pioneering GRAVITY observations of two such objects: the hypercritical accretor and exotic microquasar SS433, and the wind-accreting high-mass XRB BP Cru.

Resolving super-Eddington outflows in SS433

SS433 is unique in the Galaxy as the only known steady hypercritical accretor; the donor star provides the compact object (the nature of which remains enigmatic, but is likely to be a black hole) with matter at a rate hundreds of times above Eddington (see, for example, Fabrika, 2004 for a review of SS433). The resulting geometrically and optically thick supercritical accretion disc thermally downgrades the X-ray radiation produced close to the compact object (and typically seen in ordinary X-ray binaries) to ultraviolet (UV) and optical wavelengths, turning the compact object into an accretion-powered quasi-star that outshines its donor star at all wavelengths. In addition, the enormous radiation pressure leads to powerful outflows producing strong emission lines, seen not only from the ~ 2000 km s^{-1} accretion disc winds (the so-called "stationary" lines) but also from the ~ 80 000 km s^{-1} (0.26c) highly

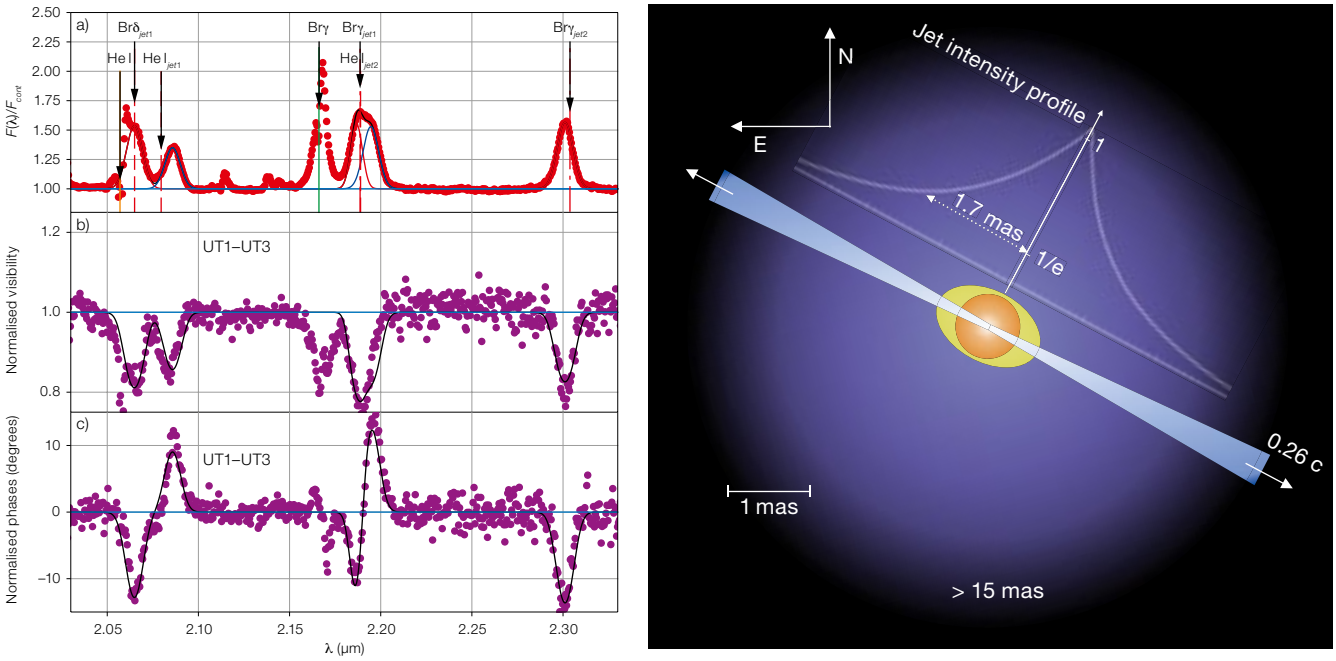

Figure 1. Left: Spectrum (a), differential visibility amplitudes (b), and visibility phases (c) across the "stationary" and baryonic jet emission lines of SS433 in the 2016 GRAVITY observation. The best-fit exponential model for the jet emission (illustrated in the schematic on the right) is shown in black.

collimated baryonic jets, with the latter's precession creating its idiosyncratic moving lines across the X-ray and optical spectra (Margon et al., 1979).

These unique properties — a very bright accretion disc at optical wavelengths and strong, broad and variable emission lines — make SS433 the ideal XRB for NIR interferometry, also providing the only opportunity to spatially study a supercritical accretion disc and its outflows. GRAVITY observations of SS433 carried out in 2016 and 2017 (GRAVITY Collaboration et al., 2017b; Waisberg et al., 2019a,b) have revealed a marginally resolved NIR continuum consisting of (i) the central unresolved binary (with a size < 0.5 astronomical units [au]), and (ii) extended emission of size ~ 40 au in the form of a wind and/or disc (contributing ~ 20% of the *K*-band flux). Much more information, however, is gathered from the spectrally resolved differential visibility amplitudes and phases across the many emission lines (Figure 1).

For instance, the observations have shown that the double-peaked "stationary" Brγ line alternates between a bipolar-outflow dominated mode (aligned with the jets) to an equatorial-outflow dominated mode (perpendicular to the jets) (Figure 2). Although the presence of equatorial outflows in SS433 had been well established from radio observations (for example, Blundell et al., 2001), this is the first time that velocity and size could be combined to show that the outflows are super-Keplerian. The outflows support the conclusion that both the compact object and the donor star in SS433 overfill their Roche lobes significantly, losing mass through their outer Lagrangian points, and that the transfer of specific angular momentum between the binary and the disc-like outflows is very significant for the binary evolution. Future observations of several hours in a single night could harvest the full power of aperture synthesis and provide velocity-resolved, model-independent images of the complex outflow structure beyond simple geometric models.

The GRAVITY observations have also spatially resolved the optical jets of SS433 for the first time, revealing exponential profiles that extend to over 20 au (i.e., several tens of times the binary size) and which peak surprisingly close to the central binary (Figure 1). These observations suggest that optical jets are heated by collimated UV radiation and, in combination with spectroscopic observations, have shown that SS433 is UV-dominated even in the jet funnel. This is important in the context of the acceleration mechanism of the ~ 0.26c jets by line-locking (Milgrom, 1979), which requires intense collimated radiation, as well as in the possible relation between SS433 and ultraluminous X-ray sources (ULXs). Future observations of several hours in a single night could directly detect the relativistic motion (8 mas d^{-1}) of the baryonic jets, providing a further probe of their heating mechanism and an accurate, self-consistent distance to SS433.

Spatially resolved wind accretion in BP Cru

BP Cru (GX 301-2) is composed of an X-ray pulsar accreting from the wind of its hypergiant B1Ia+ companion (Kaper et al., 2006). The latter has unusually powerful winds (~ 10^{-5} $M_\odot$ yr^{-1}) for a donor star in an XRB, which lead to strong emission lines of HeI and Brγ from its extended wind in its *K*-band spectrum. In addition, its unusually high eccentricity (e = 0.46) makes it an ideal target for probing the influence of the gravitational and radiation fields of the pulsar on the surrounding circumstellar environment (for example, Blondin, 1994).

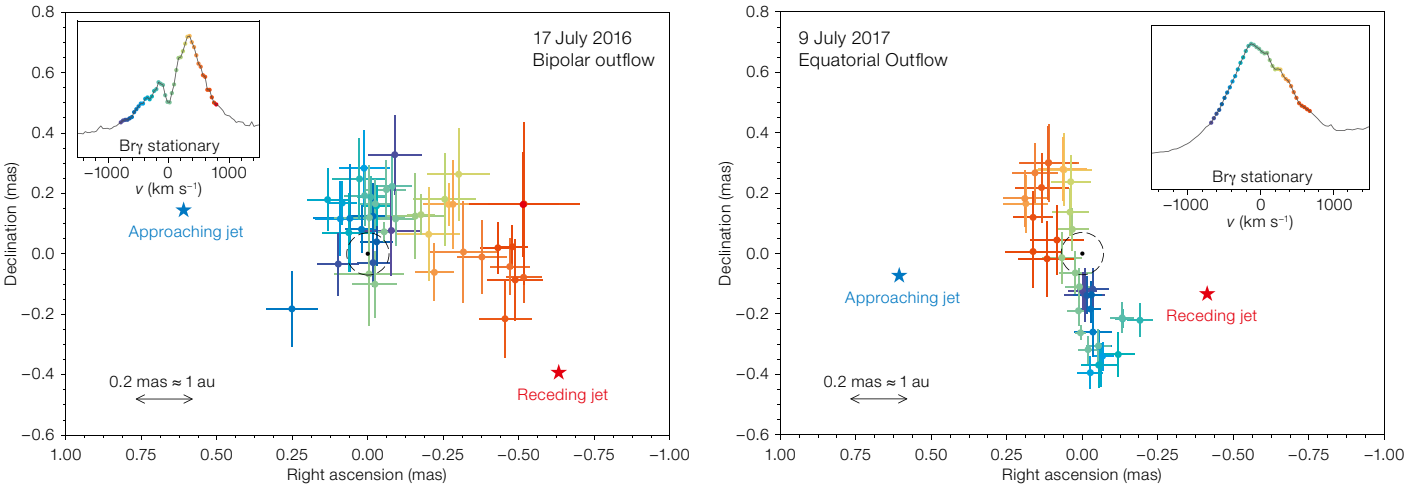

Figure 2. Velocity-resolved emission centroids across the double-peaked Brγ "stationary" line for observations in 2016 (left) and 2017 (right). The emission centroid of the spatially resolved baryonic jets is also shown. The black circles correspond to the estimated binary orbit size.

The spectral differential visibilities measured by GRAVITY (GRAVITY Collaboration et al., 2017a) reveal an extended wind with a size several times the stellar radius, which is also significantly distorted — being more extended on the side that is shielded from the pulsar — and which could be caused by the X-ray ionisation of the stellar wind facing the compact object. In addition, asymmetries revealed by the differential visibility phases across the emission lines may point to an additional component, possibly a stream of enhanced density which has been posited to exist in the system from the analysis of X-ray light curves (Leahy & Kotska, 2008). Further observations at different orbital phases could take advantage of the significant eccentricity in order to disentangle intrinsic variability of the wind from the distortion caused by the pulsar accretion.

Acknowledgements

See page 23.

References

Blondin, J. M. 1994, ApJ, 435, 756
Blundell, K. et al. 2001, ApJ, 562, L79
Fabrika, S. 2004, Space Science Reviews, 12, 1
GRAVITY Collaboration et al. 2017a, ApJ, 844, 177
GRAVITY Collaboration et al. 2017b, A&A, 602, L11
Kaper, L. et al. 2006, A&A, 457, 595
Leahy, D. & Kostka, M. 2008, MNRAS, 384, 747
Margon, B. et al. 1979, ApJ, 233, L63
Milgrom, M. 1979, A&A, 78, L9
Waisberg, I. et al. 2019a, A&A, 623, A47
Waisberg, I. et al. 2019b, A&A, 624, A127

DOI: 10.18727/0722-6691/5170

Images at the Highest Angular Resolution with GRAVITY: The Case of η Carinae

GRAVITY Collaboration (see page 20)

The main goal of an interferometer is to probe the physics of astronomical objects at the highest possible angular resolution. The most intuitive way of doing this is by reconstructing images from the interferometric data. GRAVITY at the Very Large Telescope Interferometer (VLTI) has proven to be a fantastic instrument in this endeavour. In this article, we describe the reconstruction of the wind-wind collision cavity of the massive binary η Car with GRAVITY across two spectral lines: He I and Brγ.

Interferometric imaging

With a resolving power that is a factor of tens of times better than stand-alone telescopes, infrared interferometry offers the possibility to produce milliarcsecond (mas) resolution images. Therefore, interferometric imaging is a key means to acquire information addressing a broad range of astronomical problems, ranging from the detection of planets to mapping the cores of active galactic nuclei (AGN).

Interferometers reach a level of detail proportional to the separation between each pair of telescopes in the array, known as baselines. Baselines record information, at a given orientation, of the brightness distribution of the object on the sky. Interferometric observables, called visibilities, are a series of Fourier (spatial) frequencies. These frequencies correspond to different levels of detail in the image. The highest frequencies trace the finest

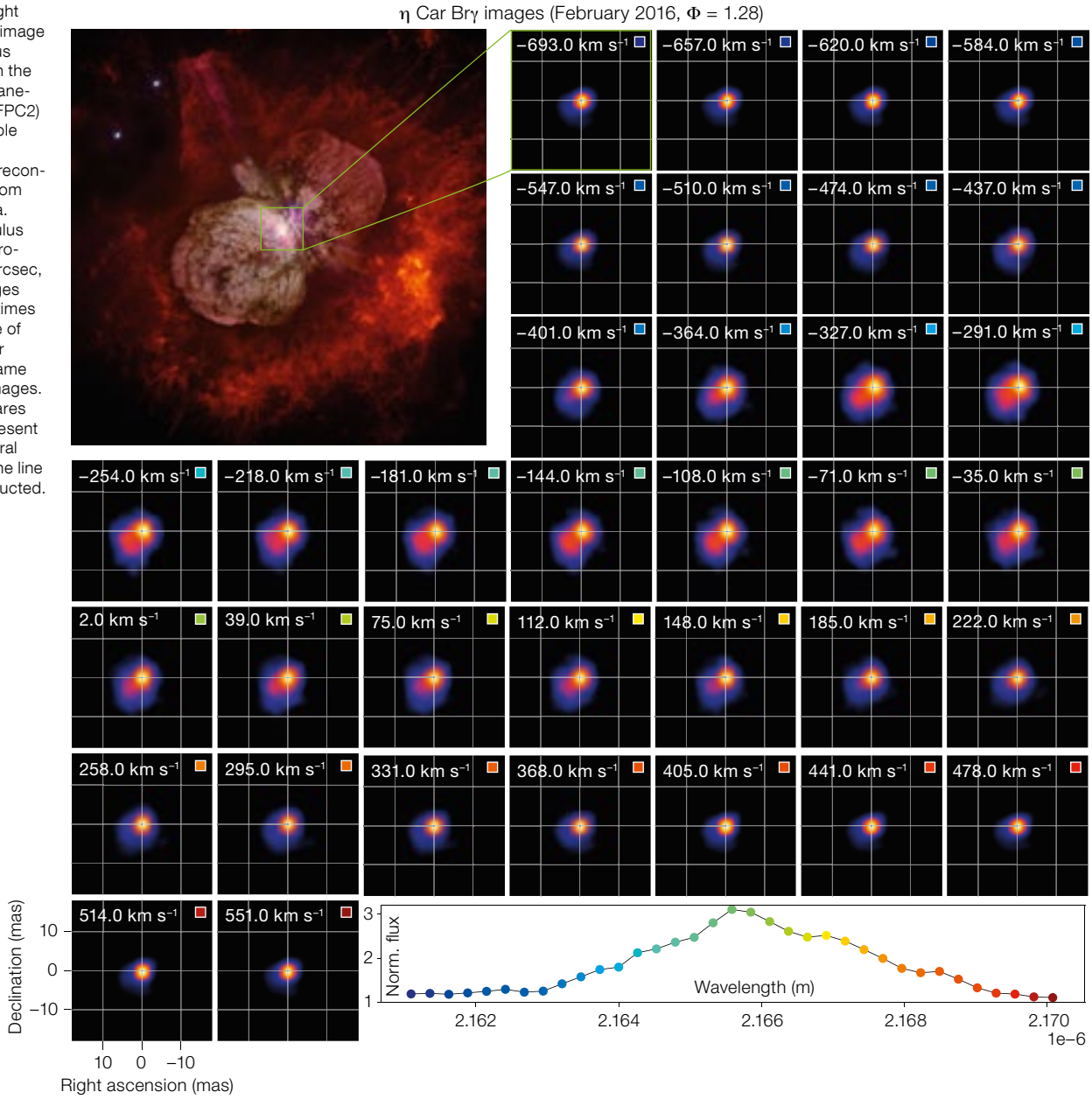

Figure 1. Upper-right panel: Composite image of the "Homunculus Nebula" taken with the Wield Field and Planetary Camera 2 (WFPC2) on board the Hubble Space Telescope. Small panels: Brγ reconstructed images from the Feb. 2016 data. With the Homunculus Nebula having a projected size of 17 arcsec, the GRAVITY images represent an 850 times zoom into the core of η Car. The Doppler velocity of each frame is labeled in the images. The coloured squares in the images represent the different spectral channels across the line that were reconstructed.

textures (like granular surfaces, or point-like objects) while the lowest ones trace extended textures (like edges and contours). An image is, therefore, composed of an infinite number of frequencies. However, interferometers only sample a few of them.

Thus, recovering an image from interferometric data is an "ill-posed" problem with more unknowns (pixels in the image) than constraints (data). Reconstructing images requires the use of iterative regularised least-squares minimisation algorithms. These algorithms minimise (i) the difference between the data and the visibilities obtained from the model image (i.e., the likelihood term), and (ii) the value of one or several priors (i.e., the regularisers), which are defined based on the knowledge of the source (see Sanchez-Bermudez et al., 2018). Reconstruction packages available to the community optimise through gradient-descent (for example, MiRA: Thiébaut, 2008; BSMEM: Buscher, 1994) or Monte-Carlo Markov-Chain methods (for example, SQUEEZE: Baron & Kloppenborg, 2010).

The massive binary at the core of η Car

Located at the core of the "Homunculus Nebula" (see Figure 1) at a distance of 2.3 kiloparsecs, η Car is a very massive and intriguing object. Indirect observations suggest that a binary with a period of 5.54 years resides in its core. The primary, η_A, is supposedly a star with a mass of around 100 $M_\odot$, while the secondary, η_B, appears to be a hotter star, perhaps a giant O-star, with a mass of around 30 $M_\odot$, but around 100 times fainter than the primary. Different observations suggest that

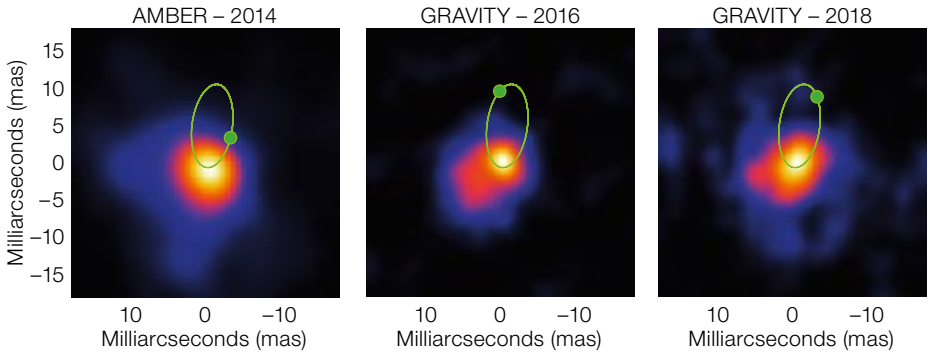

Figure 2. Comparison between the wind-wind collision zone's morphologies at different orbital phases of η_B taken with AMBER (2014) and GRAVITY (2016, 2018) at a Doppler (blue-shifted) velocity of −280 km s^{-1}. The projected trajectory of the secondary and its position are marked by the green ellipse and dot, respectively, in each of the panels. Notice how the structure of the cavity changes considerably depending on the secondary's orbital phase. For example, the south-eastern clump observed in 2016 disappears in the 2018 reconstruction.

η_A exhibits a very dense and slow wind that shocks with a much faster and lighter wind from the secondary.

The existence of η_B produces several changes in the morphology of η_A's wind. In particular, it photoionises part of the primary wind, changing the strength of lines such as Hα, He I, Fe II, or Ne II (Mehner et al., 2010, 2012; Madura et al., 2012). 2D radiative transfer models and 3D hydrodynamical simulations of the wind-wind collision scenario suggest that the high-velocity secondary wind penetrates the slow and dense primary wind creating a low-density cavity in it, with thin and dense walls where the two winds interact (Madura et al., 2013; Clementel et al., 2015a,b).

Several attempts have been made to map the core of η Car and to peer into the structure of the wind-wind collision region, and of the binary itself, at scales of 5–10 astronomical units (au) or 2–4 mas. Long-baseline infrared interferometry has been a decisive technique for such studies (van Boekel et al., 2003; Weigelt et al., 2007). Astronomical Multi-BEam combineR (AMBER) observations in 2014 allowed, for the first time, the recovery of aperture-synthesis images, at a resolution of ~ 6 mas of the wind-wind collision cavity across Brγ (Weigelt et al., 2016).

Observing η Car with GRAVITY

The unique characteristics of η Car make it a good candidate for increasing our understanding of the role of multiplicity in shaping the fate of stars at the upper end of the Initial Mass Function (IMF). It was therefore selected as a target for the Guaranteed Time Observations (GTO) GRAVITY programme (GRAVITY Collaboration, 2017), with the objective of carrying out a long-term (monitoring) analysis of the wind-wind collision cavity through interferometric imaging.

The first reconstructed images, presented in GRAVITY Collaboration (2018), included data taken during the commissioning phase (in 2016) of GRAVITY and through regular P100 programmes (in 2017). η Car was observed with the Auxiliary Telescopes (ATs) using the high-spectral-resolution mode of GRAVITY. This setup allowed us to resolve several spectral lines across the target's spectrum and thereby to monitor the morphologies of the core at different Doppler velocities. In particular, we focused our efforts on mapping Brγ and the He I 2s–2p lines.

Images were recovered using SQUEEZE. Prior information necessary for the reconstruction was included in both the spatial and spectral domains to obtain simultaneous images of 35 different spectral channels, with a resolution as good as 1.75 mas (4 au; see Figure 1). Compared with the 2014 AMBER images, the GRAVITY Brγ ones revealed structural changes associated with the orbital motion of the secondary. In particular, a bright "clump" is observed towards the southeast of the central core, which was identified as part of shocked wind flowing along the inner cavity walls after the last η_B periastron in 2014.

The He I images revealed, for the first time, the distribution of this element in η Car's core. We suggest that the partially ionised He I is formed from (i) a portion of the primary wind, which is photoionised by the strong ultraviolet radiation of the η_B wind, and (ii) by the shocked material in the cavity walls. To properly quantify this scenario new spectro-interferometric images are required in combination with dedicated modelling. Two additional imaging epochs in 2018 and 2019 have been obtained with GRAVITY. From the preliminary analysis of data taken in 2018, we can confirm that the morphology of the wind-wind collision zone changes depending on the orbital phase of the secondary (Figure 2). As demonstrated in the case of η Car, GRAVITY spectro-interferometric imaging provides unique information that can help to characterise the physics associated with the morphology of complex systems at the highest angular resolution currently possible in the near-infrared.

References

Baron, F. & Kloppenborg, B. 2010, Proc. SPIE, 7734, 77344D

Buscher, D. F. 1994, *Very High Angular Resolution Imaging*, IAU Symposium, 158, 91

Clementel, N. et al. 2015a, MNRAS, 450, 1388

Clementel, N. et al. 2015b, MNRAS, 447, 2445

GRAVITY Collaboration 2017, A&A, 602, A94

GRAVITY Collaboration 2018, A&A, 618, 125

Mehner, A. et al. 2010, ApJ, 710, 729

Mehner, A. et al. 2012, ApJ, 751, 73

Madura, T. I. et al. 2012, ApJ, 647, L18

Madura, T. I. et al. 2013, MNRAS, 436, 3820

Sanchez-Bermudez, J. et al. 2018, Experimental Astronomy, 46, 457

Thiébaut, E. 2008, Proc. SPIE, 7013, 701311

van Boekel, R. et al. 2003, A&A, 410, L37

Weigelt, G. et al. 2007, A&A, 464, 87

Weigelt, G. et al. 2016, A&A, 594, A106

DOI: 10.18727/0722-6691/5171

Precision Monitoring of Cool Evolved Stars: Constraining Effects of Convection and Pulsation

Markus Wittkowski[1]
Sara Bladh[2]
Andrea Chiavassa[3]
Willem-Jan de Wit[1]
Kjell Eriksson[2]
Bernd Freytag[2]
Xavier Haubois[1]
Susanne Höfner[2]
Kateryna Kravchenko[1]
Claudia Paladini[1]
Thibaut Paumard[4]
Gioia Rau[5,6]
Peter R. Wood[7]

[1] ESO
[2] Uppsala University, Department of Physics and Astronomy, Sweden
[3] Université Côte d'Azur, Laboratoire Lagrange, Nice, France
[4] LESIA, Observatoire de Paris, Meudon, France
[5] NASA, Goddard Space Flight Center, Greenbelt, USA
[6] Catholic University of America, Department of Physics, Washington, DC, USA
[7] Research School of Astronomy and Astrophysics, ANU, Canberra, Australia

Mass loss from cool evolved stars is an important ingredient of the cosmic matter cycle, enriching the Universe with newly formed elements and dust. However, physical processes that are not considered in current models represent uncertainties in our general understanding of mass loss. Time-series of interferometric data provide the strongest tests of dynamical processes in the atmospheres of these stars. Here, we present a pilot study of such measurements obtained with the GRAVITY instrument on the Very Large Telescope Interferometer.

Cool evolved stars

Asymptotic giant branch (AGB) and red supergiant (RSG) stars are located in the Hertzsprung–Russell diagram at low effective temperatures (about 2500–4500 K). They are major contributors to the integral luminosity of stellar systems, and they are major sources of the chemical enrichment of galaxies. Owing to the low temperatures, molecules and dust can form in their atmospheres, and are subsequently expelled into the interstellar medium via stellar winds.

Both AGB stars and RSGs are affected by pulsation and convection, but RSGs show lower variability amplitudes than AGB stars. For AGB stars, it has been shown that pulsation and convection lead to strongly extended molecular atmospheres, where the temperature is low enough for dust condensation. Radiation pressure on dust then gives rise to a general mass outflow as the surrounding gas is dragged along through friction (for example, Höfner & Olofsson, 2018).

For RSGs, it has been speculated that the same processes may explain their mass loss. However, Arroyo-Torres et al. (2015) showed that current dynamic model atmospheres of RSGs, based on pulsation and convection alone, cannot explain the observed extensions of RSG atmospheres, or how they can reach distances where dust can form. This points to missing physical processes in current RSG dynamic models. It translates into uncertainties in our general understanding of mass loss, as such processes may to some degree also affect the atmospheric structures of AGB stars and other cool giants.

1D and 3D model atmospheres

Significant advances are being made in the development of dynamic atmosphere models of cool evolved stars. Latest developments include 1D DARWIN (Bladh et al., 2019), and 3D CO5BOLD radiative hydrodynamics (RHD) simulations (Freytag et al., 2017; Höfner & Freytag, 2019). In contrast to existing CO5BOLD and CODEX models, DARWIN models include the wind acceleration region, which affects atmospheric structure and molecular features (Bladh et al., 2013, 2015; Höfner et al., 2016), and may account for some of the previously found discrepancies between AGB star models and interferometric observations. Additional processes that may contribute to larger atmospheric extension in RSG dynamic models include radiation pressure on molecular lines (Josselin & Plez, 2007) or the effects of magnetic fields and Alfvén waves (for example, Airapetian et al., 2010; Cranmer & Saar, 2011; Yasuda & Kozasa, 2019; Rau et al., 2019). Radiative pressure is currently being implemented in global CO5BOLD models. Magneto-hydrodynamical effects can, in principle, be described by CO5BOLD models (Freytag et al., 2012; Steiner et al., 2014), but an application to AGB and RSG stars requires further work.

Pilot study with GRAVITY

Time-series of interferometric observations provide the strongest tests of dynamical processes in the atmospheres of evolved stars, as they spatially resolve the star and provide constraints on different atmospheric layers, following the variability cycle of the star. However, such time-series are still very rare.

Wittkowski et al. (2018) recently conducted a pilot study measuring the variability of the continuum radius and of extended molecular layers for the oxygen-rich Mira star R Peg during science verification and early (P98) science operations, using the newly available near-infrared *K*-band beam combiner GRAVITY (GRAVITY Collaboration, 2017) at the VLTI. This became possible because of the improved performance of the GRAVITY instrument compared to, for example, the Astronomical Multi-BEam combineR (AMBER), with an increased precision in visibilities, data for six baselines in one snapshot, and a spectral resolution of about 4000 across the full *K*-band.

We showed that the continuum size and the size in a bandpass that is dominated by water vapour were anti-correlated with the visual light-curve. The size in the CO (2–0) line instead follows the visual light-curve more closely, indicating a different — possibly more stable — behaviour of CO compared to water vapour (Figure 1). The wavelength-dependent visibility variations could be reproduced by a set of CODEX (Ireland et al., 2008, 2011) dynamic model atmospheres at phases between 0.3 and 0.6. However, we noticed the following issues: (1) best-fit model phases did not correspond well

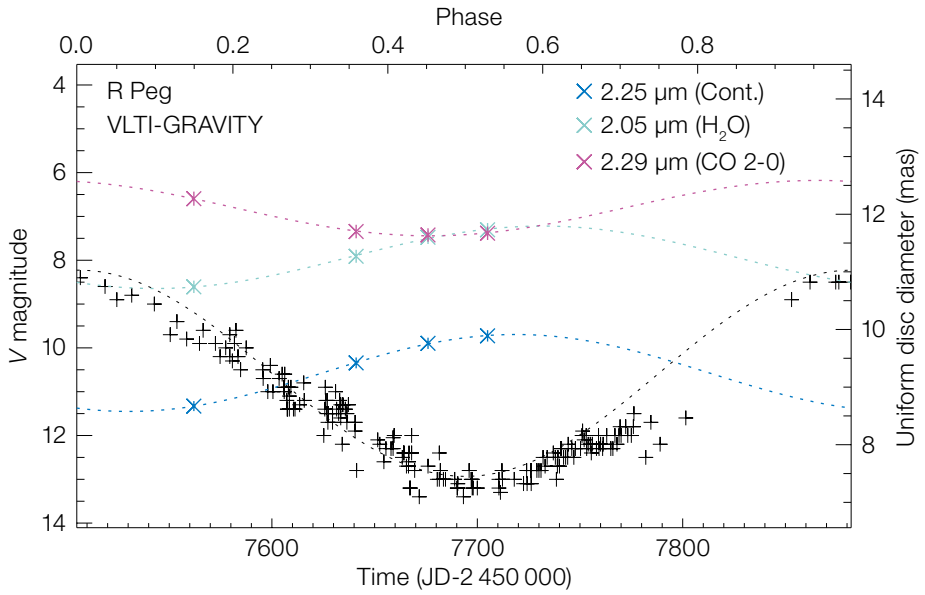

Figure 1. Variability of R Peg in the *V*-band (grey crosses) and of the uniform disc angular diameter in a near-continuum band (blue × symbols), and in bands dominated by H_2O and CO (light blue and pink × symbols, respectively). Also shown are sinusoidal fits in the corresponding colours. The minimum continuum size tracks the maximum light, which can be understood by the increase in effective temperature while the star gets smaller in radius. The minimum contribution of H_2O also tracks the maximum light, which relates to the destruction of water vapour at maximum, and formation at minimum, light. The contribution by CO is, however, largest at maximum light, indicating different, possibly more stable, behaviour compared to H_2O. From Wittkowski et al. (2018).

with observed phases, and (2) the observed amplitude of the continuum radius is 14% — this is smaller than predicted by CODEX model atmospheres (45%–67%), and closer to those predicted by 3D RHD simulations (Freytag et al., 2017). The data covered only four epochs, and more are needed to be meaningfully compared to 3D models, which show strong intra-cycle and cycle-to-cycle irregularities.

Outlook

We plan to extend the GRAVITY pilot study described above to a larger sample of cool evolved stars, and in particular to include a comparison of AGB stars, for which current models successfully predict observed extensions, and RSG stars, for which models and observations show strong discrepancies in this respect. We need a denser and wider phase sampling compared to our plot study, including intra-cycle and cycle-to-cycle variations, to be able to make meaningful comparisons to the latest dynamic models.

We will be able to use more, and better-defined, atmospheric layers compared to our pilot study by applying a tomographic method that relies on spectral masks selecting lines that form in given ranges of optical depths in the stellar atmosphere (Kravchenko et al., 2018, 2019). Combined with spectro-interferometric GRAVITY observations on the VLTI, the tomographic method will permit a simultaneous spectral and spatial characterisation of AGB and RSG star atmospheres. By extracting interferometric visibilities at wavelengths contributing to different masks, we can measure the corresponding geometrical extents of the atmosphere and recover the link between optical and geometrical depth scales.

Acknowledgements

Based on observations made with the VLT Interferometer at Paranal Observatory. We thank the GRAVITY Science Verification team[1], the GRAVITY consortium[2], the GRAVITY Collaboration (see page 20), and the ESO science operation team for the development and operations of GRAVITY, and for their great support.

References

Airapetian, V. et al. 2010, ApJ, 723, 1210
Arroyo-Torres, B. et al. 2015, A&A, 575, A50
Bladh, S. et al. 2013, A&A, 553, A20
Bladh, S. et al. 2015, A&A, 575, A105
Bladh, S. et al. 2019, A&A, 626, A100
Cranmer, S. R. & Saar, S. H. 2011, ApJ, 741, 54
Freytag, B. et al. 2012, JCoPh, 231, 919
Freytag, B. et al. 2017, A&A, 600, A137
GRAVITY Collaboration 2017, A&A, 602, A94
Höfner, S. et al. 2016, A&A, 594, A108
Höfner, S. & Olofsson, H. 2018, A&ARv, 26, 1
Höfner, S. & Freytag, B. 2019, A&A, 623, A158
Ireland, M. et al. 2008, MNRAS, 391, 1994
Ireland, M. et al. 2011, MNRAS, 418, 114
Kravchenko, K. et al. 2018, A&A, 610, A29
Kravchenko, K. et al. 2019, A&A, 632, A28
Rau, G. et al. 2019, ApJ, 882, 37
Steiner, O. et al. 2014, PASJ, 66, S5
Josselin, E. & Plez, B. 2007, A&A, 469, 671
Wittkowski, M. et al. 2018, A&A, 613, L7
Yasuda, Y. et al. 2019, ApJ, 879, 77

Links

[1] GRAVITY Science Verification: https://www.eso.org/sci/activities/vltsv/gravitysv.html
[2] GRAVITY consortium: http://www.mpe.mpg.de/ir/gravity

DOI: 10.18727/0722-6691/5172

Multiple Star Systems in the Orion Nebula

GRAVITY Collaboration (see page 20)

GRAVITY observations reveal that most massive stars in the Orion Trapezium cluster live in multiple systems. Our deep, milliarcsecond-resolution interferometry fills the gap at 1–100 astronomical units (au), which is not accessible to traditional imaging and spectroscopy, but is crucial to uncovering the mystery of high-mass star formation. The new observations find a significantly higher companion fraction than earlier studies of mostly OB associations. The observed distribution of mass ratios declines steeply with mass and follows a Salpeter power-law initial mass function. The observations therefore exclude stellar mergers as the dominant formation mechanism for massive stars in Orion.

The formation of massive stars

The formation of massive stars remains a mystery. Hidden in their parental gas and dust clouds, it is unclear how their seeds can accrete so much matter before the repulsive forces from thermal pressure and radiation prevent the formation of a protostar. The most discussed scenarios are competitive accretion and core accretion (see, for example, Tan et al., 2014 and references therein). Another possibility is the collision of two stars, merging into a more massive star.

Core accretion is a scaled-up version of standard star formation applicable to stars similar to our Sun. In this scenario it is a single core that accretes its mass independently of other sibling cores. The mass of the star is then set at the beginning of the process, determined by the available mass in the accretion volume. An alternative explanation is formation by competitive accretion (for example, Tan et al., 2014), where several cores compete for the available mass, culminating in hierarchical systems with stars of different masses. Unlike in the core-accretion model, their masses are not pre-defined, but depend on the interaction with each other. A third possibility for the formation of massive stars is stellar mergers, where two colliding stars end up in a more massive object.

High angular resolution observations are crucial to pinning down the dominant mode of massive star formation. One of the closest massive star forming regions is the Orion Nebula Cluster, located at a distance of 414 ± 7 pc (for example, Reid et al., 2014). As such the Orion Nebula has been the target of many previous observations. The superb angular resolution and sensitivity of GRAVITY using the VLTI can reveal details on the crucial scales of 1–100 au, which had remained mostly unexplored until now.

Observations with GRAVITY

We observed the 16 brightest, most massive stars in the Orion Nebula Cluster, with masses between 2 and 44 $M_{\odot}$. The observations were mostly done with the Auxiliary Telescopes in astrometric configuration. Data were reduced with the standard GRAVITY pipeline (GRAVITY Collaboration, 2017). The interferometric data were then fitted to a binary star model, providing the flux ratio of the companion to the main star, and the separation vector between the two components (GRAVITY Collaboration, 2018).

We focused first on the central region, the Orion Trapezium Cluster, home of Orion's most massive, visible star, θ^1 Ori C. The 16 observed objects have a total of 22 companions; see Figure 1 for an overview.

With GRAVITY, we found three previously unknown companions and we confirm a suspected companion for ν Ori (Grellmann et al., 2013). The newly discovered stars belong to the systems of θ^1 Ori B, θ^2 Ori B, and θ^2 Ori C. We determined their separation, and from the flux ratio we could estimate the masses of all new companions (see GRAVITY Collaboration, 2018 for more details). θ^1 Ori B is a system of particular interest, as it consists of six objects in total. These objects are all gravitationally bound, though it is suspected that the system is only temporarily stable (Close et al., 2013). θ^1 Ori C is accompanied by two companion stars, one spectroscopic companion and one known companion with a determined orbit. With GRAVITY observations, we could refine the orbit of θ^1 Ori C_2 to have a period of 11.4 ± 0.2 yr and a semi-major axis of 18.2 ± 0.3 au. Additionally, we determined a new Orbit for θ^1 Ori D_2, with a semi-major axis of 0.77 ± 0.03 au and a period of 53.05 ± 0.06 days.

Most massive stars live in multiple systems

Massive stars are more often found in multiple systems than are lower mass stars. For example, Duchene & Kraus (2013) and Sana et al. (2014) found increasing numbers of stars in companion systems with higher stellar mass. Additionally, the average number of companion stars increases with higher mass. Our observations confirm this trend and our results are comparable to those of Sana et al. (2014). Orion's O-type stars have an average of 2.3 ± 0.3 companions.

Plotting the number of all our observed stars and their companions against stellar mass, we find the mass function well described by a power law with an exponent of $\Gamma = 1.3 \pm 0.3$ (Figure 2). This matches the initial mass function (IMF) for field stars (see, for example, Salpeter, 1955).

To constrain star formation scenarios, we compare predictions to our observations. For both core accretion and competitive accretion, the number of stars in companion systems and the number of companions should rise with mass (Clarke, 2001). Therefore, both scenarios would match our observations. The situation is different for the correlation between the companion masses. While competitive accretion shows no clear correlation between the primary and secondary mass, with a mass distribution that could follow a Salpeter IMF (for example, Tan et al., 2014) or a top-heavy companion mass distribution (Bate, Bonnell & Bromm, 2002), core accretion results in a strong correlation between the companion masses, which we do not observe. Also, the companion separation should correlate with system mass for core accretion. For competitive accretion, the separation should inversely correlate with system mass (Bonnell & Bate, 2005). In Orion, we observe no correlation between separation and system mass (Figure 3), which is inconsistent with

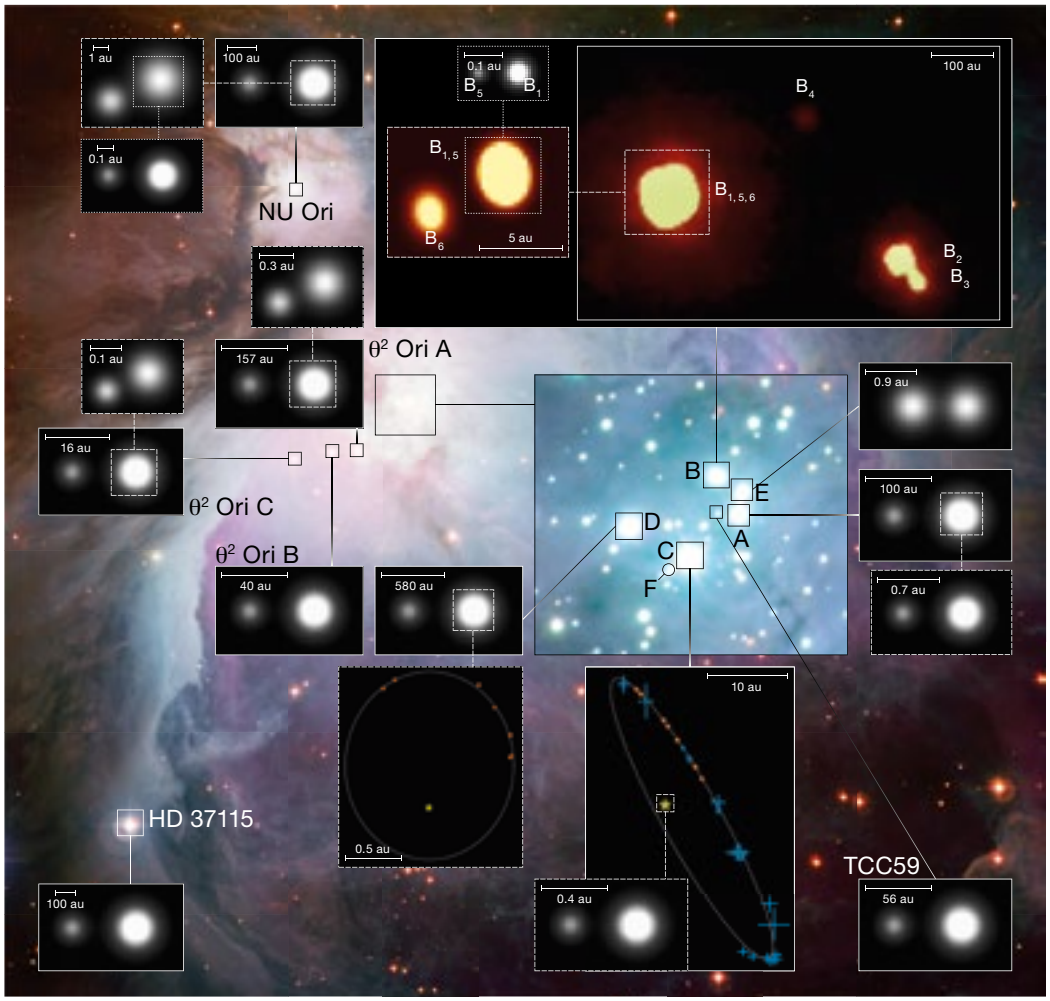

Figure 1. Overview of all observed multiple stars in the Orion Nebula. The observed 16 systems comprise a total of 22 companions. The scale of the separation of the companion is indicated in the figure. The coloured images of θ¹ Ori B are from observational data, except the greyscale B_1, B_5 system, which is only representative. The image of $B_{1,5}$ and B_6 is a reconstructed image of GRAVITY observations. The orbital positions, which are indicated for θ¹ Ori C and θ¹ Ori D, are the positions given in GRAVITY Collaboration (2018) and previous literature. The other greyscale close-up images are for illustrative purposes only. This figure is taken from GRAVITY Collaboration (2018).

Figure 3 (below). Companion separation for all of Orion's multiple star systems, sorted by mass of the primary star. Each system is indicated by a different colour. The dot size scales with the square root of the companion mass. There are as many companions in the range 0.1–1 au as in the range 1–100 au. The dashed circles around companions of θ² Ori C and TCC 59 indicate missing information about the masses. (GRAVITY Collaboration, 2018)

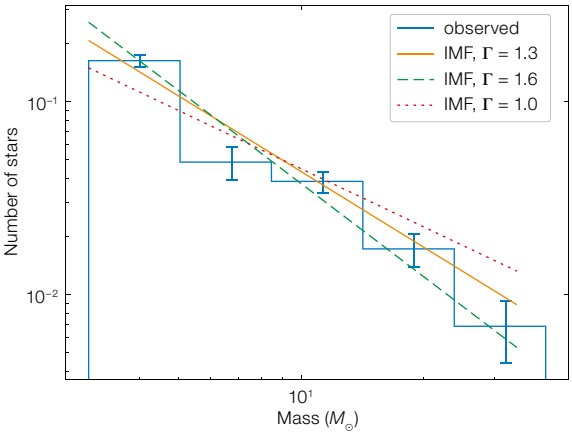

Figure 2. The observed mass distribution of the observed stars and their companions as a normalised histogram, and the initial mass functions as proposed by, for example, Kroupa (2001).

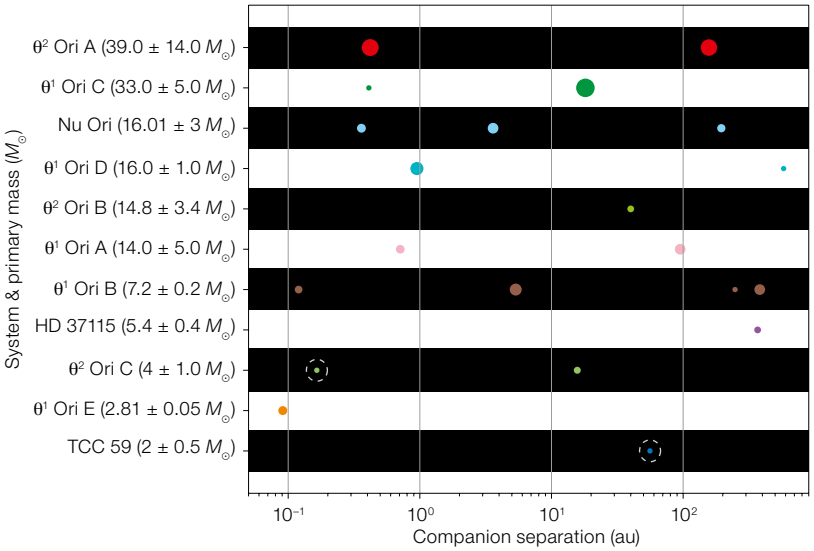

either scenario. In addition, competitive accretion predicts an anti-correlation between the mass ratio of the companion to primary star and their separation, which we do not see in our data. If stellar collisions were the dominant formation process, we would expect a strong deviation from the Salpeter IMF (Moeckel & Clarke, 2011). Thus we can exclude stellar mergers as the dominant formation mechanism for massive stars in Orion.

Summary & conclusions

We probed the Orion Nebula for massive multiple star systems with separations between 1 and 100 au. Almost all massive stars live in multiple systems. We do not see a strong preference for either core collapse or competitive accretion among the massive stars of Orion. The Salpeter IMF hints towards competitive accretion, whereas the lack of correlations between separation, system mass, primary and companion masses contradicts it. We can exclude the collision of stars as the main mechanism for the formation of high mass stars in Orion, which would result in a strong deviation from the Salpeter IMF. Our GRAVITY results highlight the crucial role of interferometry in filling the gap between 1 and 100 au, which is not accessible with traditional imaging and spectroscopic techniques.

Acknowledgements

See page 23.

References

Bate, M. R., Bonnell, I. A. & Bromm, V. 2002, MNRAS, 336, 705
Bonnell, I. A. & Bate, M. R. 2005, MNRAS, 362, 915
Clarke, C. J. 2001, *The Formation of Binary Stars*, IAU Symposium, 200, 346
Close, L. M. et al. 2013, ApJ, 774, 13
Duchêne, G. & Kraus, A. 2013, ARA&A, 51, 269
GRAVITY Collaboration 2017, A&A, 602, A94
GRAVITY Collaboration 2018, A&A, 620, A116
Grellmann, R. et al. 2013, A&A, 550, 531
Kroupa, P. 2001, MNRAS, 322, 231
Moeckel, N. & Clarke, C. J. 2011, MNRAS, 410, 2799
Reid, M. J. et al. 2014, ApJ, 783, 130
Salpeter, E. E. 1955, ApJ, 121, 161
Tan, J. C. et al. 2014, *Protostars and Planets VI*, ed. Beuther, H. et al., (Tucson: Univ. of Arizona), 149

DOI: 10.18727/0722-6691/5173

Probing the Discs of Herbig Ae/Be Stars at Terrestrial Orbits

GRAVITY Collaboration (see page 20)

More than 4000 exoplanets are known to date in systems that differ greatly from our Solar System. In particular, inner exoplanets tend to follow orbits around their parent star that are much more compact than that of Earth. These systems are also extremely diverse, covering a range of intrinsic properties. Studying the main physical processes at play in the innermost regions of the protoplanetary discs is crucial to understanding how these planets form and migrate so close to their host. With GRAVITY, we focused on the study of near-infrared emission of a sample of young intermediate-mass stars, the Herbig Ae/Be stars.

Dust in the innermost regions of the young intermediate-mass stars

The formation and evolution of protoplanetary discs are important stages in the lifetimes of stars. Terrestrial planets are born in and/or migrate into the innermost regions close to the host star. As discs evolve, different phenomena such as photoevaporation, mass-loss through winds and jets, and dynamical clearing by newly-formed planets will disperse the disc material. Thus disc evolution and planet formation are linked processes. Observing the inner regions with sufficient angular resolution is crucial for better understanding the key physical processes at play and how they combine to lead to the formation of an exoplanetary system.

Thanks to high angular resolution imaging in the optical range with the Spectro-Polarimetric High-contrast Exoplanet REsearch instrument (SPHERE; Beuzit et al., 2019), and at (sub-)millimetre wavelengths with the Atacama Large Millimeter/submillimeter Array (ALMA partnership et al., 2015), rings, gaps, spiral arms, warps, and shadows have been revealed in the outer disc on scales ranging from a few tens to a few hundreds of astronomical units (au). GRAVITY uniquely probes the innermost few au where hot gas might accrete onto the star through magnetospheric accretion or be launched through winds and jets, where dust is thermally processed, sublimated, and from where it can be redistributed into the outer disc. Identifying dust traps and other planetary signposts such as dynamical perturbations in the disc is an important goal if we are to constrain inner planet formation mechanisms.

The diverse nature of the inner discs

In this contribution, we highlight GRAVITY observations that reveal the morphology of the inner dusty discs. The near infrared emission detected with GRAVITY[1] and the Precision Integrated Optics Near-infrared Imaging ExpeRiment (PIONIER[2]; Le Bouquin et al., 2011) arises mostly in the dust sublimation front of the inner part of the protoplanetary disc. We observe wedge-shaped rims, with a smooth radial distribution of dust that is much wider than would be expected for a single dust component (GRAVITY Collaboration et al., 2019). We suggest that these inner-

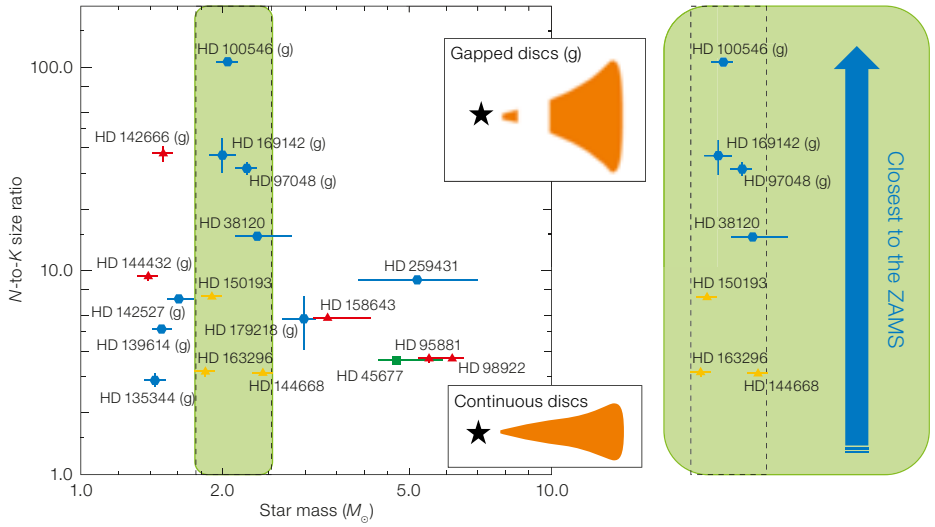

Figure 1. *N*-to-*K* size ratio of the discs as a function of the mass of the central stars. The blue diamonds denote flared/gapped discs (as sketched in the top inset), while the red triangles denote flat/continuous discs (as sketched in the bottom inset) according to the Meeus (2001) classification. The square symbol denotes an unclassified star. The gapped sources are identified as (g). The green area spots the 2 $M_{\odot}$ objects and the arrow indicates the position with respect to the Zero-Age Main Sequence (ZAMS).

most regions host grains of different sizes and/or compositions so that some can survive near the inner rim while others are further away. Moreover, GRAVITY reveals a slight asymmetry in most of these discs that could be explained by inclination effects for more than half the objects, while an intrinsic asymmetry should be invoked for others. From the observations of 27 targets, we confirm the size-luminosity relationship. For the luminous stars (around $10^3\,L_{\odot}$), a large scatter around the mean relation is observed, pointing towards a range of compositions of the inner dusty discs.

Flat, flared, gapped and continuous discs

To trace the disc regions beyond the dust sublimation rim, mid-infrared interferometry is a powerful tool, as it probes dust at temperatures down to ~ 300 K. After the MID-infrared Interferometric instrument (MIDI), the Multi AperTure mid-Infrared SpectroScopic Experiment (MATISSE[3]) can now investigate disc flaring at tens of au and can help to question disc classifications based on Spectral Energy Distributions (SEDs; Meeus et al, 2001); i.e., sources with decreasing mid-infrared SEDs exhibit a flat geometry while those with flat or rising mid-infrared SEDs have flared discs. For these latter SED shapes, Maaskant et al. (2013) proposed that they could indicate a gapped disc structure.

We compare the disc sizes in the *N*-band, derived from MIDI (Menu et al., 2015), with our *K*-band measurements. To first order, the *K*-band and *N*-band sizes increase proportionally. Using the *N*- to *K*-band size ratios as a proxy, we look for general trends for about 20 objects in our GRAVITY sample; gapped sources exhibit a large *N*-to-*K*-band size ratio, and large ratios are only observed in the low-luminosity, less massive members of our sample that are older than 1 Myr.

Evolution of the inner structure

An underlying question related to disc classification is whether the sources with flared/gapped and flat/continuous discs form an evolutionary sequence. Dullemond and Dominik (2004) proposed that discs might start out with a flared shape, then become flat when going through the process of grain growth. On the other hand, Maaskant et al. (2013) proposed that both can evolve from the primordial flared discs. More recently, Menu et al. (2015) suggested that either each group could follow a distinct evolutionary path from continuous to gapped disc, or flat gapped discs could later evolve into flared discs with larger gaps.

We use the masses and ages provided by ESA Gaia observations (Vioque et al., 2018) and focus on the relative ages of objects with similar masses to avoid well-known mass bias effects for the age estimation of the young stellar objects. For 2 $M_{\odot}$ objects, we observe a transition from flat/continuous to flared/gapped shapes, and an increase of the *N*-to-*K*-band size ratio when the relative age increases (Figure 1). However, owing to the limited size of our GRAVITY sample, we cannot establish any clear universal evolution mechanism across the Herbig

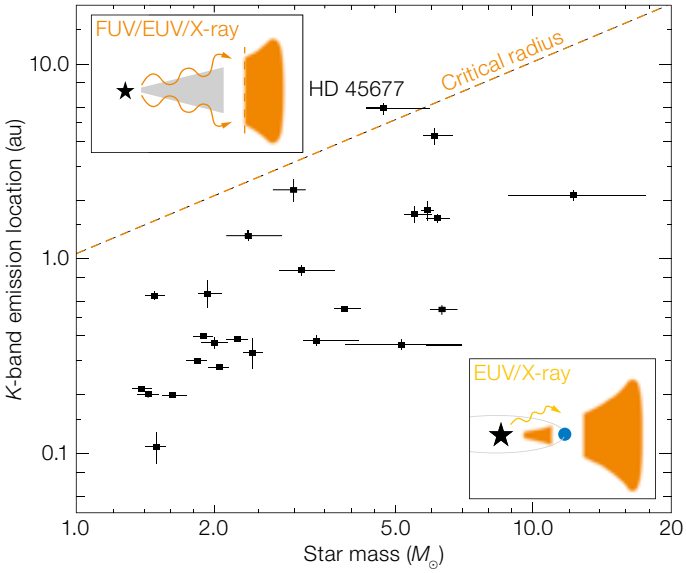

Figure 2. *K*-band emission location as measured by GRAVITY as a function of star mass. The dashed red line corresponds to the critical radius where the gap is expected to form as a result of EUV/FUV/X-ray heating from the central star. This photoevaporation phenomenon leads to a fast depletion of the inner disc and a void central cavity (as sketched in the top inset) while young planets and EUV/X-ray photoevaporation will open gaps and not deplete the inner disc quickly (bottom inset).

Ae/Be mass range and need additional observations.

Gap formation scenarios

Gaps in protoplanetary discs can be found in concentric arrangements from the inner regions out to large distances — as nicely evidenced by ALMA images (Zhang et al., 2018). Clearing by dynamical effects due to newly-born planets and photoevaporation by extreme- and far-ultraviolet (EUV/FUV) and X-ray radiation from the central star are key processes of disc dispersal through gap and inner cavity formation. In the photoevaporation scenario, gap formation takes a few 10^6 years and inner disc depletion takes about 10^5 years (Gorti et al., 2009). Since almost all the *K*-band emission we measured with GRAVITY is located at positions smaller than the critical radius where the gap is expected to form as a result of to extreme-/far-ultraviolet/X-ray heating, the discs in our sample might be shaped by forming young planets rather than by depletion resulting from photoevaporation (Figure 2).

With PIONIER, GRAVITY and MATISSE, the VLTI is perfectly equipped to reveal the gas and dust distributions in protoplanetary discs at unprecedented angular and spectral resolution.

References

ALMA Partnership et al. 2015, ApJ, 808, L1
Beuzit, J.-L. et al. 2019, A&A, 631, A155
Gorti, U. et al. 2009, ApJ, 705, 1237
Dullemond, C. & Dominik, C. 2004, A&A, 421, 1075
GRAVITY Collaboration et al. 2019, A&A, 632, A53
Le Bouquin, J.-B. et al. 2011, A&A, 935, A67
Lopez, B. et al. 2018, SPIE, 10701, 107010Z
Maaskant, K. M. et al. 2013, A&A, 555, A64
Meeus, G. et al. 2001, A&A, 365, 476
Menu, J. et al. 2015, A&A, 581, A107
Vioque, M. et al. 2018, A&A, 620, A128
Zhang, S. et al. 2018, ApJ, 869, L47

Notes

[1] GRAVITY operates in the near-infrared *K*-band, i.e., with wavelengths between 2 and 2.5 µm.
[2] PIONIER at the VLTI operates in the near-infrared *H*-band, i.e., with wavelengths between 1.5 and 1.8 µm.
[3] MATISSE at the VLTI operates in the mid-infrared *L*-, *M*-, and *N*-bands, i.e., with wavelengths between 3 and 13 µm (Lopez et al., 2018).

DOI: 10.18727/0722-6691/5174

Spatially Resolving the Inner Gaseous Disc of the Herbig Star 51 Oph through its CO Ro-vibration Emission

GRAVITY Collaboration (see page 20)

Near-infrared interferometry gives us the opportunity to spatially resolve the circumstellar environment of young stars at sub-astronomical-unit (au) scales, which a standalone telescope could not reach. In particular, the sensitivity of GRAVITY on the VLTI allows us to spatially resolve the CO overtone emission at 2.3 microns. In this article, we present a new method of using the model of the CO spectrum to reconstruct the differential phase signal and extract the geometry and size of the emitting region.

Protoplanetary discs at high angular resolution

Circumstellar discs are crucial to understanding how stars and planets form. They contain both gas and dust and, although there are many studies of the outer part of the disc, there are very few on the inner disc, in particular the inner gaseous disc. This hinders our understanding of the physical processes taking place in this inner part of the disc. In addition to the study of the size and shape of the continuum emission originating in protoplanetary discs around young stellar objects (YSOs), GRAVITY's spectral resolution of up to $R = 4000$ facilitates studies of the gaseous component of circumstellar material. The two most prominent components are hydrogen, in the form of the Brackett γ and higher levels of the Pfund recombination lines, and molecular gas as traced by CO ro-vibrational transitions. A direct tracer of the gas in the disc is the CO molecule. The CO emission is present at different scales throughout the disc: from the outer, cooler regions detected at millimetre wavelengths to the inner, warmer regions detected at near-infrared wavelengths. In particular, the CO ro-vibrational emission at 2.3 microns is a good tracer of the hot inner gaseous disc. Therefore, spatially resolved observations of the CO ro-vibrational transitions are crucial to constraining the dynamics and chemical composition of the inner dust-free disc.

The source

51 Oph is a fast-rotating star ($v \sin i$ = 267 km s^{-1}; Dunkin, Barlow & Ryan, 1997) and is located at a distance of 123 parsecs (Lindergren et al., 2016; GAIA Collaboration et al., 2018). Its spectrum is full of atomic and molecular lines and it is one of the very few Herbig Ae/Be stars that shows bright 2.3-micron CO overtone emission, making it an ideal candidate for near-infrared interferometric studies (Thi et al., 2005; Berthoud et al., 2007; Tatulli et al., 2008).

The CO spectrum of the star has been extensively studied spectroscopically

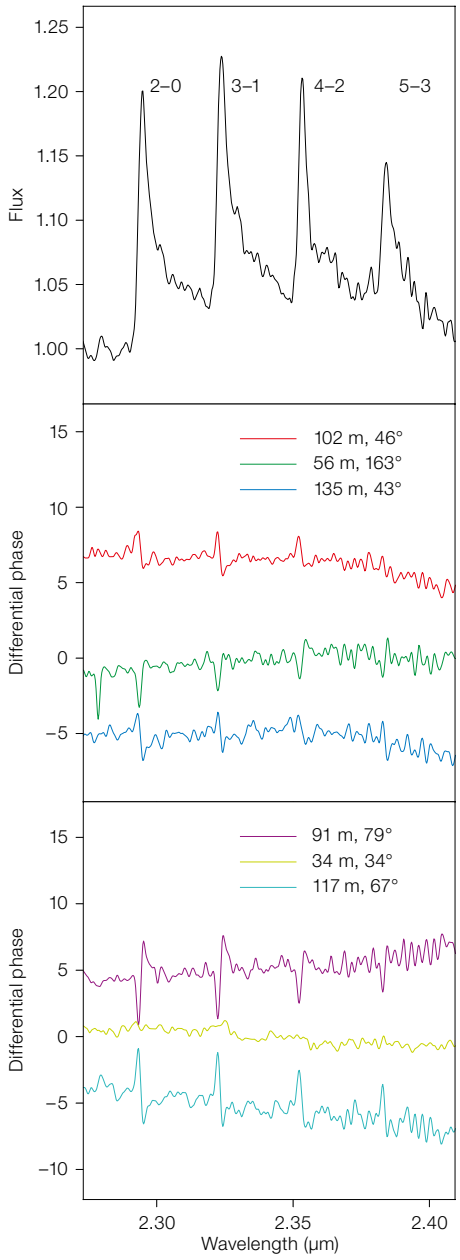

Figure 1. Spectrum (top), and differential phases of the GRAVITY interferometric data at one epoch. Each colour represents a baseline.

and indicates gas close to the star showing Keplerian rotation (Thi et al., 2005; Berthoud et al., 2007). Near-infrared interferometric observations using the Astronomical Multi-BEam combineR (AMBER) — one of the first-generation interferometric instruments on the VLTI — confirmed that the CO is emitted from the very inner disc regions, within the dust sublimation radius (Tatulli et al., 2008). Unfortunately, these observations were at low spectral resolution (R = 1500) and no differential phase signal was retrieved.

The circumstellar environment of 51 Oph

51 Oph was observed with GRAVITY during Guaranteed Time Observations (GTO) at two epochs using the 1.8-metre Auxiliary Telescopes (ATs). From an optical interferometer like the VLTI we can usually extract the following information: spectra, visibilities, differential phases and closure phases. The visibility gives an estimate of the size of the emitting region, with a visibility equal to 0 meaning a resolved source, while 1 is a point source. The differential phase is the photocentre shift of the line with respect to the continuum and the closure phase is an indicator of asymmetries in the circumstellar environment.

One epoch of our VLTI/GRAVITY observations of 51 Oph is shown in Figure 1. The spectrum shows four bright band heads (u = 2–0, 3–1, 4–2 and 5–3). The environment of 51 Oph is compact, both in the line and the continuum emitting regions. The line emitting regions originate closer to the star than the continuum. There is a strong differential phase signal (bottom panels of Figure 1) indicating a photocentre shift of the line with respect to the continuum. There is no indication of an asymmetric circumstellar environment.

By fitting our interferometric observations (i.e., spectrum, visibilities and differential phases) with a local thermodynamic equilibrium (LTE) model of the CO, we find that the CO is emitted from a relatively warm (2400 K) and dense (N_{CO} ~ 2 × 10^{21} cm^{-2}) region, consistent with gas rotating in a ring at Keplerian velocity (v sin i ~ 147 km s^{-1}) and located at roughly 0.1 au from the star (more details in Koutoulaki et al., in preparation; see also the spatial scales probed in Figure 3). From the model, an intensity map could be created since we know the intensity at each azimuthal angle. An example is shown in Figure 2 for three velocity channels at the blueshifted (left panel), peak (middle panel), and redshifted (right panel) parts of the first band head. This intensity map can be used as an input to the latest version of the interferometric software "Astronomical Software to PRepare Observations" — ASPRO2 — to simulate GRAVITY observations. By varying the inclination and position angle the software creates synthetic observations that can be compared with the real ones.

Assuming Keplerian rotation, the combination of the v sin i measurement, determination of the inclination, i, of the CO

Figure 2. Intensity maps of the blueshifted (left), peak (middle), and redshifted (right) parts of the first band head.

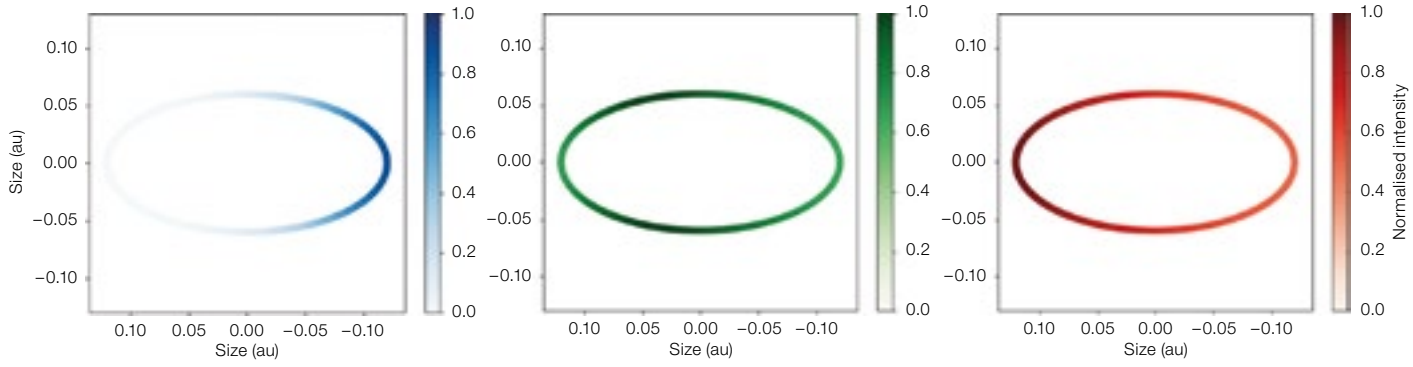

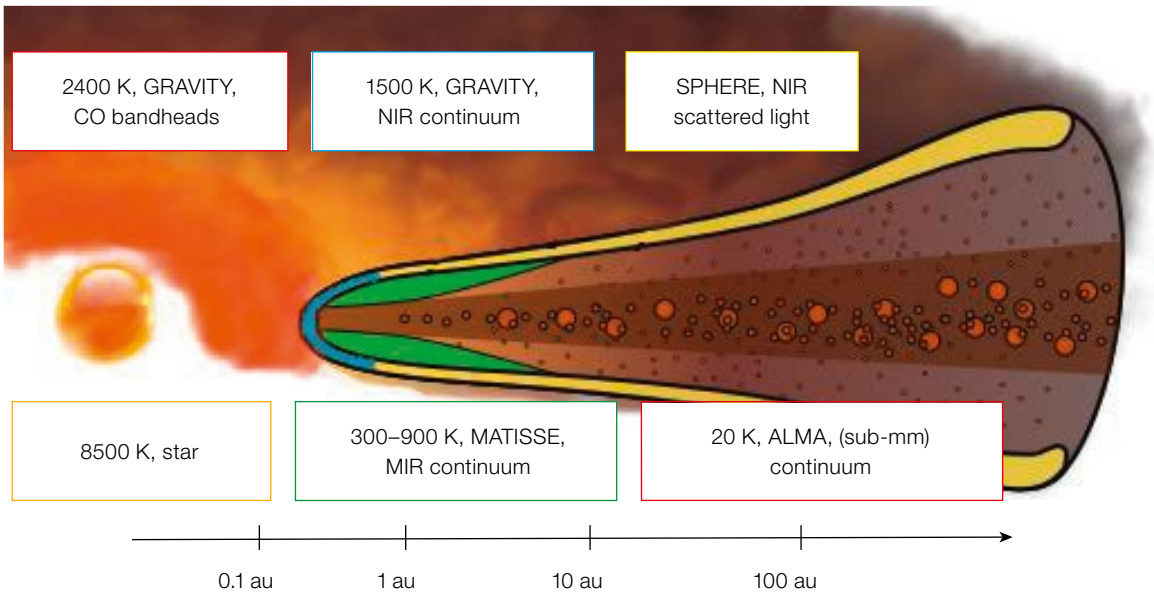

Figure 3. Cartoon of a protoplanetary disc based on Testi et al. (2014). The different boxes correspond to different spatial scales and temperatures of the disc as observed by different instruments.

ring, the angular extent of the CO, and the known distance to 51 Oph from GAIA Data Release 2, results in a direct measurement of the mass of the central star of 3.9 ± 0.6 $M_{\odot}$.

GRAVITY has opened a new window enabling the use of molecular lines to probe the circumstellar environment of young stars. This new technique of combining the spectrum fit with interferometric observables can provide new insights into the geometry and size of the gaseous disc very close to the star. In the case of 51 Oph we have been able, for the first time, to observationally constrain the physical properties of the gas at 0.1 au from the star; we find physical properties consistent with those expected from LTE models of the gas content of the disc (Muzerolle et al., 2004).

References

Berthoud, M. G. et al. 2007, ApJ, 660, 461
Dunkin, S. K., Barlow, M. J. & Ryan, S. G. 1997, MNRAS, 286, 604
Gaia Collaboration et al. 2018, A&A, 616, A1
Lindegren, L. et al. 2016, A&A, 595, A4
Muzerolle, J. et al. 2004, ApJ, 617, 406
Tatulli, E. et al. 2008, A&A, 464, 55
Testi, L. et al. 2014, *Protostars and Planets VI*, ed. Beuther, H. et al., (Tucson: University of Arizona Press), 339
Thi, W. F. et al. 2005, A&A, 430, L61

ESO/P. Carrillo

The 8.2-metre Unit Telescopes of the Paranal Observatory in silhouette against the Sun.

DOI: 10.18727/0722-6691/5175

Spatially Resolving the Innermost Regions of the Accretion Discs of Young, Low-Mass Stars with GRAVITY

Claire L. Davies[1]
Edward Hone[1]
Jacques Kluska[2]
Alexander Kreplin[1]

[1] Astrophysics Group, University of Exeter, UK
[2] Instituut voor Sterrenkunde (IvS), KU Leuven, Belgium

Low-mass, young stars — the T Tauri stars — make up the majority of young stellar objects. They have been relatively unexplored with optical long baseline interferometry owing to the cooler temperatures of their stellar photospheres which makes them fainter and more compact than the more frequently studied intermediate mass, young stars — the Herbig Ae/Be stars. With its greater flux sensitivity, GRAVITY has allowed us to explore T Tauri stars at high angular resolution in unprecedented detail. Here we present highlights from two such studies.

GRAVITY is enabling substantial progress in high-angular-resolution studies of star formation. Its spectrograph's greatly improved *K*-band flux sensitivity compared to the first-generation VLTI instrument Astronomical Multi-BEam combineR (AMBER), for example, has unlocked the previously poorly studied sample space occupied by the low-mass (T Tauri) stars — which comprise the majority of young stellar objects. The flux sensitivity is further increased by GRAVITY's unique dual-field mode which allows for longer integration observations with the spectrograph if a sufficiently bright, neighbouring star exists within a few arcseconds. GRAVITY's ability to observe with high angular and high spectral resolution across the *K*-band allows us to study the dynamic inner regions of protoplanetary discs and to directly measure the processes by which mass is accreted onto stars and launched into outflows.

Discs identified around the low-brightness stars in the binary CO Ori

Wide-separation young stellar binary systems often feature circumprimary and circumsecondary discs. During GRAVITY science verification, we used the VLTI's Auxiliary Telescopes (ATs) to observe the individual components of the CO Ori young stellar binary (Programme ID 60.A-9159; PI Davies). While the primary component (CO Ori A) was sufficiently bright (K = 6.0 magnitudes) for standard single field mode observations, the secondary (CO Ori B: K = 9.0 magnitudes) required GRAVITY's unique dual-field mode. Our observations confirmed the existence of individual circumstellar discs around both components and spatially resolved them for the first time.

CO Ori B displayed Brγ emission in its spectrum, which is typically associated with accretion and related outflow processes in young stars. This provided further evidence for the existence of a circumsecondary accretion disc. Meanwhile, the absence of Brγ emission in the spectrum of CO Ori A may indicate that accretion onto the primary star is weaker or otherwise inhibited. We investigated whether the characteristic size of the near-infrared emission is consistent with the location of the dust sublimation rim, as has been seen to be the case for discs around more massive young stars (for example, Lazareff et al., 2017). We compared the continuum visibilities to geometric models incorporating a central point source and a Gaussian component, finding a characteristic radius of 2.31 ± 0.04 milliarcseconds. At first glance, this appears large compared with the expected location of the dust sublimation rim and observations with GRAVITY on longer baselines are required to confirm this result.

CO Ori A also exhibits a 12.4-year periodicity in its optical photometry (Rostopchina et al., 2007), potentially indicating the presence of an additional, as yet undetected, companion. Using our best-fit geometric modelling result and the fringe tracker visibilities and closure phases obtained for CO Ori A, we searched for evidence of off-centre brightness contributions which may indicate the presence of such a companion. Within the field of view probed by our short baseline observations, we found no evidence for an additional companion to CO Ori A. Furthermore, we were able to rule out the presence of companions providing as much as 3.6 per cent of the total *K*-band flux within 7.3 to 20 milliarcseconds (Figure 1). These results are presented in greater detail in Davies et al. (2018).

Magnetospherically truncated discs

In 2018, we used GRAVITY's high spectral dispersion (R = 4000) mode to observe the low-mass, young star CW Tau (Programme ID 102.C-0755; PI Hone) in single-field mode. We fit the fringe tracker visibilities with a two-dimensional geometric model comprising a central point source (simulating the star), a ring (simulating

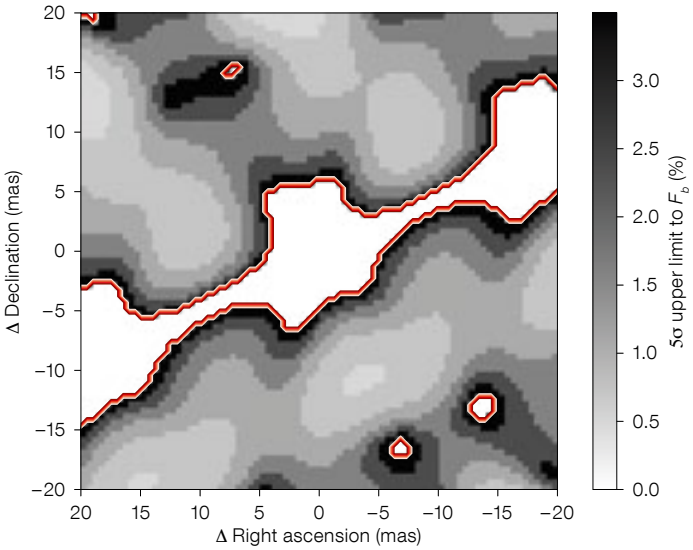

Figure 1. CO Ori A sensitivity map produced using the best-fit model from our modelling of the continuum visibilities. Each pixel in the map is coloured to reflect the maximum possible flux contribution that a companion could have at that position and remain undetected. As our observations do not sample the entire uv plane, we are not sensitive to companions in regions outlined in red.

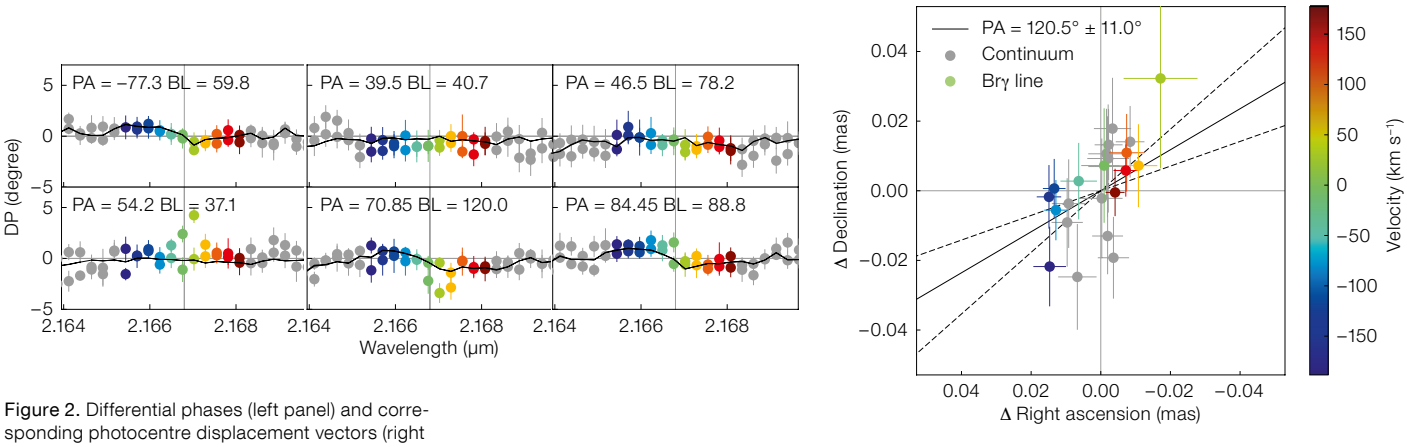

Figure 2. Differential phases (left panel) and corresponding photocentre displacement vectors (right panel) across the Brγ line for CW Tau. The black lines in the left panel indicate how well the photocentre shifts match the differential phases. The solid black lines in the right panel show the best-fit position angle of the motion between redshifted and blueshifted vectors, with the dashed line indicating the uncertainty.

disc emission on milliarcsecond scales) and an extended Gaussian component (simulating over-resolved larger-scale disc emission). The best-fit ring radius from our model (0.56 ± 0.2 milliarcseconds) corresponds to a physical distance of 0.074 ± 0.03 astronomical units. We find this distance to be consistent with the magnetospheric truncation radius and, from this, estimate a dipolar magnetic field component strength of ~ 2 kG for CW Tau. This value is consistent with those previously found for low-mass young stars via spectropolarimetric techniques (for example, Donati et al., 2010; Hill et al., 2019).

We also used our differential phases to calculate model-independent photocentre shifts across the Brγ emission line, tracing the small-scale displacement of the centroid as a function of wavelength. The photocentre displacement vectors reveal a clear displacement between redshifted and blueshifted material along a position angle of 120.5 ± 11.0 degrees, (Figure 2). The position angle of the motion traced by the photocentre shifts is closer to the minor axis of the disc of CW Tau as seen by ALMA (150.7 degrees; Bacciotti et al. 2018), suggesting that the Brγ emission predominantly traces motion out of the disc plane. This indicates the existence of a complex velocity field traced by the Brγ emitting gas, such as the launching of a jet or the motion of material being carried along magnetospheric accretion funnels. Indeed, the presence of a jet emerging away from the star-disc system, towards the south-east, along a position angle of ~ 150 degrees has been observed previously by, for example, Gomez de Castro (1993) and McGroarty, Ray & Froebrich (2007). These results form part of the PhD thesis of Edward Hone and will be presented in more detail in Hone et al. (in preparation).

GRAVITY's impact and outlook for the future

GRAVITY has extended high-resolution studies of star formation to the low-mass T Tauri stars. The availability of four-telescope beam combination has also enabled more efficient uv-plane sampling. The arrival of NAOMI, the adaptive optics system for the ATs, during the summer of 2019 has further improved the flux sensitivity and we look forward to further probing how well our understanding of star formation, garnered from the study of intermediate-mass young stars, is transferable to the low-mass T Tauri stars.

Acknowledgements

We acknowledge support from ERC Starting Grant "ImagePlanetFormDiscs" (Grant Agreement No. 639889) and help from ESO staff astronomers and the GRAVITY consortium and Science Verification team in the execution and reduction of our observations.

References

Bacciotti, F. et al. 2018, ApJL, 865, 12
Davies, C. L. et al. 2018, MNRAS, 474, 5406
Donati, J.-F. et al. 2010, MNRAS, 409, 1347
Gomez de Castro, A. I. 1993, ApJL, 412, 43
Hill, C. A. et al. 2019, MNRAS, 484, 5810
Lazareff, B. et al. 2017, A&A, 599, 85
McGroarty, F., Ray, T. P. & Froebrich, D. 2007, A&A, 467, 1197
Rostopchina, A. N. et al. 2007, Astron. Rep., 51, 55

ESO/S. Otalora

The landscape of the Chajnantor Plateau on which the antennas of the Atacama Large Millimeter/submillimeter Array (ALMA) are located.

DOI: 10.18727/0722-6691/5176

When the Stars Align — the First Resolved Microlensed Images

Subo Dong[1]
Antoine Mérand[2]
Françoise Delplancke-Ströbele[2]
Andrew Gould[3,4,5]
Weicheng Zang[6]

[1] Kavli Institute for Astronomy and Astrophysics, Peking University, Beijing, China
[2] ESO
[3] Max Planck Institute for Astronomy, Heidelberg, Germany
[4] Korea Astronomy and Space Science Institute, Daejon, Republic of Korea
[5] Department of Astronomy, Ohio State University, Columbus, USA
[6] Department of Astronomy and Tsinghua Centre for Astrophysics, Tsinghua University, Beijing, China

Using GRAVITY, we have resolved the two images of a microlensed source star for the first time, more than a century after Einstein first predicted that such image splitting could be caused by the gravity of another (lens) star along the line of sight to the source. We have measured the angular Einstein radius (almost exactly half the image separation) to be 1.87 milliarcseconds, with a precision of just 30 microarcseconds. The measurement also yields the direction of the relative motion of the lens with respect to the source. These results, combined with other, so-called microlens parallax measurements, yield the lens mass and distance. While this lens is an ordinary luminous star, the same technique could be applied in the future to measure the mass and distance of completely dark objects, such a black hole. In fact, while black holes in binaries have been found from X-ray and LIGO gravitational-wave observations, and are likely to be found in the future by Gaia astrometry, gravitational microlensing is the only known way to find isolated black holes. Our detection using GRAVITY on the VLTI opens the path to such measurements of isolated black hole masses.

Introduction

In 1936, after persistent prodding by the amateur scientist Rudi Mandl, Albert Einstein reluctantly published the idea of gravitational microlensing (Einstein, 1936), which was "a little calculation" he had carried out 24 years earlier. According to general relativity, when an object (i.e., a lens) aligns closely with a background star (i.e., a source) along the line of sight to the observer, the light rays from the source are bent when passing by the lens and subsequently form images. In the ideal case of perfect alignment, the bent light rays form a ring-like image (called the Einstein ring); more typically, there are two arc-shaped images with a separation on the scale of the Einstein ring. For microlensing in the Galaxy, the angular radius of the Einstein ring (the angular Einstein radius) is on the order of only a milliarcsecond.

Einstein's reluctance to publish was because he saw little in the way of observational prospects; he asserted that "*there is no hope of observing this phenomenon directly*". He had two reasons for thinking this, both of which relate to the minuscule angular size of the Einstein ring. First, for microlensing to occur, two stars need to align within the Einstein ring, and the probability of this is tiny, no greater than one in a million towards any star in the Galaxy. Second, he anticipated that no instruments could resolve the images, and thus the only observable effect would be the brightening of the source.

Since 1993, armed with wide-field telescopes and CCD cameras, time-domain surveys have vastly exceeded Einstein's pessimistic expectation and found tens of thousands of microlensing events so far by photometrically monitoring almost a billion stars in dense stellar fields (primarily the Galactic bulge). During these events, the brightness of the source usually varies over a few weeks as the lens star moves with a relative proper motion of several milliarcseconds per year. Microlensing events have yielded rich astrophysical results, including the discovery of nearly a hundred extrasolar planets.

Microlensing event detected by GRAVITY

It was not until November 2017 that microlensed images were successfully resolved for the first time (Dong et al., 2019), defying Einstein's dismissal. Our team achieved this by observing the microlensing event TCP J0507+2447 with the GRAVITY instrument (GRAVITY Collaboration, 2017) on the Very Large Telescope Interferometer (VLTI). Our observations allow us to measure the

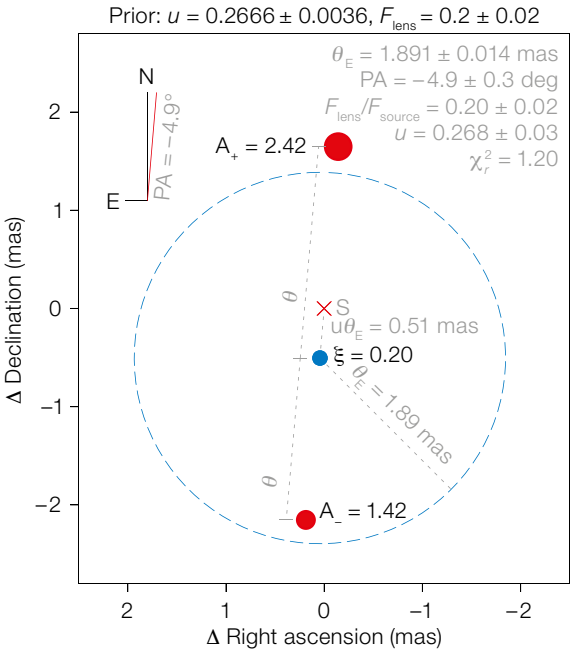

Figure 1. Model of the apparent image. The two red dots are the major and minor images — the sizes of the dots do not represent the actual apparent sizes of the images, but rather an indication of their respective fluxes. The "x" symbol is where the unlensed source would be (labelled "S"). The blue dot is the lens position with its flux, and the blue dashed circle is its Einstein ring. Flux is expressed in fractions of unlensed source flux.

angular Einstein radius at 2% precision: 1.87 ± 0.03 milliarcseconds (see Figure 1). Interferometric resolution of images can unleash microlensing's unique potential to find isolated stellar-mass black holes (BHs) lurking in the Galaxy by lifting the degeneracy between mass and distance in the analysis of microlensing light curves.

LIGO/VIRGO's astonishing discoveries of merging BHs (Abbott et al., 2016) have raised an important open question: how to form BHs with a few tens of solar masses? Whether they are the end points of massive stars or have exotic origins in the early universe, theories predict that isolated (single) BHs must exist. The relative frequency between the single and binary BH populations can provide crucial clues to the formation mechanism. However, limited by the detection techniques, all known stellar-mass BHs are found in binaries.

Microlensing holds great promise in probing the important yet uncharted parameter space of isolated BHs. Estimates by Gould (2000) suggest that, amongst the microlensing events detected to date, many hundreds may involve BH lenses. But thus far only a few BH candidates have been reported. This is due to the mass-distance-velocity parameter degeneracy, which makes it impossible to definitively distinguish BHs from low-mass stars. All existing BH candidates have relatively long event timescales, which can be due to the large Einstein radii of BH lenses with high masses. But a large Einstein radius can also be produced by a low-mass stellar lens at a close distance. Alternatively, a slow relative proper motion between the lens and source stars may induce a long timescale even with a moderate Einstein radius.

To completely break the degeneracy, two additional observables are required besides the microlensing event timescale. One is called the "microlensing parallax", which depends on the Einstein radius projected onto the observer's plane. It can be constrained for long events from the distortion of the light curves induced by the acceleration of the Earth while it orbits the Sun or by comparing the ground-based observations with simultaneous light curves from a space telescope in heliocentric orbit. The angular Einstein radius measured from the VLTI resolution of microlensed images is the other missing ingredient that can yield unambiguous determination of the lens mass and thereby definitively identify a BH lens.

The lens of TCP J0507+2447 is not a BH but a low-mass star. Nevertheless, it can serve as a testbed for the above-mentioned approach of lens mass determination. In an independent effort, another research team has measured the lens flux with Keck adaptive optics images, and by combining this with our precise VLTI angular Einstein radius measurement, they find that the lens is a dwarf star of 0.58 ± 0.03 $M_{\odot}$ (Fukui et al., 2019). Our team (Zang et al., 2019) has measured the microlens parallax using the Spitzer light curves, and by combining the VLTI angular Einstein radius, the lens is found to be 0.50 ± 0.06 $M_{\odot}$. The good agreement between the results of these two approaches demonstrates the robustness of our method. Remarkably, around the peak of the light curve of TCP J0507+2447, there was a short-lived anomaly lasting a few hours, suggesting that the lens star has a 20-Earth-mass planet at around 1 astronomical unit (Nucita et al., 2018; Fukui et al., 2019).

The possibility of using the VLTI to resolve microlensing images was first proposed by Delplancke et al. (2001), but it had proven to be extremely challenging, with numerous failed attempts prior to our observations. The major challenge had been the difficulty of identifying a sufficiently bright target for the interferometric observations. A confluence of lucky circumstances facilitated our success. Unlike the vast majority of microlensing events found by professional wide-field surveys towards the Galactic bulge, TCP J0507+2447 was serendipitously discovered by the Japanese amateur astronomer T. Kojima, and the source is at 800 pc towards the Galactic anti-centre, making it one of the closest microlensing events ever found. Our DDT proposal (2100.D-5031) was quickly accepted, and an ongoing VLTI run allowed our GRAVITY observations to be conducted within about a week of the initial discovery. And thanks to the exceptional site conditions, we were able to observe it near the magnitude limit of VLTI/GRAVITY at a relatively high airmass of ~ 1.5.

The exceptional sensitivity of VLTI/GRAVITY and the advent of all-sky bright transient surveys such as ASAS-SN and Gaia provide an unprecedented opportunity to obtain more resolved microlensing images. We hope to carry out a systematic survey towards the first definitive identification of an isolated stellar-mass black hole.

References

Abbott, B. et al. 2016, Phys. Rev. Lett., 116, 1102
Einstein, A. 1936, Science, 84, 506
Dong, S. et al. 2019, ApJ, 871, 70
Delplancke, F. et al. 2001, A&A, 375, 701
Fukui, A. et al. 2019, AJ, 158, 206
Gould, A. 2000, ApJ, 535, 928
GRAVITY Collaboration 2017, A&A, 602, 94
Nucita, A. et al. 2018, MNRAS, 476, 2962
Zang, W. et al. 2019, submitted to ApJ, arXiv:1912.00038

DOI: 10.18727/0722-6691/5177

Hunting Exoplanets with Single-Mode Optical Interferometry

GRAVITY Collaboration (see page 20)

The GRAVITY instrument was primarily conceived for imaging and astrometry of the Galactic centre. However, its sensitivity and astrometric capabilities have also enabled interferometry to reach a new domain of astrophysics: exoplanetology. In March 2019, the GRAVITY collaboration published the first spectrum and astrometry of an exoplanet obtained by optical interferometry. In this article, we show how this observation is paving the way to even more exciting discoveries — finding new planets, and characterising their atmospheres.

New opportunities, new challenges

With the 2019 Nobel Prize, jointly awarded to Michel Mayor and Didier Queloz, the field of exoplanet research received worldwide recognition. It is true that for the first 20 years, the domain was more akin to a giant search for Easter eggs. The rarity of each discovery meant it had a major impact. The field was later significantly boosted by the space-based missions CoRoT (Convection, Rotation and planetary Transits), Kepler and now TESS (Transiting Exoplanet Survey Satellite), resulting in the discovery of thousands of exoplanets, and the development of a large community including many young scientists. The success of transit photometry, accompanied by a steady increase in the capabilities of stable high-precision radial velocity instruments — in which ESO has invested significantly; for example, the High Accuracy Radial velocity Planet Searcher (HARPS) and the Echelle SPectrograph for Rocky Exoplanet and Stable Spectroscopic Observations (ESPRESSO) — now allows the analysis of the mass-separation distribution of planets, revealing gaps such as the hot Neptune desert (Neptune-sized planets within ~ 1 astronomical unit).

The next challenge in the field is the characterisation of exoplanetary atmospheres through spectroscopy. Until now, the technique has been dominated by high-resolution spectroscopy of evaporating atmospheres. With the CARMENES instrument (Calar Alto high-Resolution search for M dwarfs with Exoearths with Near-infrared and optical Échelle Spectrographs), for example, it is possible to constrain the level of atmospheric evaporation from the observation of a He I line (Alonso-Floriano et al., 2019). However, transit spectroscopy is limited to probing the upper atmosphere, and is inherently constrained by the duration of the transit. In the long term, the most promising technique is direct spectroscopy, where the light of the planet (either reflected light or thermal emission) is directly imaged on a spectrograph.

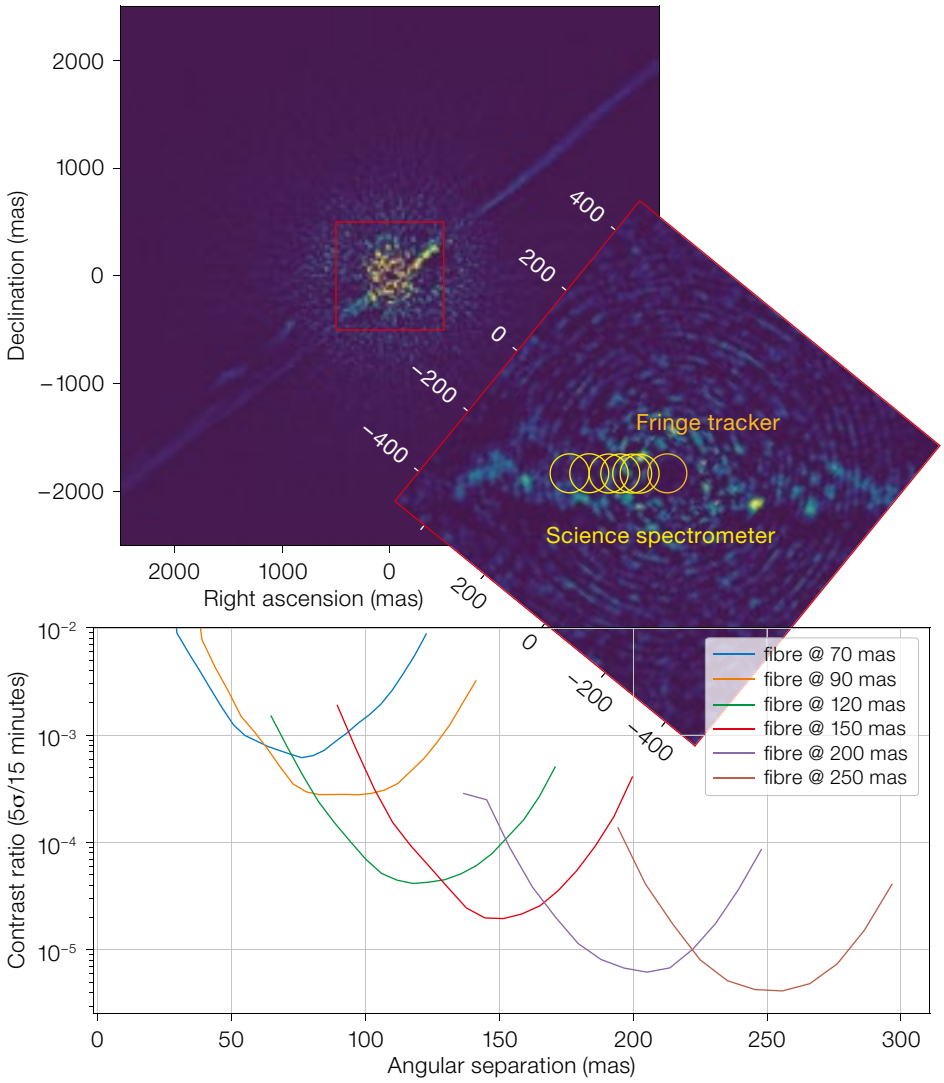

Figure 1. Upper panels: SPHERE observations of AU Mic (data from the InfraRed Dual-band Imager and Spectrograph [IRDIS] and the infrared Integral Field Spectrograph [IFS]; Boccaletti et al. 2018). Over-plotted on the IFS observation are the GRAVITY single-mode fibres. The sizes of the circles correspond to the field of view of GRAVITY. The fringe-tracker fibre is situated on the star, while the spectrometer's fibre is positioned at separations between 70 and 250 mas to the south-east of the star. From each position of the fibre, a 5-σ dynamic range is extracted and is plotted on the contrast curve. At 120 mas, a dynamic range of 4×10^{-5} is achieved. At 250 mas, the dynamic range is 4×10^{-6} (13.5 magnitudes).

This is where GRAVITY enters the field. A good exoplanet imager must have two main characteristics: an instrumental capability to remove the stellar diffraction pattern (to decrease the photon noise), and a numerical capability to remove the stellar speckles (to distinguish the planet). On an instrument like the Spectro-Polarimetric High-contrast Exoplanet REsearch (SPHERE) instrument, the former is done by means of a coronagraph,

while the latter uses angular or spectral differential imaging techniques (ADI and SDI). On GRAVITY, an off-axis single-mode fibre plays the role of a coronagraph: placed on the planet, its limited field of view filters out the stellar light. The GRAVITY interferometer surpasses single-dish instruments in post-detection speckle removal: the angular resolution of about 3 milliarcseconds (mas) yields an unprecedented capability to distinguish speckles from planetary photons.

GRAVITY as a planet hunter

GRAVITY's high dynamic range at angular separations as small as 100 mas is obtained thanks to this exquisite post-processing. Figure 1 shows GRAVITY observations of the star AU Mic. The disc of AU Mic has prominent structures, which are resolved with SPHERE (Boccaletti, Thalmann & Lagrange, 2015). GRAVITY looks for point-like sources, of size smaller than its interferometric resolution (< 3 mas). Larger objects are not seen in the coherent flux of the interferometer.

The disadvantage of the single-mode interferometer is its field of view, which is given by the diffraction limit of the telescope (60 mas in the *K*-band for the VLT Unit Telescopes). Therefore, while the fringe tracker fibre stays on the star, the science fibre (which feeds the spectrograph) is placed at different positions across the disc. This is how GRAVITY hunts for exoplanets; it dithers the position of the fibre to cover a large area. In the case of AU Mic, we took advantage of the fact that we are only looking for a planet along an edge-on disc, so we only had to scan one line, thereby minimising the required telescope time.

In the resulting dataset, which covers only the south-eastern part of the disc, no detection was made. The dynamic range achieved by GRAVITY, with 15-minute exposures, is 11 magnitudes at 120 mas (5-σ). At 250 mas the dynamic range is even higher, reaching 13.5 magnitudes. This is several magnitudes fainter than what was achieved with aperture masking (Gauchet et al., 2016), and a completely new domain compared to what could be done with ADI and SDI techniques on a single 8-metre telescope.

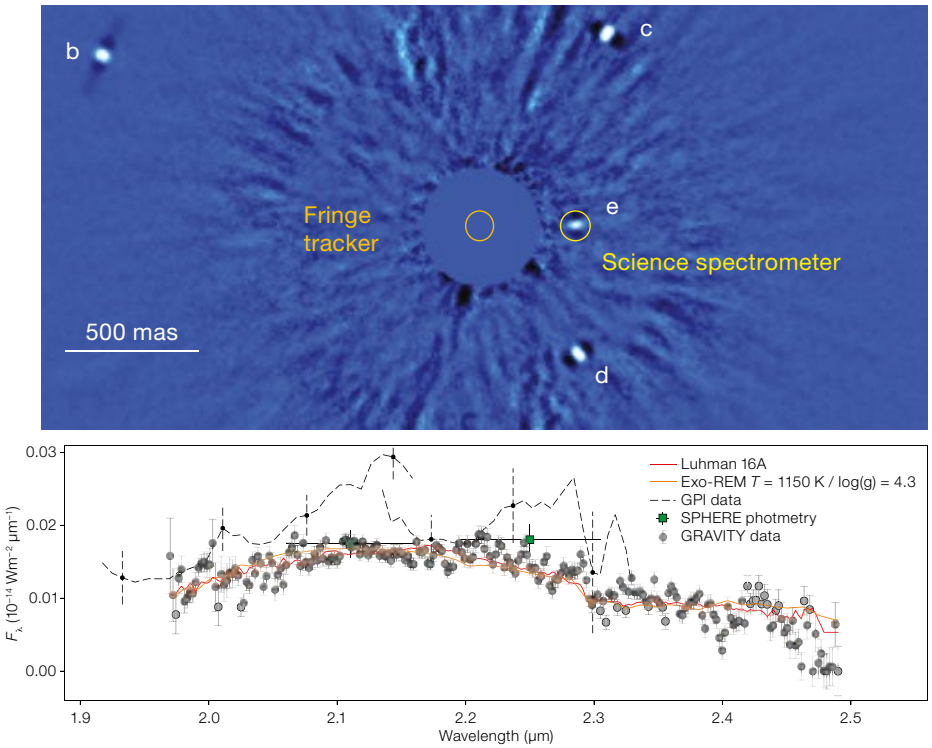

Figure 2. Upper panel: SPHERE/IRDIS image of HR8799 acquired with a broadband *H*-filter (from Wertz et al., 2017). As in Figure 1, we put the fringe-tracker fibre on the star. The science spectrometer fibre is on HR8799e. The sizes of the circles correspond to the GRAVITY field of view. Below: GRAVITY *K*-band spectrum of HR8799e at spectral resolution 500 (grey points) after 2 hours of integration. The dashed curve is the *K*-band Gemini Planet Imager (GPI) spectrum from Greenbaum et al. (2018), showing speckle contamination. (GRAVITY Collaboration et al., 2019).

GRAVITY as a way to characterise exoplanet atmospheres

In addition to its dynamic range, GRAVITY's angular resolution yields i) precise astrometry (between 10 and 100 µas) and ii) *K*-band spectra mostly unbiased by stellar light. Fortunately, such near-infrared spectra are rich in many molecular absorption lines: for example, H_2O, CO, CO_2, CH_4, N_2O. We applied this to HR8799e in GRAVITY Collaboration et al. (2019). HR8799e is the innermost object in a multi-planetary system. The angular separation to its host star is 380 mas, and the contrast is close to 11 magnitudes in the *K*-band. The young planet has an effective temperature of 1150 K, still hot from its formation. The spectra, shown in the bottom panel of Figure 2, show the CO absorption bands — no CH_4 absorption is detected. This gives clues that help to characterise the atmosphere. The difficulty in interpreting the data lies in the complex physical processes at work. Radiative transfer is used to derive the pressure-temperature curves, but clouds at different altitudes, with various compositions and possibly also heterogeneous, modify the temperature distribution. Chemical disequilibrium also adds complexity, with the necessity to add chemical timescales and mixing coefficients. In short, models need to be challenged by observations, and GRAVITY data is meeting that challenge.

In the near future, following the recent upgrade of GRAVITY's high-resolution grism, a resolution of 4000 will be achievable on exoplanets — a significant increase compared to the previous resolution of 500 (because of limited sensitivity). GRAVITY will therefore continue to challenge models of exoplanetary atmospheres, requiring simulations with more resolution and more complex chemical processes. One exciting prospect, for example, is the detection of C_{13} isotopes (Mollière & Snellen, 2019). In parallel, the recent development of atmospheric parameter retrieval is an exciting new technique, which performs better than

fitting a grid of models. The aim is to obtain direct estimates of atomic ratios. One of them, the atmospheric C:O ratio, is currently believed to be a key tracer of an exoplanet's formation history (Öberg, Murray-Clay & Bergin, 2011). With GRAVITY, we will soon show that we are able to measure this C:O ratio (GRAVITY Collaboration et al., in press).

Acknowledgements

See page 23.

References

Alonso-Floriano, F. J. et al. 2019, A&A, 629A, 110
Boccaletti, A., Thalmann, C. & Lagrange, A. M. 2015, Nature, 526, 230
Boccaletti, A. et al. 2018, A&A, 614A, 52B
Gauchet, L. et al. 2016, A&A, 595A, 31G
GRAVITY Collaboration et al. 2019, A&A, 623, 11
Greenbaum, A. Z. et al. 2018, AJ, 155, 226G
Mollière, P. & Snellen, I. A. G. 2019, A&A, 622A, 139
Öberg, K. I., Murray-Clay, R. & Bergin, E. A. 2011, ApJ, 743L, 16O
Wertz, O. et al. 2017, A&A, 598, A83

ESO/Digitized Sky Survey 2. Acknowledgement: Davide de Martin

Wide-field image showing the field in the constellation of Pegasus centred on HR8799.

ESO/M. Zamani

Students and project supervisors at the First ESO Summer Research Programme pose for a photo at the Supernova Planetarium and Visitor Centre (see p. 57).

The ESO contract for the design and production of the cell for the M5 mirror of the Extremely Large Telescope was signed with SENER Aerospacial (Spain) on 29 November 2019. The contract was signed by the ESO Director General Xavier Barcons and the General Director of SENER Aeroespacial José Julián Echevarría.

DOI: 10.18727/0722-6691/5178

Light Phenomena Over ESO's Observatories IV: Dusk and Dawn

Lars Lindberg Christensen[1]
Petr Horálek[1]

[1] ESO

Several interesting atmospheric phenomena take place during dusk and dawn, associated with the setting and rising of the Sun and Moon. Here, the most important of these are discussed in the context of ESO observing sites. This is the fourth article in a series about a range of light phenomena that can be experienced at ESO observatories.

Sunsets

Sunsets mark the daily transition from light to darkness and can be among the most beautiful and evocative light phenomena that can be seen in the sky[a]. Everyone on the planet has experienced the change in light and its effects on their mood when the Sun disappears and the night begins.

The colours of sunrise and sunset are usually very dynamic in the Atacama Desert. At the Paranal and La Silla observatories, they are enhanced by three additional factors: the high altitude, where the air is thinner and clearer; unobstructed views; and the relative vicinity to the ocean, where high levels of humidity lead to strong scattering effects[1] (Zieger et al., 2013). The sunsets in particular often paint deep colours over the horizon (Figure 1).

G. Hüdepohl (atacamaphoto.com)/ESO

Figure 1. Looking east at dusk at the Paranal Observatory. The pink-coloured Belt of Venus is followed by the Earth shadow over the horizon.

The colour and appearance of the sunset are very sensitive to clouds and the aerosol content of the upper atmosphere — no two sunsets are identical. Exceptional circumstances can have a big impact too; powerful volcanic eruptions, for example, can increase the dust content at 15–30 km altitude in the atmosphere which can create particularly magnificent sunsets (Moreno et al., 1965). In 1883, the volcano Krakatoa erupted in Indonesia and spectacular sunrises and sunsets were subsequently seen all over the world, glowing with unusual colours. There have also been strong "volcanic sunsets" in living memory, including those related to Mount St. Helens in 1980, El Chichón in Mexico in 1982, and Mt. Pinatubo in the Philippines in 1991–92. The most significant sunsets observed in recent times were seen worldwide after the eruption of Mount Kasatochi (Waythomas et al., 2010). They lasted from the end of August 2008 until at least January 2009. It may well be considered an irony of nature that volcanoes, which are so powerfully destructive, give rise to such beautiful light phenomena.

At least once within the last hundred years or so there has been a different, quite exciting, cause of exceptional sunsets: an astronomical event. In 1908, an object — most likely a 100-metre sized meteoroid — exploded over Tunguska in Siberia (Gladysheva, 2007), and in the following period unusual colours at sunset followed by very bright nights were observed in many parts of the world (Kundt, 2001; Longo, 2007).

Figure 2. Alpenglow seen from above ESO's Paranal Observatory. The VLT and VISTA domes are coloured red during the sunset.

Alpenglow

When the Sun is just below the horizon, the colour of the sky on the western horizon takes on a warm yellow or yellow-red hue and mountains and buildings to the east appear to glow red (Figure 2). This phenomenon is named Alpenglow. A well-known example is Uluru in Australia, whose red colour becomes intensified at twilight. Alpenglow can even be seen in cities.

Crepuscular and anticrepuscular rays

Most of you will have witnessed the rays of light that sometimes shine through gaps in cloud cover and illuminate the land below. Especially in rainy weather,

R. Wesson/ESO

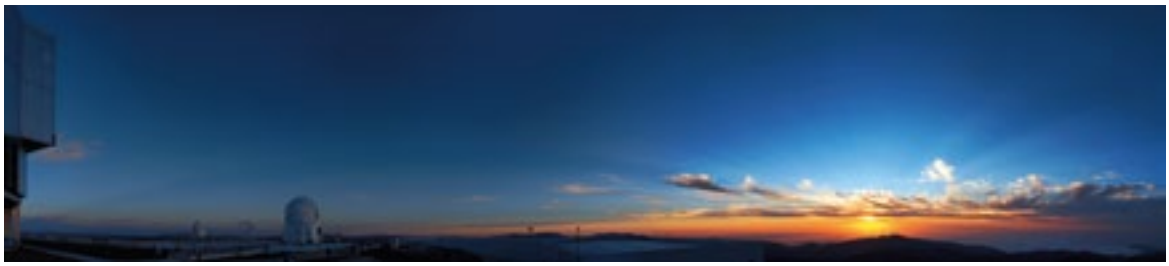

ESO/R. Wesson

Figure 3. The Sun sets over Paranal Observatory, painting an array of subtle hues across the sky. Crepuscular rays — and shadows from the clouds — are streaming from the Sun and appear to converge at the antisolar point.

these rays can make for a dramatic scene. They are also quite often visible at sunset, when they shine over the tops of clouds or through gaps within the clouds (Figure 3). They are called crepuscular rays and have been known by various poetic names in different cultures, for example, "Maui's rope" — based on a Maori tale; "Buddha's rays" in parts of south-east Asia; and "Jacob's ladder" in the UK (Lynch & Livingston, 2001).

When the Sun sets behind high mountains to the west, the mountains create broad crepuscular rays by partially blocking the light. Some dust or haze in the air will serve to highlight the rays. Under perfect conditions, when crepuscular rays can be followed all the way across the sky, they appear to expand at first and then narrow towards the east. In reality, they remain in parallel but only appear narrower at greater distances from us. Crepuscular rays in the east are called anti-crepuscular rays (Figure 4).

Refraction, differential refraction and the green flash

There is a whole subset of interesting phenomena related to the shapes of the Sun and Moon as they rise and set.

Few people are aware that we still see the Sun for a few minutes after it has moved below the horizon. The reason we still see it in the sky is that its rays are refracted by the atmosphere, raising the image of the solar disc by about a diameter on average as it sets[2]. In other words the Sun's apparent movement towards the horizon is slowed down by the refraction.

The refraction happens because light rays travel more slowly as they pass through the Earth's atmosphere. The lower the Sun is, the further the light rays travel through the atmosphere, the slower they become, and thus the more they are refracted. The effect is measurable — even when the Sun is high in the sky — and it can be important for navigators and astronomers. The extent of the refraction varies from day to day, so the observed sunset time can change from one day to the next by as much as 5 minutes. We cannot therefore rely on an ephemeris to predict the observed sunset time with perfect accuracy.

A more specific variation of this phenomenon is visible in the Arctic regions. In 1596, the ship carrying polar scientist Willem Barents (c. 1550–1597) was caught in the ice on what is now called the Barents Sea at Novaya Zemlya Island. There were two weeks until sunrise, but the tip of the solar disc had already peaked above the horizon (de Veer, 1876). Polar explorer Sir Ernest Henry Shackleton (1874–1922) also reported repeated sunrises "ahead of time" in the Arctic

Figure 4. During the early evening of 7 August 2017, a partial lunar eclipse was visible in the sky above the ESO Headquarters. While the Moon was rising, significant anticrepuscular rays were visible in the antisolar direction.

ESO/P. Horálek

P. Horálek/ESO

Figure 5. The setting crescent Moon deformed by the atmosphere over the Pacific Ocean, as seen from Paranal on 19 November 2017. The effect of layers with different temperature and density in the atmosphere caused different parts of the Moon's image to be refracted by different amounts as it neared the horizon.

(Shackleton, 1919). The explanation is once again the atmosphere's refraction of light or rather, the variation in that refraction. In the case of Barents, the refraction must have lifted the solar disc by about 5 degrees to peek over the horizon, but this is one of the more extreme cases. The phenomenon is known as the Novaya Zemlya effect (Lehn, 1979; Lehn & German, 1981).

Figure 6. Several effects are seen on the setting stars in this multi-exposure photo: atmospheric scattering (reddening) and absorption, and differential refraction ("lifting" of the stars).

Another effect of refraction is that the Sun and Moon never appear perfectly round as they approach the horizon, they appear flattened — as also evidenced in many of the photographs in this article. The amount by which the rays are refracted increases closer to the horizon, so rays from the upper edge of the solar disc are refracted less than those from the lower edge, flattening its shape. Occasionally, the shape of the disc may be further disturbed if the layers in the atmosphere have different temperatures and refract the light by different amounts — called differential refraction. It gives rise to a Chinese lantern effect in which the solar or lunar disc appears layered. The subtle details of the layered lantern effect can best be observed with the Moon (see Figure 5), as the Sun often saturates on pictures. The "lifting" effect of the lower layers of the atmosphere can also be seen on stars as they set (Figure 6).

Compared to other natural light phenomena, the green flash has an aura of mystery and supernaturality. The green flash is rare and very difficult to observe, but, when the conditions are right, the observer's perseverance is rewarded with a quick green gleam at the top of the setting Sun, amid the red and orange shades.

At sunset the blue and green light rays are refracted a little more than the red light, which means that the blue-green colours are "lifted" slightly more in the sky. You could almost say there are two solar discs — one blue-green and one red (Young, 2013). Where they overlap, we see a yellowish-red Sun, with the reddening of the Sun due to atmospheric

R. Wesson/ESO

scattering. With the right equipment it is not so rare to see the Sun with a greenish top, called the green segment, even before it reaches the horizon (Figures 7 and 8).

However, differential refraction alone does not result in more than the green and red segments. To produce a proper flash such as those seen in Figures 8 and 9, the red light is spectrally separated from the blue-green light. Without spectral separation, only a green (upper) or a red (lower) fringe would be seen in the solar image. The ozone layer is responsible for the spectral effect, since the light path through the atmosphere is longer at sunrise and sunset and the ozone layer covers altitudes between about 12 and 40 km. The Chappuis band of ozone absorbs light in a broad band centred close to 590 nm in the orange. Owing to the long path, the effect from this band strengthens when the Sun is near the horizon, effectively removing much of the yellow, orange and red light. In the right conditions this can produce the apparent spectral separation needed to produce a noticeable flash.

Simple atmospheric modelling[3] shows that in order to see a green flash at all, the aerosol content of the atmosphere needs to be very low where the sunlight grazes the horizon. It also turns out that in rare circumstances, when the light path is guided by differential refraction to take an unusually long track through the ozone layer, the flash is significantly shifted towards shorter wavelengths to produce the magnificent (and very rare, Figure 9) blue flash; lucky is the person who witnesses that!

Dutch researcher Marcel Minnaert (1893–1970) saw the green flash shoot up like a flame from the horizon (Minnaert, 1993). Because the green-blue rim on the solar disc is very thin (just a few arc-seconds), it is only alone over the horizon for approximately one second. Accordingly, the green flash is seen to last for a similarly short length of time at ESO observatories. It can, however, last much longer. Polar explorer Richard E. Byrd (1888–1957) and his crew claimed to have seen a "green sun" persist for up to 35 minutes while on an expedition to Antarctica in 1929 (Lock, 2015). Despite this unique observation, there are relatively few pictures of the

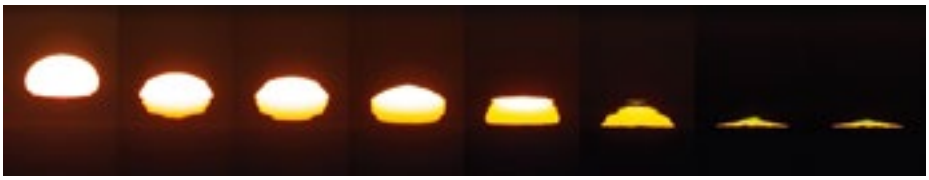

P. Horálek/ESO

Figure 7 (above). This sequence taken at La Silla on 16 November 2017 shows the phenomena of red (below the solar disc) and green flashes (above) that can occur when the Sun sets and the atmosphere refracts the sunlight into different colours.

Figure 8 (below). An example of a green segment seen from Cerro Paranal. The image was taken by Stéphane Guisard (ESO). Light phenomena connoisseurs argue that this is strictly speaking not the green flash.

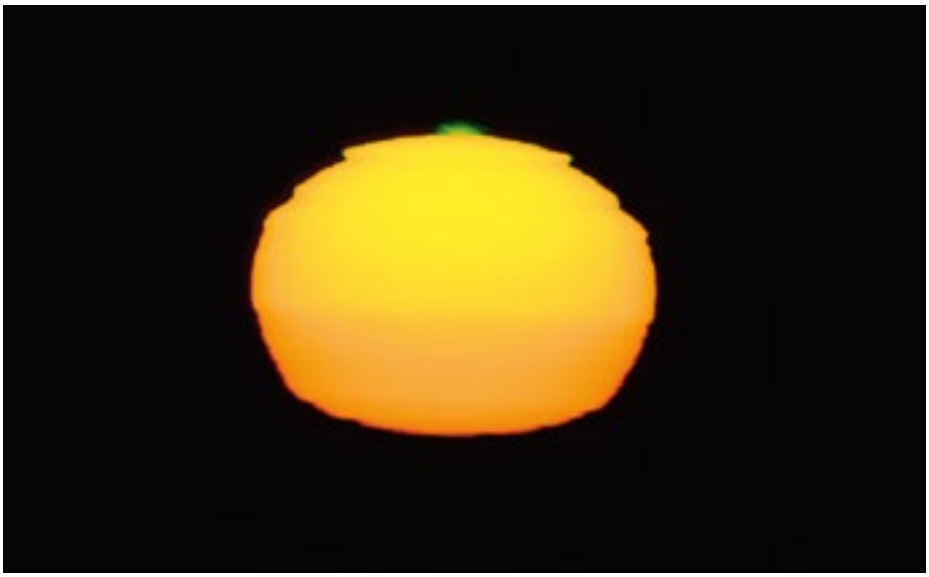

ESO/S. Guisard

G. Blanchard/ESO

Figure 9. ESO staff member Guillaume Blanchard was able to capture the very rare blue flash while observing the sunset on Christmas Eve 2007 from the Paranal Residencia.

phenomenon, which contributes to the whole mystery surrounding the flash and makes it something quite special to look for.

The green flash is best seen on a completely unobstructed western horizon, like the view from the Paranal platform. The weather must be very clear, and the atmosphere needs to have complex layers and a low aerosol content. Happy hunting!

ESO/C. Malin

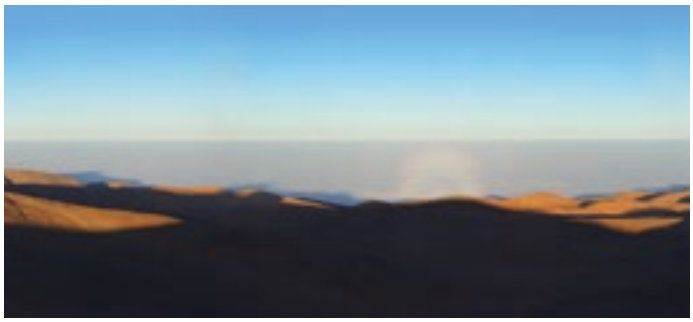

Figure 11. A glory caused by sunlight backscattering off tiny droplets of water in the atmosphere. Glories appear at a point directly opposite the position of the Sun, so they are only visible at sunrise or sunset.

The Earth shadow and the Belt of Venus

As the Sun reaches the horizon, an orange-yellow twilight arch forms to the west, and the blue-grey Earth shadow slowly rises to the east; stretching from the horizon upwards as the Sun goes down. The twilight arch is the arc of light that forms over the place where the Sun has set. It is usually red at the bottom, yellow for a wide stretch above the red, and arches over in a peach-coloured, green, turquoise or slightly purple band that merges with the background colour. It is created by scattered sunlight in the atmosphere. Even when the Sun has set, it can continue shining on parts of the atmosphere that lie on the horizon or high above our heads. The Earth shadow emerges and its visibility is best when there is little dust or haze in the air.

The clarity and low humidity of the air at the high altitudes of the Atacama Desert provide extraordinary opportunities to regularly observe the phenomenon called the Belt of Venus, followed by the projection of the dark Earth shadow onto the

Figure 10. The pink Belt of Venus and Earth shadow as seen at ALMA.

D. Kordan/ESO

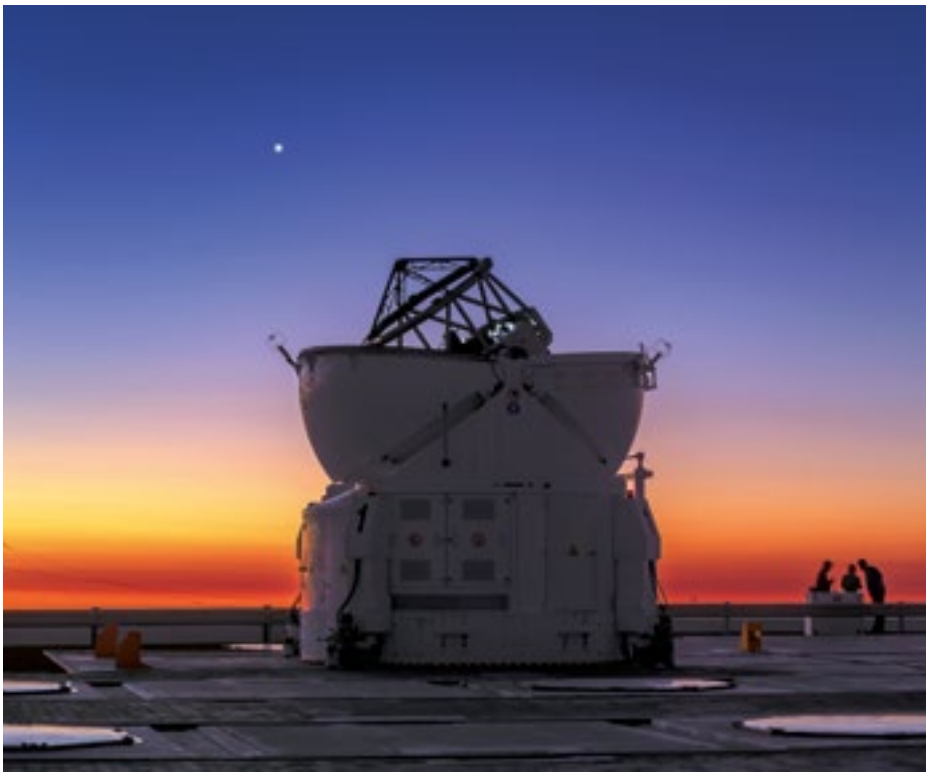
ESO/P. Horálek

Figure 12. Looking west just after sunset at ESO's Paranal Observatory on 25 January 2015. The bright object is Venus. In this view rich dusk colours can be seen. They were likely caused by volcanic ash from the January 2015 eruption of Tongan volcano and possibly even the 2014 eruptions of the Indonesian volcano Mount Sinabung.

atmosphere (Figure 10). Looking towards the antisolar point some minutes after the sunset or before the sunrise, the sky over the horizon seems like a dark curtain bounded by pink, while the dusk or dawn sky above is much brighter.

Seen from the ground when the Sun is below the horizon, the Belt of Venus is the result of light from the setting or rising sun being backscattered by fine dust particles and aerosols that are present higher in the atmosphere (Lee, 2015). It is most easily visible just a few minutes after sunset or before sunrise. The belt appears as a glowing, pinkish arch that extends roughly 10–20 degrees above the horizon.

The glory

Observers at La Silla or Paranal can at times see a phenomenon called a glory when looking down on a cloud layer. Glories are concentrated coloured rings around the shadow of the observer's head (or the shadow of a camera; see Figure 11). They occur by backscattering on tiny water droplets in clouds or fog at the antisolar point and look like circular rainbows (Nussenzveig, 2011). This is a rather complicated case of Mie scattering (and not the special divine importance of a person!). If two people are standing on a mountain and look at both of their shadows, they will each see only one glory and claim it to be around their own head. Looking down at a plane's shadow when flying, you will often be able to see a glory on the cloud tops.

Planets in dusk and dawn

The clear air at the high altitudes of the observatories makes dawn and twilight colours very intense, but also followed by a steep darkening gradient. For these reasons, very bright objects, such as planets in our Solar System or the brightest stars in the sky, can be visible in the sky very early after sunset (Figure 12) or very shortly before sunrise. Usually just minutes after sunset the brightest stars appear while the Belt of Venus becomes larger and the sky above is "swallowed" by the Earth's shadow.

Acknowledgements

The authors are grateful for helpful conversations with Bob Fosbury. Sarah Leach and Laura Hiscott are thanked for improvements to an earlier version of the text.

Notes

[a] Please don't forget that looking at the Sun itself, especially through an optical device (camera, telescope, binoculars, etc.), is very dangerous, and could cause immediate blindness. Do not attempt to observe the Sun unless you know what you are doing.

Links

[1] The colors of sunset and twilight (Corfidi, S. F. 2014, NOAA/NWS SPC): https://www.spc.noaa.gov/publications/corfidi/sunset/

[2] Effect of atmospheric refraction on the times of sunrise and sunset (Tong, Y. 2017, HKO): https://www.hko.gov.hk/m/article_e.htm?title=ele_00493

[3] The telluric spectrum of the green flash (Fosbury, R. 2018): https://www.flickr.com/photos/bob_81667/39604010580/

[4] Green and red rims (Young, A. T. 2013): https://aty.sdsu.edu/explain/simulations/std/rims.html

References

Christensen, L. L. et al. 2016, The Messenger, 163, 40
Gladysheva, O. 2007, Solar System Research, 41, 314
Horálek, P. et al. 2016a, The Messenger, 163, 43
Horálek, P. et al. 2016b, The Messenger, 164, 45
Kundt, W. 2001, Current Science, 81, No. 4, 399
Lee, R. L. 2015, Applied Optics, Vol. 54, Issue 4, B194
Lehn, W. H. 1979, Journal of the Optical Society of America, Vol. 69, Issue 5, 776
Lehn, W. H. & German, B. A. 1981, Applied Optics, Vol. 20, No. 12, 2043
Lock, J. A. 2015, Applied Optics, Vol. 54, Issue 4, B54
Longo, G. 2007, *Comet/Asteroid Impact and Human Society*, 303
Lynch, L. K. & Livingston, W. 2001, *Color and Light in Nature*, (Cambridge: Cambridge University Press)
Minnaert, M. G. J. 1993, *Light and Color in the Outdoor*, (New York: Springer)
Moreno, H. et al. 1965, Science, 148, 364
Nussenzveig, H. M. 2012, Scientific American, 306, 68
Shackleton, E. H. 1919, *South: The Story of Shackleton's 1914–1917 Expedition*, (London: William Heinemann)
de Veer, G. 1876, *The Three Voyages of William Barents to the Arctic Regions: 1594, 1595 and 1596*, (London: Forgotten Books, 2017)
Waythomas, C. W. et al. 2010, Journal of Geophysical Research, 115, B12
Zieger, P. et al. 2013, Atmospheric Chemistry and Physics, 13, 10609

DOI: 10.18727/0722-6691/5179

The ESO Summer Research Programme 2019

Carlo F. Manara[1]
Christopher Harrison[1]
Anita Zanella[1]
Claudia Agliozzo[1]
Richard I. Anderson[1]
Fabrizio Arrigoni Battaia[2]
Francesco Belfiore[1]
Remco van der Burg[1]
Chian-Chou Chen (T. C.)[1]
Stefano Facchini[1]
Jérémy Fensch[1]
Prashin Jethwa[1]
Rosita Kokotanekova[1]
Federico Lelli[1]
Anna Miotello[1]
Anna Pala[1]
Miguel Querejeta[1]
Adam Rubin[1]
Dominika Wylezalek[1]
Laura Watkins[1]

[1] ESO
[2] Max Planck Institute for Astrophysics, Garching, Germany

For the first time ever, a summer research programme was organised at ESO Garching. Seven students, enrolled in universities all around the world, were selected from more than 300 applicants. They each spent six weeks from June to August 2019 carrying out a scientific project under the supervision of teams of ESO Fellows and postdocs, while engaging in the scientific life of ESO. The students carried out research in different fields of astronomy, from comets to high-redshift galaxies and from pulsating stars to protoplanetary discs. In this report we present the programme and describe the main outcomes of the projects.

Motivation and organisation

Summer studentship programmes for undergraduate students are becoming the preferred way for an enterprising student to gain their first research experience; these programmes can last from a few weeks to months at top-class international universities or research centres. Such programmes have a wide range of benefits to students and hosts alike. The ESO Fellows in Garching identified this as an opportunity that had been missing at Garching until now and decided to organise a six-week-long Summer Research Programme at ESO for up to seven university students.

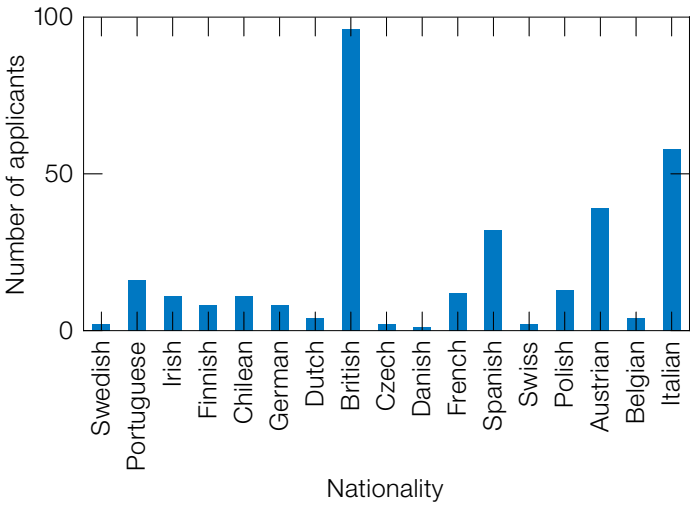

Figure 1. Distribution of the nationalities of the applicants for the first ESO Summer Research Programme.

A proposal was submitted by the Garching ESO Fellows requesting funds from the Director for Science to cover travel costs and to provide a basic stipend to cover lodging and living expenses for the students. The proposal was accepted and ESO Fellows, with the support of ESO administrative assistants, organised the first-ever ESO Summer Research Programme. This involved booking ESO apartments and office space, setting up the website[1], organising the application process and the selection of students, planning and delivering a lecture series and, most importantly, designing and leading the research projects.

The response from the community was incredible. More than 300 valid applications were received from university students in most Member States, from our Host Country Chile, and from ESO's strategic partner, Australia (Figure 1). Participants were selected by first distributing the applications amongst all potential supervisors for an initial ranking, followed by a final selection by a committee comprising three fellows, one student and one staff member. The final list included seven students — four females and three males — from seven different countries. After a short video interview all seven students accepted the offer.

Programme overview

The programme started with a workshop, open to all ESO staff, on 1 July 2019. At this workshop the seven research projects were introduced by the advisors, and the students introduced themselves. An introduction to ESO was delivered by the head of the ESO User Support Department Marina Rejkuba, and the Director General greeted all participants from the control room of the La Silla Observatory (he was visiting La Silla for the total solar eclipse at the time).

The students were each working on their own research project, with the supervision of one or more ESO Fellows, for the duration of the programme (Figures 2 & 3). The schedule in the first three weeks also consisted of a set of eight lectures on astronomical topics, a visit to the ESO Supernova including a planetarium show, and a telecon with Anita Zanella (an ESO Fellow observing at Paranal). The final three weeks were mainly focused on the research projects, but with an additional two lectures and one visit to the Extremely Large Telescope (ELT) primary mirror test stand. Most of these additional activities and lectures were organised following an explicit request from the students who had expressed enthusiasm about the first set of lectures. Throughout the duration of the programme the students were among the most active attendees of scientific activities at ESO Headquarters, including talks, science coffees, and informal meetings.

Figure 2. Student Tania Machado with her supervisor Chris Harrison.

Figure 3. ESO Summer Research Programme student Aisha Bachmann with supervisors Jeremy Fensch and Remco van der Burg.

The last days were all focused on the preparation of the most thrilling event for the students: their 15-minute presentation to be given in front of ESO staff, students and fellows during the final workshop in the old ESO auditorium. This event was very well attended by ESO personnel (Figure 4) and showcased the great science that the students were able to achieve during this relatively short programme; some examples are described in the next section.

Students and their research projects

Understanding the formation mechanism of galaxies at their extremes

Advisors: Remco van der Burg & Jérémy Fensch
Student: Aisha Bachmann (German), University Bochum, Germany

One of the most surprising recent results in the field of galaxy formation is the discovery of a significant population of ultra-diffuse galaxies (UDGs) in local galaxy clusters. These are galaxies of the size of the Milky Way, but with a stellar mass similar to dwarf galaxies. Theorists are proposing models that can produce such galaxies in simulations; these generally invoke tidal heating scenarios arising from interactions with neighbouring galaxies, or outflows coming from the galaxies themselves. To distinguish amongst these different scenarios it is important to study the abundance of UDGs as a function of cosmic epoch. This is a very challenging task because only the Hubble Space Telescope (HST) can spatially resolve UDGs at high redshift, and cosmological surface brightness dimming makes them extremely difficult to detect.

Aisha looked for UDGs, at redshifts beyond 1, in the deepest cluster images that were ever taken with the HST. She wrote a detection algorithm and tested it on mock galaxies that she inserted into the data; she then used the algorithm to search for real UDG candidates. Finally, Aisha identified which UDGs, among the candidates she found, are cluster members rather than projections along the line of sight by statistically comparing her detections with those of a reference field. Her preliminary results look extremely interesting and Aisha aims to finalise them during the next months and write up her findings in a publication.

Comet evolution from the Kuiper Belt to a dormant comet in the near-Earth asteroid population

Advisors: Rosita Kokotanekova
Student: Abbie Donaldson (UK & Ireland), University of St Andrews, UK

This project focused on analysing photometric observations of the comet 169P/NEAT taken between February and June 2019 with the FOcal Reducer/low dispersion Spectrograph 2 (FORS2) on the Very Large Telescope (VLT) and with the Wide Field Camera (WFC) on the Isaac Newton Telescope (INT) on La Palma. Since the comet was observed close to aphelion and was therefore inactive, the photomet-

Figure 4. One of the research students, Matthew Wilkinson, presents his research to fellow participants and ESO staff.

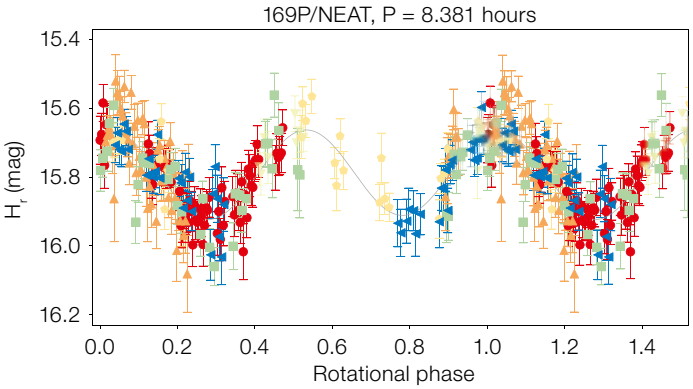

Figure 5. Rotational light curve of comet 169P/NEAT derived from INT/WFC data. The different symbols correspond to data taken during each of the six observing epochs between February and May 2019.

ric observations could be used to extract the brightness variation of the nucleus due to rotation and change of geometry. Abbie derived the rotational light curve of 169P/NEAT using the most likely rotation period of 8.381 hours (Figure 5) and constrained the comet's albedo and the slope of the phase function. Abbie's results will be included in a publication comparing the surface properties of two of the darkest Jupiter-family comets, 169P/NEAT and 162P/Siding Spring with other comets and asteroids.

Preparing for the Extremely Large Telescope: how will high-redshift star-forming galaxies appear with HARMONI?

Advisors: Anita Zanella & Chris Harrison
Student: Tania Machado (Portugese), Technico Lisbon, Portugal

The ELT, with its 39-metre diameter primary mirror, will have the angular resolution and light gathering power to revolutionise our understanding in many astrophysical fields. This project is in preparation for the use of the High Angular Resolution Monolithic Optical and Near-infrared Integral-field spectrograph (HARMONI), a first-generation ELT integral-field spectrograph, to spatially resolve the interstellar medium of high-redshift (z ~ 2–5) galaxies and to measure the physical processes occurring on scales of individual star-forming regions. Tania created simulated HARMONI datacubes of how galaxies at z ~ 2–3 will appear when observed with different observing strategies and observing conditions. The most important result from Tania's work was that our ability to extract key physical properties from the simulated data was limited by applying standard analysis techniques and not limited by the data quality. Work is now required to optimise the techniques before the arrival of the exquisite HARMONI data. Tania has a strong interest in keeping in contact with her advisors and with ESO to continue this work and she hopes to show her results at the conference "Spectroscopy with HARMONI at the ELT" to be held in Oxford in September 2020.

Caught in the act: witnessing the formation of the most massive galaxy clusters across the cosmic time

Advisors: Chian-Chou Chen (T. C.) & Fabrizio Arrigoni Battaia,
Student: Marta Nowotka (Polish), Colorado College, USA

In the hierarchical model of structure formation, the most massive galaxies often form through merging processes within the highest density peaks, known as protoclusters. Identifying these protoclusters and characterising their properties is key to reaching a full understanding of galaxy formation. Recently, new prime candidates for signposts of massive protoclusters have been discovered: they are enormous (> 200 kpc) Lyman-α nebulae (ELAN) which host multiple active galactic nuclei and are surrounded by over-densities of Lyman-α emitters.

To better understand their formation history, Marta developed complex Python algorithms to analyze SCUBA-2 850-micron data and found evidence of dust-obscured star formation around one ELAN. This is an exciting result and we expect it to be published in high-impact journals. Marta will continue to work on the project by investigating similar data sets in other ELAN fields, as well as enjoying a trip to Hawai'i to carry out observing runs at the James Clerk Maxwell Telescope (JCMT) on Maunakea.

Modulated variability: a new window into stellar pulsations

Advisors: Richard I. Anderson
Student: Samuel Ward (UK), University of Durham, UK

What causes the variability patterns of classical Cepheid variable stars to change over time? More and more modulated variability is being discovered among Cepheids, yet its origin remains elusive, and the properties of the modulation challenge the classical paradigm of Cepheids as other well-understood, more simple, variable stars.

Samuel analysed an 8-year-long set of high-resolution optical spectra of a bright Cepheid to unravel the nature and cause of the star's modulated variability. He created his own method for modeling spectral line profiles using multiple components and used it to trace the changes in complex line profiles over time. Additionally, he investigated how different atmospheric layers move at different velocities. Samuel found compelling evidence that the observed modulated line splitting is most likely caused by non-radial pulsation modes, rather than by atmospheric shock related to the dominant pulsation mode, as previously proposed.

Dark matter content of galaxies from globular cluster kinematics

Advisors: Prashin Jethwa & Laura Watkins
Student: Matthew Wilkinson (Australian), University of Queensland, Australia

How well can we measure the amount of dark matter in a galaxy? This was the central question of this project, and its answer will have important consequences for our understanding of cosmology and galaxy formation. Questions about dark matter certainly motivated our pool of potential students, with 115 eager applicants for this project. Out of this talented pool, we selected Matthew, who tested

the accuracy of calculations of galactic dark matter content.

Matthew tested calculations which use observations of globular clusters — dense, bright clusters containing tens of thousands of stars. This very same calculation had recently been applied to observations in the Milky Way, so testing its accuracy is of real, present importance. To do this test, Matthew applied the calculation to simulations and compared the results to the correct answer known from the simulations. The results suggest that the calculation may be underestimating the amount of dark matter in galaxies. This is a tentative result and confirming it would require more tests. Prashin and Laura remain in touch with Matthew and are enthusiastically supporting him as he applies for PhD positions in astronomy.

Testing disc evolution with ALMA surveys of CO emission

Advisors: Stefano Facchini, Anna Miotello & Carlo Manara
Student: Francesco Zagaria (Italian), University of Pavia, Italy

How protoplanetary discs evolve is a long-standing question. How they evolve determines the planet formation potential of discs and is a key ingredient in any planet formation model. The two main theoretical paradigms describe disc evolution as driven by viscosity, or by magnetically supported winds. The two lead to different predictions about the evolution of gas disc radii, with the former predicting that the disc radii should expand. In this project, Francesco tested the viscous scenarios by comparing statistical properties of CO fluxes measured by ALMA for the disc populations of Lupus and Upper Sco, two star-forming regions spanning ages between 2 and 10 Myr. Francesco developed a code aimed at reproducing the observed CO fluxes within the viscous evolution framework, with interesting results. While the model reproduces the statistical properties of individual star forming regions well, it is not able to fit all of the star forming regions simultaneously. This suggests either that the viscous evolution scenario has to be revisited, or that the two star forming regions had different initial conditions in their disc mass and radius distributions. The results are presented in a draft paper that will be submitted soon.

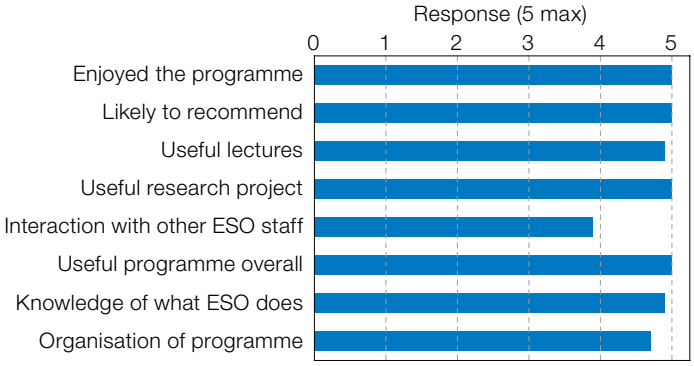

Figure 6. Average results from the feedback given by students at the end of the programme; 5 is the most positive score.

Feedback and future programmes

We asked students to give feedback on the programme, and the responses were extremely positive (Figure 6). Interviews carried out with the students are presented in the ESOBlog[2] and highlight how much they enjoyed their research experience and the programme overall.

The great success of the programme has not been overlooked by the ESO Director of Science and by ESO management and we are pleased to report that funding has been secured to run the programme again in the summer of 2020. This is great news for many, including future potential applicants who have already started to inquire about the deadline for applications. How this programme continues will depend on the efforts of many, and its expansion to include more ESO staff, including Fellows in Santiago and/or other ESO departments, is very much encouraged.

Acknowledgements

The ESO Fellows and postdocs in Garching acknowledge the active support and encouragement of the Director for Science Rob Ivison, the ESO Faculty, and several ESO students, staff and administrative assistants. In particular, we thank Stella-Maria Chasiotis-Klingner for her excellent support with logistics. We acknowledge funding from the Directorate for Science to cover the travel costs and stipends for the students.

Links

[1] ESO summer research programme website: http://eso.org/summerresearch/
[2] ESOBlog entry *Meet Our 2019 Summer Research Programme Students*: https://www.eso.org/public/blog/from-comets-to-cosmology/

ESO/S. Otalora

The ALMA array on the Chajnantor Plateau from October 2019.

DOI: 10.18727/0722-6691/5180

Report on the ESO Workshop

Artificial Intelligence in Astronomy

held at ESO Headquarters, Garching, Germany, 22–26 July 2019

Henri M. J. Boffin[1]
Tereza Jerabkova[1,2,3]
Antoine Mérand[1]
Felix Stoehr[1]

[1] ESO
[2] Helmholtz-Institut für Strahlen- und Kernphysik, Universität Bonn, Germany
[3] Astronomical Institute, Charles University, Prague, Czech Republic

In July 2019, ESO hosted one of the first international workshops on artificial intelligence in astronomy, with the double aims of presenting the current landscape of methods and applications in astronomy and preparing the next generations of astronomers to embark on these fields. In addition to a wide range of review and contributed talks, as well as posters, the ~ 150 attendees could learn the techniques through several dedicated tutorials.

It is certainly an understatement that artificial intelligence (AI), i.e., intelligence demonstrated by machines, has taken the world by storm, with breakthroughs appearing in the news almost daily. Indeed, the incredible progress in computer power, the availability of large amounts of data and the ability to process them (even if they are unstructured), coupled to a theoretical understanding of techniques such as machine learning, and, more generally, data mining, have allowed AI to advance at a frantic rate, including in science. Astronomy is no exception. The sheer volume of astronomical data (which is increasing exponentially; see for example, Stoehr, 2019) necessitates a new paradigm. Data analysis must become, to a large extent, more automated and more efficient, in particular through AI. And this is indeed what is happening. A look at the NASA Astrophysical Data System shows that before 2005 only 21 refereed papers had "machine learning" in their abstract. Since then the number has been multiplied by 41, with 663 papers published within the last five years, in an almost exponential way (there were twice as many published in 2018 than in 2017, for example).

As AI methods become more commonly used, a fundamental understanding of their limitations, assumptions, and performance is due. The rigour of the scientific process requires that such methods are applied with extreme care and to ensure that "the machine is being taught to take into account certain relevant known facts" (Griffin 2014). Moreover, the perspectives of information theory, neural science, and other areas on AI are expected to stimulate and guide the development of the next generation of intelligent methods used in astronomy and elsewhere. It was therefore thought to be an ideal time to host an international workshop on AI in astronomy. ESO organising such a workshop was important for several reasons, but perhaps less known is that ESO has had an interest in AI for a long time (for example, Adorf, 1991).

Artificial intelligence covers a wide range of algorithms and methods. The first goal of the workshop was to provide a clear map by which to navigate this jungle and show which techniques are used for which kind of science. This was done in a few invited talks by prominent speakers to clearly set the scene. Laura Leal-Taixé provided an introduction to deep learning using computer vision and its application to autonomous driving as a clear example that will affect our lives more and more. She stressed the importance of increasing the diversity in the data, but also in the community which is building the algorithms, in order to avoid biases (that, in daily life, can be fatal). Emille Ishida showed the need for active learning in astronomy, as the basic assumption of supervised machine learning — that the training set is fully representative of the target sample — is often not fulfilled. It is thus essential that humans intervene in the process to enhance the efficiency of the learning. She stressed the need for optimised samples and algorithms for machine learning applications and that interdisciplinarity is the key, but also that serendipitous discoveries will only get more difficult with the next generation of large-scale surveys and it is therefore essential to plan for the unknown with adaptable algorithms. Alberto Krone-Martins presented the other way to achieve results in astronomy: with unsupervised learning, that is, essentially

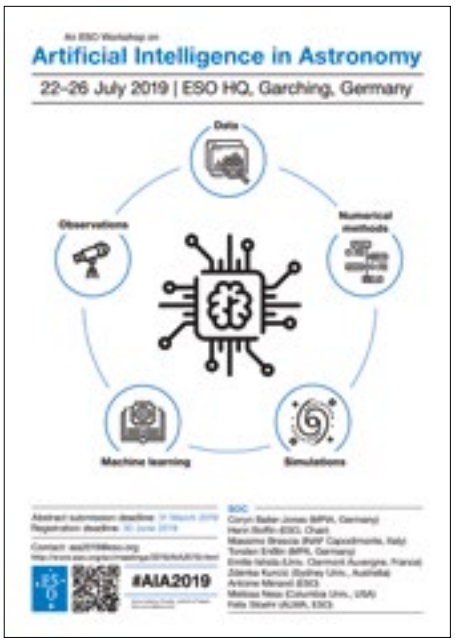

Figure 1. Conference poster.

clustering and dimensionality reduction. These can be done through a variety of methods and it is important to know which one is best suited to a given problem. He presented several applications, such as how to find 101 new stellar clusters in the Milky Way or several lensed quasars thanks to Gaia or how to discover hundred of thousands of new galaxies by combining WISE and Gaia data. These results would have been hard, if not impossible, to obtain without the use of machine learning, but it is important to note that while unsupervised learning is powerful, it also requires some taming and a clear understanding of the limitations. That this is true was reviewed by Giuseppe Longo, who also explained that the use of these methods will lead to often unexpected results that make sense to humans only *a posteriori*. Dalya Baron showed in impressive fashion how one can mine for novel information in large and complex datasets using outlier detection and dimensionality reduction algorithms (Baron, 2019). Particularly impressive was how such techniques allowed astronomers to find a new correlation amongst active galactic nuclei.

Finding the right method is not an easy task and it is important to bring together experts from different fields.

Figure 2. Conference photo.

Mi Dai presented the Photometric LSST Astronomical Time series Classification Challenge (PLAsTiCC) and described how to involve the community at large and its thousands of machine learning experts via, for example, the Kaggle platform[2], to come up with the best algorithms to classify the very many transient sources that will be found by the Large Synoptic Survey Telescope. Similarly, Rafael de Souza presented the Cosmostatistics Initiative, an endeavour aimed at fostering interdisciplinary collaborations around astronomy and characterised by a residence programme.

It was also important to make sure that the ground covered by the workshop was as wide as possible. Accordingly, John Skilling spoke on how to do computation in big spaces, presenting the framework of inference, i.e. the Bayes therorem, and how the prior space is often much bigger than the small posterior space, leading to a lot of confusion. Only by reducing dimensionality can one hope to solve the problems. Jens Jasche showed how to perform large-scale Bayesian analyses of cosmological datasets, using computer programs and not analytic functions to perform a hierarchical Bayes analysis. This allows one, for example, to infer the mass density in a super-galactic plane or estimate galactic cluster masses. In the same vein, Torsten Enßlin presented both in a contributed talk and in a tutorial the fully Bayesian information field theory and the Numerical Information Field Theory (NIFTy) library[3].

Perhaps even further from what we usually see in astronomical conferences, Zdenka Kuncic presented a special, and quite inspiring, talk about emergent intelligence from neuromorphic complexity and synthetic synapses in nanowire networks. After presenting a brief history of AI, she showed that to reach the ultimate goal of general intelligence, one needs to move away from mainstream computing. She told us that companies are already developing sophisticated neuromorphic chips, which consume orders of magnitude less power than conventional processors and which try to emulate the brain. She also described how scientists and engineers are now creating biomimetic structures of nanowires that self-assemble into a complex, densely interconnected network, with a topology similar to a biological neural network and characterised by a collective memory.

This very impressive series of invited talks was complemented by numerous contributed talks and posters, covering the whole range of applications of AI methods in astronomy, from meteorite hunting to augmenting *N*-body simulations with deep learning models, through applications in adaptive optics. A poster competition was organised, and participants were asked to vote for the best posters. The three winners each received a mounted ESO image; they were: Philipp Baumeister (Using Mixture Density Networks to Infer the Interior Structure of Exoplanets); Timothy Gebhard (Learning Causal Pixel-Wise Noise Models to Search for Exoplanets in Direct Imaging Data); and Colin Jacobs (Using Deep Learning in the Cloud to find Strong Lenses).

As already indicated, there were also four three-hour tutorials and hands-on sessions that allowed the participants to delve directly into the techniques. These covered an introduction to machine learning using Python notebooks, machine learning and deep learning using disitributed frameworks and optimised libraries, and how to use NIFTy.

The workshop closed with a final discussion led by Torsten Enßlin which proved that AI is needed in astronomy and will be even more in the future, especially as we won’t be able to store all the data and on-the-fly decisions will have to be made. It was also stressed that interdisciplinary teams are required, as well as a new kind of physicist who will have to be trained. The need to better understand the methods that are used was also stressed — as scientists, we shouldn’t rely on “black boxes” and need to be very critical. This requires us to learn the language of the data scientists and the basic underpinning of the methods, such as Bayesian probability.

The workshop was a great success and participants praised the overall quality of the talks and tutorials, as well as of the abstract booklet[4]. Many were already hoping that a related workshop would take place next year! We therefore invite the community to organise such events as regularly as possible. The PDFs of all the talks and posters and the material of two of the three tutorials are available on the workshop webpage[1]. All in all, the talks, tutorials and posters covered a very wide range of topics in artificial intelligence and the workshop fulfilled its aim. The available material will surely be very useful for many years to come.

Demographics

The workshop had a very high level of participation, with about 130 registered participants coming from all parts of the world and approximately two dozen unregistered participants from ESO and neighbouring institutes, including several software engineers, highlighting the great interest generated by the topic.

The Scientific Organising Committee worked hard to ensure fair representation from the community. Among the 10 invited speakers, five were female. Three of the five sessions were also chaired by women. Among the abstracts submitted, a quarter were by women, and this was also the female/male ratio among the contributed speakers. We had a very high level of participation from young researchers, most likely due to a combination of a highly discounted registration fee for students and the fact that this field is relatively young. Thus, among the registered participants, we had 41% students, 22% postdoctoral researchers, and 37% tenure-track or tenured faculty. The talk selection was made blindly (the chair of the SOC removed names and identifying information about the authors, including their seniority and their affiliation), and was based solely on the merits of the abstract and its relation to the themes of the workshop. This resulted in 62% of the talks and 50% of the posters being given by students.

Acknowledgements

It is a great pleasure to thank the members of the Scientific Organising Committee (Coryn Bailer-Jones, Henri Boffin, Massimo Brescia, TorstenEnßlin, Emille Ishida, Zdenka Kuncic, Antoine Mérand, Melissa Ness, and Felix Stoehr) for setting up an amazing programme, the invited speakers for remarkable and clear reviews, and the organisers of the four tutorials (Patrick van der Smagt, Fabio Baruffa, Luigi Iapichino, Philipp Arras, Torsten Enßlin, Philipp Frank, Sebastian Hutschenreuter, and Reimar Leike) for their exceptional work. We especially thank Stella Chasiotis-Klingner for her efficient organisation of many practical aspects of the Workshop, as well as ESO catering and ESO logistics, for ensuring the best conditions during the meeting.

References

Adorf, H.-M. 1991, The Messenger, 63, 69
Baron, D. 2019, arXiv: 1904.07248
Griffin, R. F. 2014, The Observatory, 134, 109
Stoehr, F. 2019, ASPC, 387, 523

Notes

[a] Machine learning is one of the most commonly used subsets of AI.

Links

[1] Workshop website: https://www.eso.org/sci/meetings/2019/AIA2019.html
[2] The Kaggle platform website: kaggle.com
[3] Numerical Information Field Theory: http://ift.pages.mpcdf.de/nifty/
[4] 2019 AIA workshop programme: https://www.eso.org/sci/meetings/2019/AIA2019/Booklet_final.pdf

DOI: 10.18727/0722-6691/5181

Report on the IAU Conference

Astronomy Education — Bridging Research & Practice

held at the ESO Supernova Planetarium & Visitor Centre, Garching, Germany, 16–18 September 2019

Wolfgang Vieser[1]
Tania Johnston[1]
Saeed Salimpour[2,3]

[1] ESO
[2] Deakin University, Burwood, Australia
[3] Edith Cowan University, Joondalup, Australia

Astronomy education contributes to the spread of scientific literacy among successive generations, helping to attract students into science, technology, engineering and mathematics (STEM) subjects and potentially also into astronomy research. Although the field of research into astronomy education has grown significantly, the sustainable transfer from research institutes into the classroom is lacking. The goal of this conference was to bring together all stakeholders — teachers, educators and researchers — to communicate and discuss their various needs in order to effectively bridge the gap between astronomy education research and its practical application.

Astronomy is not only one of the oldest sciences, but also a perennially fascinating one to the broader public, who often ask educators questions such as, “where do we come from?”, or “are we alone?” For this reason, astronomy has always been a relatively easy area of science to convey to the public and it can serve as a gateway to other scientific concepts, especially in young people.

Astronomy therefore plays a special role within public science communication. The literature is full of suggestions and advice about how to best communicate astronomy to the public. Astronomy education or teaching astronomy is different from communication, however. Whereas communication and outreach are processes aimed at generating inspiration and awareness, education aims to develop knowledge, skills and competences, and core values and attitudes through a range of pedagogies and methodologies that account for the abilities and development level of the learner. Astronomy education is less prominent within the scientific community than

astronomy communication and outreach even though the International Astronomical Union (IAU) established Commission 46 on "The Teaching of Astronomy" in 1964. The Commission's designation changed from 46 to C1 in 2015 but its mandate has remained essentially the same: *to further the development and improvement of astronomical education at all levels throughout the world through various projects developed and maintained by the Commission and by disseminating information concerning astronomy education.*

To foster this mandate, the IAU will establish the Office of Astronomy for Education (OAE) this year; its objective will be to provide structured support to for astronomy education in all countries. This includes, but is not limited to, providing training and resources for encouraging the use of astronomy as a stimulus for teaching and learning from primary to secondary school levels. At a workshop between 17 and 19 December 2019 at the Institut Astrophysique de Paris, the IAU revealed that the location of the OAE would be at the Haus der Astronomie in Heidelberg, Germany. In addition, at that same workshop the remit of the new office was presented along with its plans regarding the goals set out in the IAU Strategic Plan for 2020–2030.

The field of astronomy education has grown significantly over the last few decades, with an increasing number of research articles having been published by a growing number of researchers. Despite this, there has been no regular international conference for astronomy education researchers and practitioners around the world to convene and discuss their work. This conference is intended to be the first of a regular, biennial, IAU-Commission C1 Astronomy Education Conference series. The aim is to increase the quality, quantity, community and impact of astronomy education research and practice by bringing together astronomers, astronomy education researchers and education practitioners to communicate, discuss and tackle common issues.

The three key themes of this conference — Astronomy Education Research; Astronomy Education Standards, Curriculum and Instruction; and Primary and Secondary Teacher Education — span traditional and practical research, exploring the purely theoretical issues encountered when attempting to embed research results into practical situations, usually mediated by standards, curriculum and instruction.

This conference was organised by IAU Commission C, together with ESO, the ESO Supernova, and Leiden University. It was hosted at the ESO Supernova using all its facilities, including the planetarium as the lecture theatre. The programme comprised three invited talks, 44 contributed talks, 10 hands-on workshops and 50 posters. As it is an educational facility, the ESO Supernova proved to be the perfect location for this conference and the participants were enthusiastic about this inspiring environment. Details of the programme can be found via the conference webpage[1]. Each talk was followed by a five-minute session dedicated to questions and discussion that continued during the breaks. Poster viewing took place during all coffee breaks and was particularly encouraged during 30-minute poster sessions every day.

The IAU President Ewine van Dishoeck, the IAU General Secretary Teresa Lago and ESO's Director General Xavier Barcons all acknowledged the necessity of such a conference in their welcome addresses. The IAU President also gave a summary of the activities and events commemorating 100 years of the IAU, including the travelling exhibition, and announced the inauguration of the OAE.

Astronomy education research

The invited talk by Janelle Bailey summarised the broad field of astronomy education research (AER), highlighting upcoming projects, for example a two-volume work about astronomy education, and introduced modern education concepts like active learning. Future directions of AER were also discussed, such as the use of qualitative and mixed methods, robust quantitative analyses and longitudinal studies.

Contributed talks covered more specialised topics such as students' (mis-)conceptions about astronomical topics and how these could be organised into coherent patterns of understanding. A new AER study now provides a wider and more coherent framework about the high conceptual understanding of astrophysics that is necessary to develop research-based teaching-learning sequences for high school students — something that will be developed in the near future. Other contributed talks focused on how multidimensionality in the field of astronomy or astronomical time- and length-scales can be made understandable for students. In both fields, models can help students learn about relevant aspects, but they need to be built by experienced teachers. Some contributed talks surveyed and analysed the production of AER studies in different countries like Brazil, France, Japan and Portugal, focusing not only on school grade levels or the type of academic research but also on gender balance.

Astronomy education standards, curriculum and instruction

In his invited talk Robert Hollow discussed opportunities and issues regarding curricula at the school level, particularly in the context of the recent IAU Framework for Astronomy Literacy. The science curriculum of Australia served as an example to illustrate the possibilities and the challenges of using astronomy in teaching science. A contributed talk by Saeed Salimpour gave a review of how often astronomy is encountered in the school curriculum of 37 countries (OECD, China and South Africa), highlighting that 77% of all curricula in Grade 1 include astronomy, 54% in Grades 2 & 7 and 27% in Grades 1 to 12. The highest percentage of astronomy (85%) can be found in Grade 6. The study also revealed that one curriculum explicitly mentioned only two women astronomers and only three of the 37 countries explicitly mentioned indigenous astronomy.

Several contributed talks highlighted the importance of research-based science education, in which real data are analysed with research-quality tools to investigate questions for which the answer is not known. One talk recounted how the practices employed to use archival image and spectral data have evolved over time

Figure 1. Conference participants gathered on balconies inside the ESO Supernova, overlooking the exhibition space called The Void.

and described some of the challenges of working with real data. The lack of user-friendly interfaces aimed at non-experts and documentation emerged as the main bottlenecks preventing the broader use of archive data.

Another talk described an activity in which potential targets for the James Webb Space Telescope are identified via spectroscopic observations of stars taken by the Spitzer Space Telescope. This activity turned out to be beneficial not only for students, who showed an increased inclination to pursue a career in science after this activity, but also for the teachers' levels of motivation. Another contributed talk addressed the diversity of curricula in a big country like Canada, which creates a challenge for pan-Canadian programmes. It was shown that this issue can be overcome by offering online astronomy workshops and webinars that focus on science topics that are common to all curricula.

Internet resources like videos were shown to be extremely helpful for hearing-impaired or deaf people in a contributed talk about astronomy education among deaf children and school-age youth in Brazil, through the Brazilian sign language project Libras (*Língua Brasileira de Sinais*). Another contributed talk by Marco Brusa described how video games for educational purposes that are free of violence and focused on STEM related science can result in a growing interest in STEM.

Other internet-based education resources were discussed like the IAU AstroEDU platform[2] for high-quality, peer-reviewed astronomy education activities, whose Italian version was launched in 2017. The Open University (UK) is also accessible online and its curriculum is open to all and delivered entirely by distance teaching. Its OpenSTEM Labs allow students to perform remote experiments, including the use of robotic observatories.

Primary and secondary teacher education

The invited talk by Agueda Gras-Velazquez focused on the struggles of teachers in their daily work; challenges include a lack of time, excessively large curricula, and often isolation within the faculty. A promising way to overcome these problems is via professional development and collaboration, taking advantage of the many European initiatives on offer. These collaborations in science, technology, engineering and mathematics in general, and astronomy education in particular, were intensively discussed.

A contributed talk by An Steegen focused on the level of the teacher's awareness of student ideas and on the possible strategies they use in class related to astronomical concepts. Studies found that this level of awareness varies considerably among teachers and attention should be paid to misconceptions, in both pre-service teacher programmes and professional development activities.

Another contributed talk described continuous professional development workshops for primary and secondary school

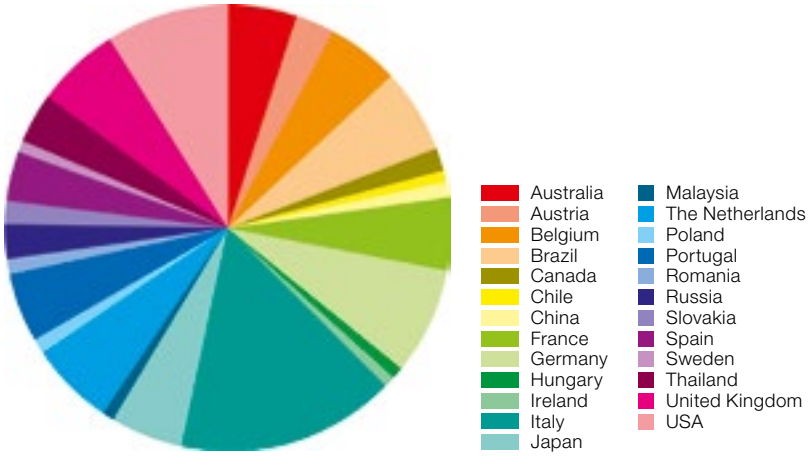

Figure 2. Pie chart showing the distribution of countries from which the 114 participants came.

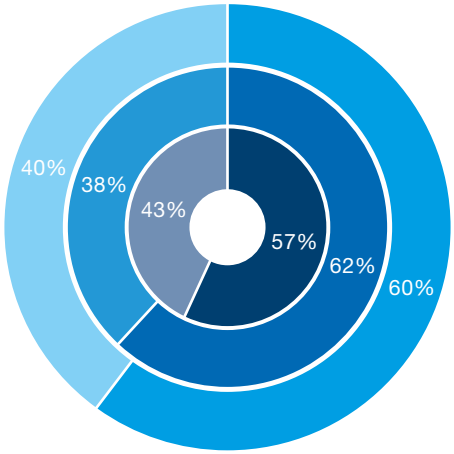

Figure 3. Multi-level pie chart showing the gender ratio amongst participants (outer ring), talks (middle ring), accepted posters (inner ring); in each of these the lighter and darker colours represent the female and male ratios, respectively.

teachers based around the Irish National Junior Certificate theme of Earth and Space. With these workshops, teachers are kept informed of current research and discoveries, and are provided with content and material to engage students using space research. A further contributed talk presented teacher trainings in the use of robotic telescopes. The focus was to bring astronomy closer to teachers in an enjoyable way, so that they lose the fear of working on these topics with their students, and to provide them with the tools and knowledge so that they can introduce them in a practical way and develop enquiry-based projects.

Workshops

The workshops covered a broad range of activities:
- the positive and negative effects of the use of technology in the classroom;
- the use of real astronomical data in the classroom;
- presentation of the recently published booklet *Big ideas in Astronomy: A proposed Definition of Astronomy Literacy;*
- two workshops combining STEM with the arts (STEAM), one dealing with programmable materials that are important for future space travel, the other with the creative use of satellite images;
- an art-based approach to teaching astronomy via Visual Thinking Strategies;
- limitations and opportunities of planetariums, often seen as natural places to run informal education activities;
- how to make astronomy projects more diverse and inclusive;
- developing and testing new interdisciplinary and inclusive educational and outreach activities;
- links between astronomy and environmental education;
- how to design inquiry-based workshops for secondary school students and teacher trainings that are relevant to curricula and cost effective.

The conference highlighted that astronomy education is a well-established field with a global community. Education — alongside research, outreach and development — is one of the main activities of the IAU. Some trends in astronomy education recurred throughout the conference, such as multidisciplinary approaches, the options for online collaboration, training, and distribution. Also, the societal relevance of education was addressed and discussed with topics like inclusion and diversity and climate change. Very fruitful discussions took place during the conference and the majority of participants felt that they are acting towards a common goal. However, there is still a need to improve knowledge transfer between researchers and practitioners, as the wheel tends to be reinvented too often, with efforts being duplicated. After this meeting, the baseline has now been set, and the community looks forward to marking its progress by the next conference in 2021.

Demographics

The demand for this conference was extremely high, but owing to the limited seating in the planetarium, the number of possible participants had to be capped at 114. The participants came from 25 countries, including 13 ESO member states, the Host Country Chile and Strategic Partner, Australia (see Figures 1 & 2). In total, 112 talk abstracts were submitted, 46% of which came from female colleagues (Figure 3). The gender balance among the speakers in the final programme reflected the 40:60 (female:male) distribution of the participants, similar to that of the Scientific Organising Committee (SOC), which had a corresponding ratio of 44:56 (female:male).

Links

[1] Conference webpage: https://iau-dc-c1.org/astroedu-conference/
[2] AstroEdu platform: https://astroedu.iau.org/en/

DOI: 10.18727/0722-6691/5182

Fellows at ESO

Rosita Kokotanekova

Rosita Kokotanekova

My path in astronomy began before I can remember, and it has led to my becoming an ESO Fellow thanks to the support of a long list of teachers, mentors, and friends. However, in the first place, I owe my inspiration to be an astrophysicist to my parents, Joanna Kokotanekova and Dimitar Kokotanekov. They have devoted their lives to outreach and teaching extracurricular astronomy classes to high-school students in Haskovo and Dimitrovrad in Bulgaria.

When my brother Georgi and I were little, our parents took us along to almost every observation they organised: astrophotography sessions, observations of partial and total solar and lunar eclipses, meteor showers, Venus and Mercury transits — you name it. Later, I participated in the Bulgarian National Astronomy Olympiad, as well as in two International Astronomy Olympiads in Crimea (2004) and China (2005). I also completed my first small research projects and had my first contact with ESO, both through the Catch a Star contest [1].

These experiences convinced me that I would like to become an astrophysicist and in my bachelors degree I chose to study Earth and Space sciences at Jacobs University Bremen, Germany. This programme was a great choice because it allowed me to learn more about geosciences and environmental studies alongside astrophysics. Besides, the education at Jacobs University had a hands-on approach and prepared me very well for a research career.

After only my first year at Jacobs, I contacted Marcus Brüggen and Elke Roediger to ask whether I could work with them on a small research project over the summer. During this summer project and my subsequent bachelors thesis research, Elke taught me a great deal about galaxy clusters and hydrodynamical simulations, but most importantly introduced me to the research process — how to start with an idea and find the right collaborators, and how to complete it and produce a high-quality scientific publication.

After my second year at Jacobs University — in 2011 — I joined the Laboratory of Astrophysics (LASTRO) at the École Polytechnique Fédérale de Lausanne (EPFL) in Switzerland where I worked with Frédéric Courbin, Cécile Faure and Georges Meylan on a six-week project to discover strong gravitational lenses in optical images from the Wide Field Camera 3 (WFC3) on the Hubble Space Telescope (HST). I greatly enjoyed the friendly environment at LASTRO and the Observatory of Geneva, as well as living so close to the Alps, so I decided to go back for another two-month project the year after.

Straight after completing the second internship, I joined the AstroMundus Masters Course in Astrophysics. This program took me on a two-year journey through four different countries, at the University of Innsbruck, the University of Padua, Belgrade University and Göttingen University. After three semesters of courses covering almost every area of astronomy, I spent the final semester of the programme researching X-ray weak quasars with Wolfram Kollatschny at Göttingen University and Luka Popović in Belgrade. This project gave me my first experience of spectroscopy and taught me how to work independently — a skill that has come in handy during my PhD, and especially during the ESO fellowship.

I had reserved the AstroMundus summer break in 2013 for a three-month internship at the Harvard Smithsonian Center for Astrophysics working with Ralph Kraft and Akos Bogdan. This project was a continuation of my work with Elke Roediger and would not have been possible without her generous efforts to expand my skill set and to develop my resumé. My work at CfA was extremely interesting and introduced me to X-ray and radio observations of galaxy cluster centres. In addition to the amazing science environment at CfA, that summer also brought me many wonderful experiences which I shared with old and new friends in Boston.

The next step of my career was determined by a lucky coincidence. Straight after the internship at CfA, I started looking for PhD positions. While I was fascinated by extragalactic astronomy, and in particular by X-ray observations of galaxy clusters, I was not looking forward to yet another relocation. This motivated me to keep my eyes open for other PhD opportunities that would let me stay in Göttingen or at least in Germany. Then suddenly, in November 2013, the press was filled with reports about the unexpected complete disintegration of comet ISON. This got me very intrigued because up to that point I had not had any courses in Solar System science and I naively thought that small bodies were very well studied, and that their behaviour could be predicted with great accuracy.

That same week, a friend sent me a link to the home page of Pedro Lacerda who was looking for PhD students to join his newly formed research group in Cometary Science at the Max Planck Institute for Solar System Research in Göttingen.

After reading his webpage and meeting him in person, I was captivated by his way of thinking and his approach to doing research. He also managed to convince me that minor planets in the Solar System hide many unanswered questions.

I joined Pedro's research group in October 2014 and chose to work on his large observing programme with ESO's New Technology Telescope (NTT) at La Silla. The programme was awarded 40 nights with the ESO Faint Object Spectrograph and Camera 2 (EFOSC2) to study the rotational light curves and surface colours of up to 60 Trans-Neptunian Objects (TNOs). In only the third week of my PhD, I went for my first observing run at La Silla with my other PhD advisor Colin Snodgrass. This was the first time I had the chance to spend time with Colin, and I quickly became convinced that my PhD was going to lead to many exciting projects and fun trips. Soon after that run, I enrolled as a PhD student at the Open University, UK and Simon Green joined the supervision team as a third advisor. While most people are lucky to find one good advisor, I was fortunate to work with three great mentors on my PhD.

Like most PhDs, mine did not go as planned. The data from the large programme turned out to be very challenging to analyse, and instead I focused on publishing our side projects on photometric observations of Jupiter-family comet (JFC) nuclei. This led to many new ideas and accepted observing proposals on nine different telescopes. The work on that project did not always go smoothly either, but in the end resulted in a coherent PhD thesis, which I managed to write mainly during an eight-week window while being stuck at home with a broken foot.

Ever since my first trip to La Silla, I had been hoping to follow in Colin's footsteps to become an ESO Fellow. When the time came, and I was about to look for postdoc positions, my advisors encouraged me to put my ideas together and design a research programme to propose for the ESO fellowship application.

This led to an offer from ESO and I started my fellowship in November 2018, two months after I defended my PhD thesis. At ESO, I chose to take up support astronomer duties on VLT/UT3 as my functional work and now, after four shifts in Paranal, I have finally completed my extensive training as a support astronomer. My duties in Paranal are very challenging but extremely rewarding. On the one hand, the trips to Chile are physically exhausting, but on the other hand I have become part of the amazing Paranal community, and I have already learned even more about the telescopes and instruments than I had hoped.

Stefano Facchini

As this is the first year of my first postdoc, the past twelve months have been full of many new adventures in the world of research. Probably the most rewarding one of them was mentoring a talented and enthusiastic summer student — Abbie Donaldson — during the first ESO Summer Research Programme (see page 57). For the coming year, I have an ambitious plan, which among other things includes: completing a few projects on TNOs and JFC nuclei; organising the second ESO Summer Research Programme together with the other fellows; securing more observing time for the ideas I developed over the past year; four trips to Paranal; many important conferences and meetings; more time spent working with collaborators; and last but not least, a couple of vacations that my husband and I have been looking forward to for years.

Links

[1] ESO Catch a Star contest: http://www.eso.org/public/outreach/eduoff/cas/

Stefano Facchini

Since I was a kid, I have had a passion for science — in, I would say, two different flavours. First of all, I have always been touched and fascinated by the beauty of nature, by the constantly varying shades of colour in the sea, by the powerful heights of the Alps during a hike in the summer, or by the fragility of field flowers in my grandparents' farm. I strongly believe that my sense of awe in front of the beauty and apparent order of nature is one of the main driving forces that led me to become a scientist. Secondly, I have always been interested in and fascinated by mathematics, showing a strong propensity towards scientific topics since my first years at school.

My passion for the night sky grew later, during the first years of high school. I have a clear memory of one evening being in the countryside close to Lake Como in Italy with a friend of mine and his father. His dad started pointing at the sky and naming the constellations that were visible during that summer evening. What impressed me the most is that he had a familiarity with the beauty of the sky we were looking at; he could recognise and name stars, whereas for me everything was beautiful but totally unknown. From that evening, I started studying the constellations of the northern hemisphere, and I developed an enthusiasm for getting to know and being able to describe the beauty of the sky.

I continued to follow my passion for natural sciences, and I started attending

physics courses at the University of Milan in Italy. The choice of the subject of my undergraduate studies was the easiest choice of my life by far! Even though I loved many topics, in particular solid state physics and statistical mechanics, I opted for a masters degree in astrophysics. What attracted me the most is that this subject required one to study and understand many areas of physics: general relativity, classical mechanics, quantum mechanics, molecular physics, etc. All aspects had to be taken into account! One of the topics I loved the most was compact objects — in particular the book *Black holes, white dwarfs and neutron stars: the physics of compact objects* by Teukolsky and Shapiro — where the three main forces of physics interplay to produce beautiful objects such as neutron stars and black holes.

For my masters thesis, I decided to work with Giuseppe Lodato, who had recently arrived in Milan from the UK. During my thesis, I started working on a research topic that is what I still work on seven years later: protoplanetary discs and planet formation. The thesis project was deeply theoretical, and we were trying to answer the question: what would happen if a protoplanetary disc orbits around a binary that is misaligned with respect to the disc itself? Developing semi-analytical models and hydrodynamical simulations, we figured out that the disc can warp, and in some extreme cases, it can break into separate annuli. At the time I approached this as a theoretical game. How impressed I was years later when high-resolution images of protoplanetary discs started to be available, in particular thanks to the VLT instruments NAOS-CONICA (NACO) and Spectro-Polarimetric High-contrast Exoplanet REsearch (SPHERE), and signatures of these broken discs were directly observed as we had predicted!

The masters thesis was such a great experience that I decided to keep on doing research with a PhD. To do this, I managed to go to Cambridge in the UK, to work with Cathie Clarke on a variety of topics, and in particular on the effects that ultraviolet radiation from massive stars can have on the evolution of protoplanetary discs in young massive clusters. The PhD was mostly theoretical; the most important thing I learnt is to ask myself the question that Cathie asked me many times: "how do you understand this equation empirically?" In other words, how is this mathematical formula describing a physical phenomenon in a simple way? This way of looking at the mathematical formulation of physics has changed my way of doing theory forever, leading me to understand a physical process with very simple principles.

Towards the end of my PhD, however, I felt that I was lacking something, so much so that I wondered whether to continue to do research. At some point, I understood that I was missing a closer connection to observations, and I tried to find a postdoc that could allow me to develop this new side of research. I was lucky enough that Ewine van Dishoeck invited me to join her group at the Max Planck Institute in Garching, and the three years with her group have been key for who I am today as a scientist. In particular, with her I broadened my expertise, and started working on thermochemical models of discs, and more directly on observations at different wavelengths (from millimetre to ultraviolet). Those same years, since 2015, have been transformational in my field. The tremendous capabilities of the Atacama Large Millimeter/submillimeter Array (ALMA), in terms of sensitivity and angular resolution, together with high-performance infrared imaging instruments such as SPHERE, completely revolutionised the field of planet formation, showing images of the environments where planets form with unprecedented detail. Doing research in a field that was being transformed every six months by a new set of observations has been among the most exciting experiences of my life.

During the last year, I have been working at ESO as a fellow. This has allowed me to move even more towards observational astronomy, getting even more involved with ALMA (through my functional work) and with other instruments on the VLT (such as SPHERE, MUSE, X-Shooter). To me ESO is the perfect environment to do astrophysical research in the way I love: led by observations, but with a strong theoretical background to interpret the data and to predict what to expect. I look forward to the next two years and to even more exciting discoveries!

Johanna Hartke

It is hard to pinpoint exactly when I discovered my passion for astronomy. I grew up in the northern German countryside, so even though the skies were relatively dark, it was often cloudy. My parents had a small refracting telescope which stood forgotten in front of the living room window, waiting for clear skies. However, as a child, I was more drawn towards the piano that stood right next to it. One of my first (of many) career goals was to become a pianist, then followed by a desire to be a teacher, an actress, a mathematician, and eventually, a physicist.

Following a summer school on quantum physics for gifted high-school students the year before I graduated high school, I was convinced my career lay in theoretical physics. A year later, I enrolled to study physics at Jacobs University, a small, international university in Bremen. I had a great experience living on campus with students from over a hundred different countries, but soon realised that theory was not my calling. While I enjoyed experimental physics lectures, I was also

Johanna Hartke

notorious for clumsy accidents in the lab. However, there was one topic I excelled in and that was astrophysics. Unfortunately, the astronomy branch was closed in my second year of study. The subject was not uppermost in my mind anymore, and struggling with the prospect of becoming a researcher, I seriously considered reverting to one of my earlier career choices: becoming a teacher. I had just made it to the state final of a youth music competition in Germany and teaching music and physics in high school seemed like the perfect combination of subjects for me.

Everything changed, however, when I was selected for a summer internship at Mount Stromlo Observatory of the Australian National University. For the first time, I got an insight into the day-to-day life of a researcher and could work independently on a small project on stellar streams in the Milky Way. My supervisor Ken Freeman introduced me to the beauty and elegance of galaxy dynamics. All of a sudden, I could appreciate classical mechanics as a great tool to describe the motions of the stars. After the internship, I abandoned my idea to go to the conservatory and instead focused on finding an opportunity to carry out my bachelor thesis research project in astronomy; so I found a placement in nearby Groningen to work with Amina Helmi.

I decided to stay at the Kapteyn Institute for another two years to complete my Master of Science, thoroughly enjoying a curriculum centred on astronomy. Soon an opportunity came up to enroll in a course on observational astronomy which was to take place at the Isaac Newton Telescope on La Palma. During our five nights at the telescope, we experienced first-hand how it felt to be an astronomer and the patience it required in case of bad weather! Yet I had found a new passion. It was rewarding to see our project grow from a little idea in our heads to typing the coordinates of targets into the telescope, and to finally present the science to our peers after reducing the data. One year later, I again found myself on La Palma, this time observing at the William Herschel Telescope for my master thesis project with Eline Tolstoy.

It was clear that I wanted to pursue a PhD in observational astronomy. In the same year, I was accepted into the International Max Planck Research School (IMPRS) on Astrophysics in Munich for a three-year studentship at ESO under the supervision of Magda Arnaboldi. For my PhD, I investigated how the halos of early-type galaxies grow through mergers and accretion. This is a challenging endeavour, as the closest early-type galaxies are already millions of light-years away, but the faint halos are very extended on the sky. I therefore use a particular type of stars — planetary nebulae — which are like green beacons in the sky, and whose velocity can be measured even at a distance of hundreds of millions of light-years.

I enjoyed being in the middle of one of the astronomy hubs in Europe and got to participate in many exciting seminars and conferences that were taking place on campus. I travelled again to La Palma to observe the halos of giant elliptical galaxies with the custom-built Planetary Nebula Spectrograph (PN.S) for my thesis. Since the PN.S is a visitor instrument, we spent many afternoons leading up to our observations tuning the filters and aligning the CCDs in the instrument arms. Six months later, I got the opportunity to join my ESO Fellow mentor during his duties at Paranal observatory. At last I was convinced that the next step for me would be an ESO Fellowship in Chile to get even more exposure to the forefront of astronomical research and instrumentation.

And here I am now. I have just completed the first year of my fellowship and therefore the first 80 days and nights as a support astronomer on Paranal. It has been an exciting year with a steep learning curve! I am part of the Multi Unit Spectroscopic Explorer (MUSE) instrument operations team and currently work on a project to investigate how well the adaptive optics improve the image quality. It is great working in an international and interdisciplinary team. I particularly enjoy the ritual of watching the sunset from the platform before the night starts. I also recently started to experiment with astrophotography. I like to share the wonders of the night sky with my friends in the city, where due to the bright lights, one can barely make out the Southern Cross. When I am not observing or working from Vitacura, one is likely to find me rehearsing music. While living in Munich, I was a soprano with the Münchner Motettenchor and spent a good part of my leisure time in churches and concert halls in the region. Now in Santiago, I have again taken up singing, although on a smaller scale. It is a relaxing balance to the academic world and a great way to practise my Spanish.

In Memoriam

ESO staff member, Cristian Herrera González, sadly passed away in August 2019 and will be much missed. He joined ESO and the Science Operations Department as Telescope and Instrument Operator (TIO) in 2001. During his 18 years at Paranal, Cristian worked on most of the telescopes, instruments and subsystems of the observatory. He held the role of nighttime TIO Coordinator for more than 10 years, leading the night crew and was the coordinator of the Instrument Operations Teams activities for the operators during his shifts.

Personnel Movements

Arrivals (1 October–31 December 2019)

Europe

Andersson Lundgren, Andreas (SE)	Apex Support Astronomer Gentile Fellow
Fusillo, Nicola (IT)	Student IMPRS
Girdhar, Aishwarya (IN)	Fellow
Heida, Marianne (NL)	Student DFG
Izquierdo Cartagena, Andrés (CO)	Student IMPRS
König, Pierre-Cécil (FR)	Fellow
Lansbury, George (UK)	Fellow
Marchetti, Tommaso (IT)	Accountant
Oliveira Teixeira, Emanuel Pedro (PT)	Technical Writer/ Documentation Specialist
Paredes, Amaya (ES)	Student IMPRS
Szakacs, Roland (AT)	Administrative Assistant
Teuber, Karin (DE)	Public Information Officer
Trovão Ferreira, Bárbara (PT)	

Chile

Campana, Pedro (CL)	Electronics Engineer
Dauvin, Louise (CL)	System Engineer
De Rosa, Robert (UK)	Operation Staff Astronomer
Farias, Cecilia (CL)	Telescope Instruments Operator
Hsieh, Pei-Ying (TW)	Fellow
Leon, Angelica (CL)	Telescope Instruments Operator
Saint-Martory, Georges (FR)	ELT Deputy Site Manager
Santamaría Miranda, Alejandro (ES)	Fellow
Scicluna, Peter (UK)	Fellow
Slumstrup, Ditte (DK)	Fellow

Departures (1 October–31 December 2019)

Europe

Bordelon, Dominic (IE)	Library Technology Specialist/ System Administration & Classification Specialist
Harrison, Christopher (UK)	Fellow
Heijmans, Jeroen (NL)	Instrumentation Engineer/Physicist
Hellemeier, Joschua Andrea (DE)	Student
Hughes, Meghan (UK)	Student
Iani, Edoardo (IT)	Student
Kolwa Sthabile, Namakau (ZA)	Student IMPRS
Lelli, Federico (IT)	Fellow
Møller, Palle (DK)	User Support Astronomer
Slater, Roswitha (DE)	Administrative Employee
Zanella, Anita (IT)	Fellow

Chile

Milli, Julien (FR)	Operation Staff Astronomer
Silva, Karleyne (BR)	Operation Staff Astronomer
Vogt, Frédéric (CH)	Fellow

DOI: 10.18727/0722-6691/5183

Erratum

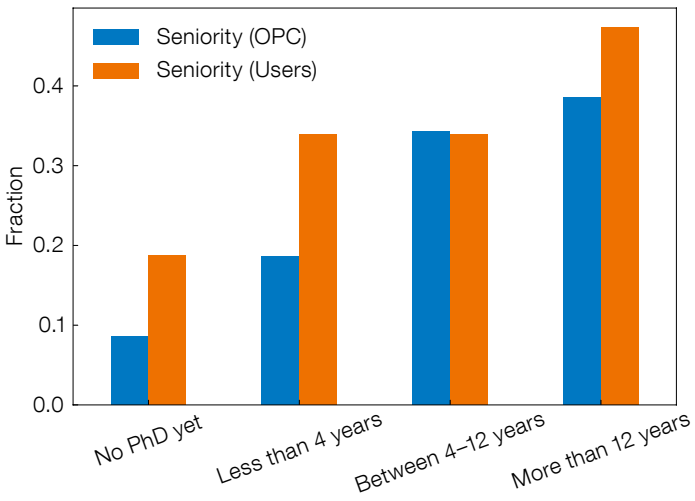

Figure 1. Scientific seniority distribution of the DPR sample (blue) compared to the ESO users sample (orange) from Patat et al. (2016). Note that the two central orange bars correspond to the middle seniority class in Patat et al. (2016).

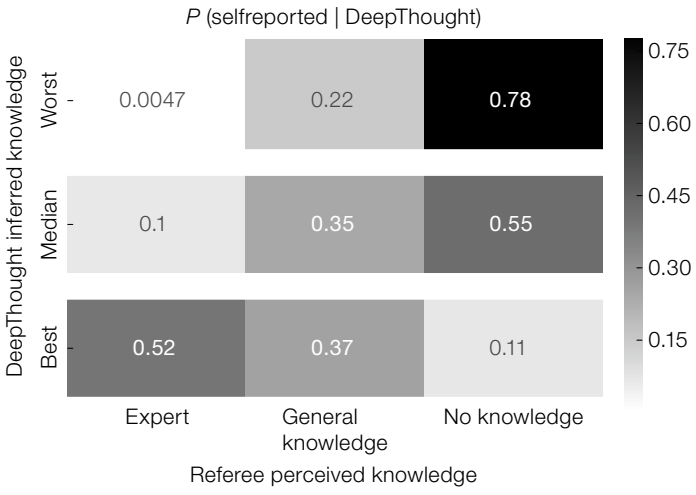

Figure 5. Conditional probability for the various combinations of self-reported and DeepThought-inferred knowledge level.

We would like to correct and update Figures 1 and 5 in *The Distributed Peer Review Experiment* by Patat et al. (2019, The Messenger, 177, 3). Figure 1 is the same as previously published and only has an updated caption and labels, Figure 5 has been updated and corrected. The rest of the article, its discussion and conclusions remain unchanged.

2ND ESO SUMMER RESEARCH PROGRAMME

2 July–11 August 2020

ESO Headquarters, Garching bei München, Germany

Fully funded programme for undergraduate (pre-PhD) students in astronomy, physics or related subjects

Application deadline

5 February 2020

Research a cutting-edge astronomy project

Collaborate with top researchers

Discover ESO and its telescopes

Learn new skills and astrophysics

Find out more and apply online:
http://eso.org/summerresearch/